Transactions of the Royal Society of Edinburgh: Earth Sciences, **96**, 131–162, 2006 (for 2005)

Cranial morphology and ontogeny of the Permo-Carboniferous temnospondyl *Archegosaurus decheni* Goldfuss, 1847 from the Saar–Nahe Basin, Germany

Florian Witzmann

ABSTRACT: Morphology and ontogenetic changes in the skull and hyobranchium of the Permo-Carboniferous temnospondyl *Archegosaurus decheni* from the Saar–Nahe Basin (SW Germany) are described in detail, based on 181 skulls ranging from 18 to 279 mm in length. Three-dimensional skull reconstructions including the palate of different growth stages are provided. The extremely elongate choanae and up to four median symphyseal teeth are unique to *A. decheni*. Among neurocranial elements, the exoccipital is well ossified and forms the paroccipital process as in stereospondyls. The shaft of the stapes which projects into the squamosal embayment grows with positive allometry and possesses a distinct lateral process. The basibranchial is well ossified in adults and exhibits a complex, spoon-like morphology. Small larvae were euryphagous and used non-directed suction and jaw prehension during prey capture. Larger larvae and adults were mainly ichthyophagous, as is indicated by the increasingly elongated snout, differentiation of marginal teeth, and nutrition remains. After a prolonged larval period, juvenile and adult *A. decheni* remained in the aquatic habitat, as suggested by the presence of lateral line sulci, the 'aquatic type' of septomaxilla and choana, and the absence of a nasolacrimal duct.

KEY WORDS: cranium, feeding, hyobranchium, ontogeny, Temnospondyli.

Among Permo-Carboniferous temnospondyls, *Archegosaurus decheni* is known from an exceptional high number of individuals in an extensive size range. Adult specimens reach more than 15 times the length of the smallest known individuals. In this respect, *Archegosaurus decheni* is comparable only to the actinodontid *Sclerocephalus haeuseri* (Boy 1988; Schoch 2003). Small growth stages possess larval characteristics, such as branchial dentition and external gills, that cannot be demonstrated in large individuals. *Archegosaurus* thus permits the study of larval development to the juvenile and adult phases. The excellent preservation of skulls allows not only the analysis of the dermal skull and mandible, but also of the neurocranial and palatoquadrate ossifications.

Scientific investigations of *Archegosaurus* date back to the first half of the 19th century when palaeontology was established as an independent field. Dechen (1847) discovered concretions in the *Toneisenstein* quarries near Lebach in SW Germany which contained remains of differently sized tetrapods. Goldfuss (1847) published the first description of Dechen's findings, placing the specimens into a new genus, *Archegosaurus*. Jäger (1850) noticed that remains of *Archegosaurus* had already been erroneously referred to the fish *Pygopterus lucius* by Agassiz (1833). Goldfuss distinguished three species, naming the large specimens *Archegosaurus decheni*, the medium- sized *A. medium*, and the small ones *A. minor*. Jordan (1849) published additional notes on the skull morphology of *Archegosaurus decheni* and described a further tetrapod species of the Lebach fauna which he called *Archegosaurus latirostris*. Burmeister (1850) provided a more detailed description of *Archegosaurus*, recognising that the differently-sized specimens of *Archegosaurus* represent various growth stages of only one species, i.e., *Archegosaurus decheni*.

Meyer (1858) published his seminal monograph on *Archegosaurus*, including a restoration of the dorsal skull roof of an adult specimen. He also elaborated on the individual growth of *Archegosaurus* and documented changes in skull proportions. A description of the lower jaw of an adult specimen of *Archegosaurus decheni* was published by Jaekel (1896). Watson (1919) discovered remains of the ossified neurocranium in *Archegosaurus decheni*. However, his material was not adequately preserved to allow a detailed description. Hofker (1926) described the neurocranium of *Archegosaurus decheni*, misinterpreting some of the neurocranial bones. He used the teleostean skull for comparison because only little was known about the morphology of the temnospondyl neurocranium at that time. Additionally, Hofker was able to demonstrate new details of the hyobranchial skeleton. Whittard (1928) provided a reconstruction of the palate with important new characteristics, and a reconstruction of the lower jaw.

After 1928, no original work on *Archegosaurus* was published for decades. Romer (1939) referred to individual growth stages of *A. decheni* within the scope of his study on 'branchiosaurs', and Boy (1974) and Boy & Sues (2000) mentioned aspects of the ontogeny of *A. decheni* in comparison with other temnospondyl larvae. In his palaeoecological work on the Lower Rotliegend of Rheinland–Pfalz and the Saarland (SW Germany), Boy interpreted *A. decheni* as a specialised fish hunter (Boy 1976, 1993a). Milner (1978) revised a tetrapod from the Košť álov-Kalná Horizon (Autunian) in the Czech Republic that was described by Steen (1938) as *Memonomenos dyscriton*. He identified it as temnospondyl and transferred it to the genus *Archegosaurus* as the species *A. dyscriton*. Boy (1993a) provided a reconstruction of the skull roof and the anterior part of the palate of a medium-sized *A. decheni*. In 1997, a paper was published by Gubin which exclusively deals with the skull morphology of *A. decheni*. All dermal bones of the palate were illustrated for the first time. In addition, parts of the neurocranium were described. Many morphological

aspects, however, remained unconsidered because only few specimens were available to Gubin. Witzmann (2004) described external gills and associated structures of the hyobranchial skeleton in larval *A. decheni* and compared them to those of other Palaeozoic anamniotic tetrapods.

The first aim of the present study is to provide a detailed description and reconstruction of the cranial anatomy of *A. decheni*. Since the pioneer work of Meyer (1858), numerous new specimens of *A. decheni* have been collected and newly prepared. In addition to a re-examination of material that was the subject of earlier works, previously undescribed and in parts exceptionally well preserved specimens were considered. The second aim is to describe the ontogenetic changes in the skull and visceral skeleton of *A. decheni*. Because the extensive size series of *A. decheni* reveals ontogenetic information that is unavailable in the majority of other temnospondyls, its study sheds light on temnospondyl ontogeny and evolution in general. A further aim is the reconstruction of the mode of life including feeding behaviour of *A. decheni* on the basis of the morphologic results, taking into account the associated tetrapod and fish fauna.

1. Stratigraphic and geographic range

The upper part of the Rotliegend (Autunian, which dates around the Permo–Carboniferous boundary) in the Saar–Nahe Basin was divided by Boy & Fichter (1982) into ten members, L-O 1 to L-O 10. The occurrence of *Archegosaurus decheni* is restricted to the Humberg Black Shale which belongs to L-O 10 (Boy 1987; Boy *et al*. 1990).

A basin facies in the northeast (Nahe Syncline) and a marginal facies in the southwest of the Saar–Nahe Basin can be distinguished within the Humberg Black Shale (Boy 1987; Boy *et al*. 1990). In the basin centre, finely laminated shales with alternating content of carbonate occur, together with poorly laminated and bituminous black claystones. According to Boy (1987), only one specimen of *Archegosaurus decheni* has been discovered in this facies. The basin facies merges into the marginal facies to the southwest. The black shales wedge out, whereas layers and concretions (geodes) of siderite become more abundant. They increase to a clay–iron–stone facies in the area of Lebach near Saarbrücken, the so-called 'Tonsteinlager'. The siderite concretions frequently contain remains of *Archegosaurus decheni* and rarely of the intasuchid temnospondyl *Cheliderpeton latirostre*. The fish fauna consists of the acanthodian *Acanthodes*, the palaeoniscoids *Rhabdolepis*, *Paramblypterus*, and *Gardinerichthys*, rare finds of the xenacanthids *Triodus*, *Xenacanthus*, and *Lebachacanthus* (*Orthacanthus*), as well as the lungfish *Conchopoma* (Schultze 1975).

In the 19th century, intensive excavations of *Toneisenstein* were undertaken in the area around Lebach, especially in the Gresaubach, Rümmelbach, and Berschweiler quarries, in which *Archegosaurus decheni* was frequently recorded (Burmeister 1850; Meyer 1858). The opencast mining has been abandoned, and the quarries are no longer accessible. Boy (1987) reconstructed the habitat of the Lebach-fauna as a vast, relatively deep lake which he called 'lake of the type Lebach'.

2. Material and methods

The following completely or partially preserved skulls of *Archegosaurus decheni* were examined for this study:

BSM (Bayerische Staatssammlung für Paläontologie und Historische Geologie, München, Germany): 1869 III 6, 1869 III 7.

GMBS (Geologisches Museum der Bergingenieursschule Saarbrücken, Germany): P/403, 426, 494, 495, 497, 498, 503, 505, 635, 828.

GPIT (Institut und Museum für Geologie und Paläontologie Tübingen, Germany): Am 20, 21, 233, 685.

IGS (Institut de Géologie Strasbourg, Université Louis Pasteur, France): UII 1/1, 1/2, UIII 2, 2/1, 2/2, 2/3, 3/3, 4/5, 5/3, Saa 145.

IPB (Institut für Paläontologie der Universität Bonn, Germany): A 7, 26, 1344 (Goldfuss 1847, pl. 3, fig. 1), 1352 (Goldfuss 1847, pl. 1, figs 1–3), 1357 (Goldfuss 1847, pl. 3, fig. 2), R 432, 438.

IPFUB (Institut für Paläontologie, Freie Universität Berlin, Germany): 13.

MB (Museum für Naturkunde, Humboldt-Universität zu Berlin, Germany): Am 118 (Meyer 1858, pl. 16, figs 4, 5), 121 (Meyer 1858, pl. 13, fig. 1), 122 (Meyer 1858, pl. 16, fig. 1), 123, 124, 126, 127 (Meyer 1858, pl. 23), 134, 136, 138–140, 145 (Meyer 1858, pl. 16, fig. 6), 146 (Meyer 1858, pl. 16, fig. 2), 148 (Meyer 1858, pl. 16, fig. 3), 149 (Meyer 1858, pl. 11, figs 1–4), 150, 152–156, 160, 167, 169, 171–175, 178–189, 191, 193–195, 197, 201–208, 213, 216, 218–223, 225, 227–230, 233–237, 245 (Meyer 1858, pl. 15, fig. 2), 248 (Meyer 1858, pl. 15, fig. 1), 253, 257, 258, 272, 275, 300 (Meyer 1858, pl. 13, fig. 4), 317, 323, 329, 953, 986, 994.

NNM (Naturalis Museum, Leiden, the Netherlands): 18154, 39027, 39029, 39031, 39034, 39036, 39040, 39043, 39044, 39046, 39048, 39051, 39053, 39065, 39066, 39070, 39072, 39074, 39080–39084, 39087, 39097, 446474, 446478, 446479.

PIM (Paläontologisches Institut Mainz): N n.reg.

PIMUZ (Paläontologisches Institut und Museum der Universität Zürich, Switzerland): A/II 0019–0023, 0061.

SMF (Forschungsinstitut und Naturmuseum Senckenberg, Frankfurt am Main, Germany): A3, 3/1, 4, 8, 14, 21, 24, 32, 35, 71, 487.

SMNK (Staatliches Museum für Naturkunde, Karlsruhe, Germany): 39/13, 39/17, 119, 124, 131.

SMNS (Staatliches Museum für Naturkunde, Stuttgart, Germany): 3706, 11512, 81850, 81993–81995.

TM (Teylers Museum, Haarlem, the Netherlands): 1154, 1169.

Professor J. A. Boy (Mainz) provided plaster casts of two skulls housed in the Natural History Museum London (BMNH) and in the Museum of Comparative Zoology of the Harvard University, Cambridge, (MCZ) respectively.

The skull length was measured in each case as the distance from the tip of the snout to the posterior margin of the postparietals. Small specimens of *Archegosaurus decheni* have two-dimensionally flattened skulls, caused by the superimposed load of the sediment. For three-dimensional reconstruction of the skull of a small larva, a wax model was prepared to determine outline and depth of the skull.

Anatomical abbreviations used in text: ml – mandible length; sl – skull length.

3. Systematic palaeontology

Tetrapoda Goodrich, 1930
Temnospondyli Zittel, 1888
Stereospondylomorpha Yates & Warren, 2000
Archegosauriformes Schoch & Milner, 2000
Archegosauridae Lydekker, 1885
Archegosaurus Goldfuss, 1847
Memonomenos Steen, 1938

https://doi.org/10.1017/S0263593300001279 Published online by Cambridge University Press

Archegosaurus decheni Goldfuss, 1847
For a detailed synonymity list until 1889 see Ammon (1889).

1896 *Archegosaurus decheni*. – Jaekel, pp. 505–521, figs 1–10
1919 *Archegosaurus decheni*. – Watson, pp. 9–10, fig. 2
1926 *Archegosaurus decheni*. – Hofker, pp. 109–130, figs 1–16
1928 *Archegosaurus decheni*. – Whittard, pp. 225–264, pl. 13
1932 *Archegosaurus decheni*. – Pfannenstiel, p. 24, fig. 10
1939 *Archegosaurus decheni*. – Romer, pp. 757–758, fig. 3
1947 *Archegosaurus decheni*. – Romer, pp. 151–153, fig. 28
1974 *Archegosaurus decheni*. – Boy, pp. 251–254, 256–260, fig. 13 e, f
1976 *Archegosaurus decheni*. – Boy, p. 57, fig. 27 a
1977 *Archegosaurus decheni*. – Boy, pp. 133–134, fig. 8
1978 *Archegosaurus decheni*. – Milner, pp. 670, 673–676
1983 *Archegosaurus decheni*. – Haubold, pp. 191–192, figs 134, 138
1991 *Archegosaurus decheni*. – Gubin, p. 13
1993a *Archegosaurus decheni*. – Boy, p. 158, fig. 1
1997 *Archegosaurus decheni*. – Gubin, pp. 103–121, figs 1–8
2000 *Archegosaurus decheni*. – Schoch & Milner, p. 56, fig. 48
2004 *Archegosaurus decheni*. – Witzmann, pp. 388–389, fig. 3

3.1. Shared derived characters of archegosaurids (emended from Schoch & Milner 2000) that are found in *A. decheni*

1. Slender supratemporal, forming a long suture with the squamosal.
2. Maxillary-vomer contact excludes premaxilla from anterior choanal margin.
3. Double anterior palatal fossae (or very bilobed single).
4. Six to 22 ectopterygoid teeth and no ectopterygoid fang (shared with *Cheliderpeton latirostre*).

3.2. Derived characters of adult *A. decheni* in relation to other archegosaurids

1. Choanae extremely elongate and narrow, laterally concave, reaching more than one fifth of skull length and more than 3 times naris length.
2. Four symphyseal fang loci on the dentary medial to the marginal tooth row on each mandibular ramus.
3. Crest on the ventral side of the tabular that extends beyond the posterior margin of the tabular horn and forms the posteroventrally directed tabular extension.

3.3. Differences between different growth stages of *A. decheni*

1. Preorbital region proportionally distinctly shorter in small larvae; its length increases proportionally during ontogeny in juveniles and adults.
2. Tabular extensions not present until approximately 40 mm skull length.
3. Choanae proportionally distinctly less elongate in small larvae; their length grows with positive allometry.
4. Larval specimens (up to 150 mm skull length) with branchial dentition.

Neotype: The three syntypes of the original description of *Archegosaurus decheni*, '*A. medius*', and '*A. minor*' by Goldfuss (1847) were housed in the Institut für Paläontologie der Universität Bonn. The skull of approximately 150 mm length illustrated by Goldfuss as *A. decheni* (1847: pl. 1, figs 1–3) is lost, and only a plaster cast (IPB A 1352; Fig. 1a) of it is available. IPB A 1344 is a skull of approximately 70 mm in length plus trunk, described by Goldfuss (1847: pl. 3, fig. 1) as '*A. medius*', and IPB A 1357 is the plaster cast from a specimen of 43 mm skull length plus anterior trunk designated by Goldfuss (1847: pl. 3, fig. 2) as '*A. minor*'. Because the only available original specimen of the syntypes (IPB A 1344) was described as '*A. medius*' by Goldfuss (1847), it cannot be chosen as the lectotype of *A. decheni*. Therefore a neotype of *A. decheni* has to be determined. This is MB.Am.116 (a+b) with a skull length of 279 mm. It consists of a natural mould of the dermal skull roof plus mandible (MB.Am.116a), and of almost the complete palate plus parts of the neurocranium (MB.Am.116b). Both '*A. medius*' and '*A. minor*' are non-valid species and must be assigned to *A. decheni*.

Locus typicus: Lebach near Saarbrücken, between Rümmelbach and Gresaubach, Lebach/Saar, Saarland, Germany.

Stratum typicum: Upper part of the Humberg Black Shale (Boy *et al*. 1990), L-O 10 after Boy & Fichter (1982), Lower Rotliegend, Autunian.

Geographic and stratigraphic distribution: Saar–Nahe Basin, Meisenheim Formation, Humberg Black Shale (Königer *et al*. 2002).

3.4. Non *Archegosaurus*

'*A. latirostris*' Jordan, 1849 from the Early Permian Humberg Black Shale of the Saar–Nahe Basin is referred to as *Cheliderpeton latirostre* by Boy (1993b).

'*A. austriacus*' Makowsky, 1876 from the Early Permian of the Boskovice Furrow (Czech Republic) is not a temnospondyl but a seymouriamorph. Kuhn (1933) introduced the name *Discosauriscus austriacus*.

Credner (1882, pp. 231–234, pl. 13, figs 9–14) reported findings of *A. decheni* from the Early Permian Niederhäslich–Schweinsdorfer Schichten of Saxony (Döhlen Basin, Niederhäslich near Dresden). However, the described cranial and postcranial remains can be assigned to the eryopid *Onchiodon labyrinthicus*.

Cf. Archegosaurus sp. from the Upper Goldlauter Beds of Friedrichroda, Thuringia (Early Permian) is pictured by Langenhan (1909, addendum-plate 2) and consists of the anterior part of a mandibular symphysis whose rami meet at an acute angle. The original specimen is lost (R. Werneburg, pers. comm. 2003). According to the figure, the mandibular teeth possess a cap that can be interpreted as a cap of acrodine. Acrodine is a unique character of actinopterygians (Janvier 1996).

'*A. ornatus*' Woodward, 1905 from the Late Permian Vihi Beds, Mamal Formation of Kashmir, is referred to as *Kashmirosaurus ornatus* by Werneburg & Schneider (1996).

Konzhukova (1956) assigned a lower jaw from the Late Permian of the Inta region (Russia) to *Archegosaurus* sp. Gubin (1986) described this specimen as an intasuchid incertae sedis.

'*A. kashmiriensis*' Tewari, 1960 is a junior synonym of '*A. ornatus*' (=*Kashmirosaurus ornatus*; Werneburg & Schneider 1996).

Haubold (1983) and Werneburg (1986) reported questionable postcranial remains of *Archegosaurus* in the Upper Oberhof Beds of Friedrichroda, Thuringia (Germany). Werneburg (1988) assigned these remains to the eryopid *Onchiodon labyrinthicus*.

4. Dermal skull roof

4.1. Outline and proportions of the skull

Figures 2–5 show reconstructions of skulls of *A. decheni* ranging from 18 to 279 mm length (measured from the tip of

https://doi.org/10.1017/S0263593300001279 Published online by Cambridge University Press

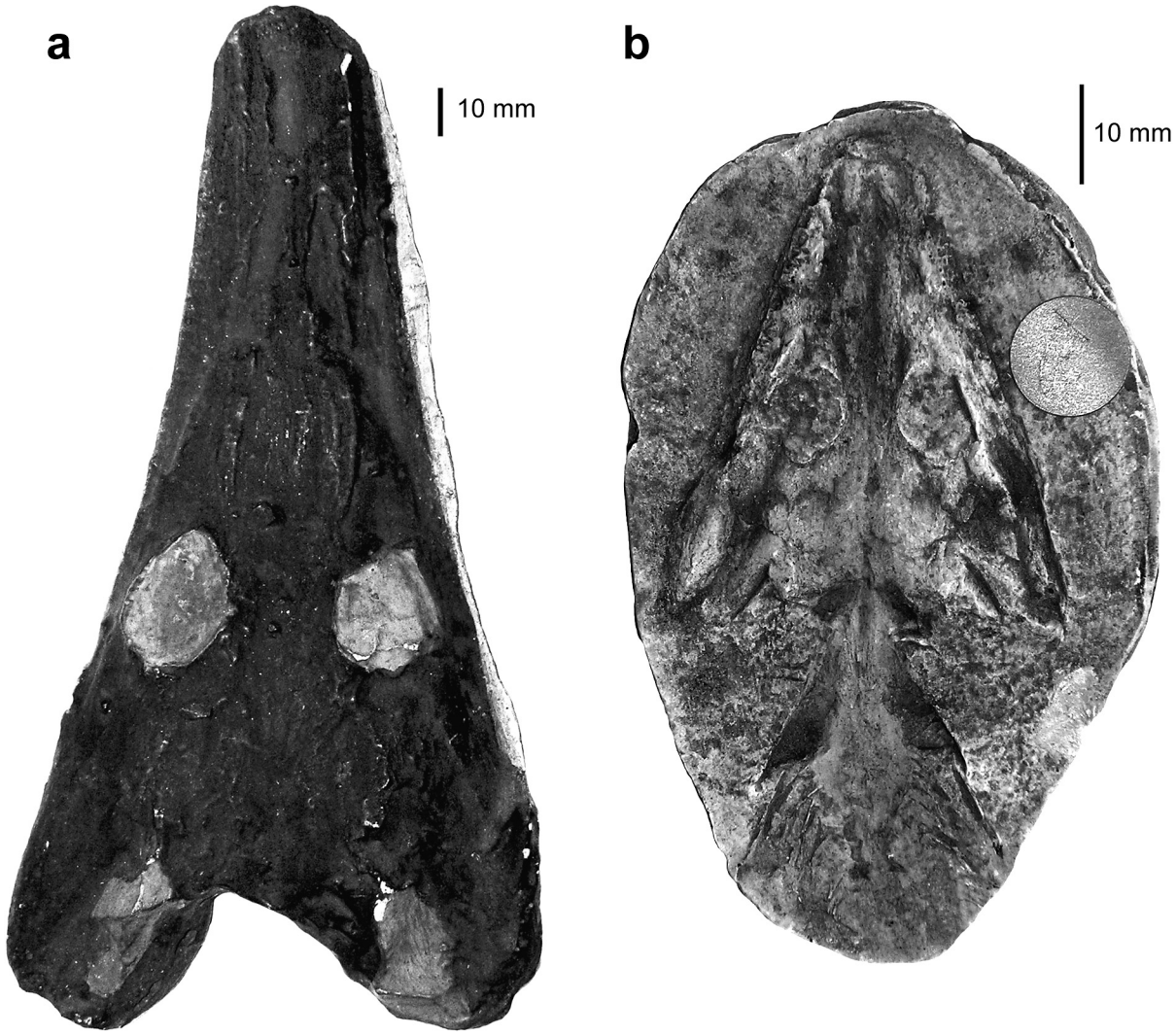

Figure 1 *Archegosaurus decheni*. Plaster casts of the lost type specimens: (a) IPB A 1352 (sl=150 mm); (b) IPB A 1357 (sl=43 mm).

the snout to the posterior margin of postparietals). The skull forms an isosceles triangle that tapers distinctly in its anterior part with increase of skull length. The anterior end of the snout is blunt and slightly broadened in the larger skulls. During size increase, the preorbital length ('length of snout') exhibits distinct positive allometry. The smallest skulls have a preorbital length that accounts for approximately 40% of skull length. In middle-sized skulls, preorbital length amounts around 60% of skull length, and in the largest skulls it is almost 70%.

The shape of the orbits is oval, with the longitudinal axis aligned nearly parallel to the lateral margin of the skull. In most specimens, a slight anteromedial constriction of the orbits is present. The maximum orbital length measures almost 30% of skull length in the smallest specimens. During further ontogeny, the orbits decrease proportionally in size, so that their length accounts for only 10% in the largest skulls. The orbits face upwards and laterally and are surrounded by a torus in large specimens. During growth, the interorbital width increases proportionally with respect to individual orbital width. In the smallest skulls, the interorbital width accounts for approximately 70% of orbital width, whereas it is about 1·5 times the orbital width in the largest skulls. Ossified round-oval sclerotic rings can be found in the orbits. They consist of 28–29 bony platelets which do not overlap. The platelets are longer and broader in the anterior and median part of the ring. Carbonised remains, which may derive from the retina, are often preserved inside the ring.

The parietal foramen is situated a short distance posterior to the orbits in the smallest specimens. It shifts posteriorly during increase of skull length, so that it lies more than one third of the postorbital skull length posterior to the orbits in the largest skulls.

The external nares open dorsolaterally and are situated approximately 2·5 times their length posterior to the tip of the snout in the largest specimen, but are close to the snout tip in small specimens. The external nares are proportionally slightly more elongate in large specimens than in the small larvae.

In large skulls, a thickened ridge extends from the tabular horn and runs anteriorly and slightly medially on the lateral part of the supratemporal; it turns in anterolateral direction towards the orbit at the level of the supratemporal-postorbital suture (Figs 4, 5). The skull table is clearly concave between these two ridges. This concavity decreases slightly in the interorbital area, whereas the surface of the skull roof is slightly convex in the preorbital part. Similar ridges begin at the anterior end of each orbit and extend anteriorly. They are not as strongly developed as the ridges on the posterior skull table. The ridges are best visible on the prefrontals and are only faintly visible anterior to them.

https://doi.org/10.1017/S0263593300001279 Published online by Cambridge University Press

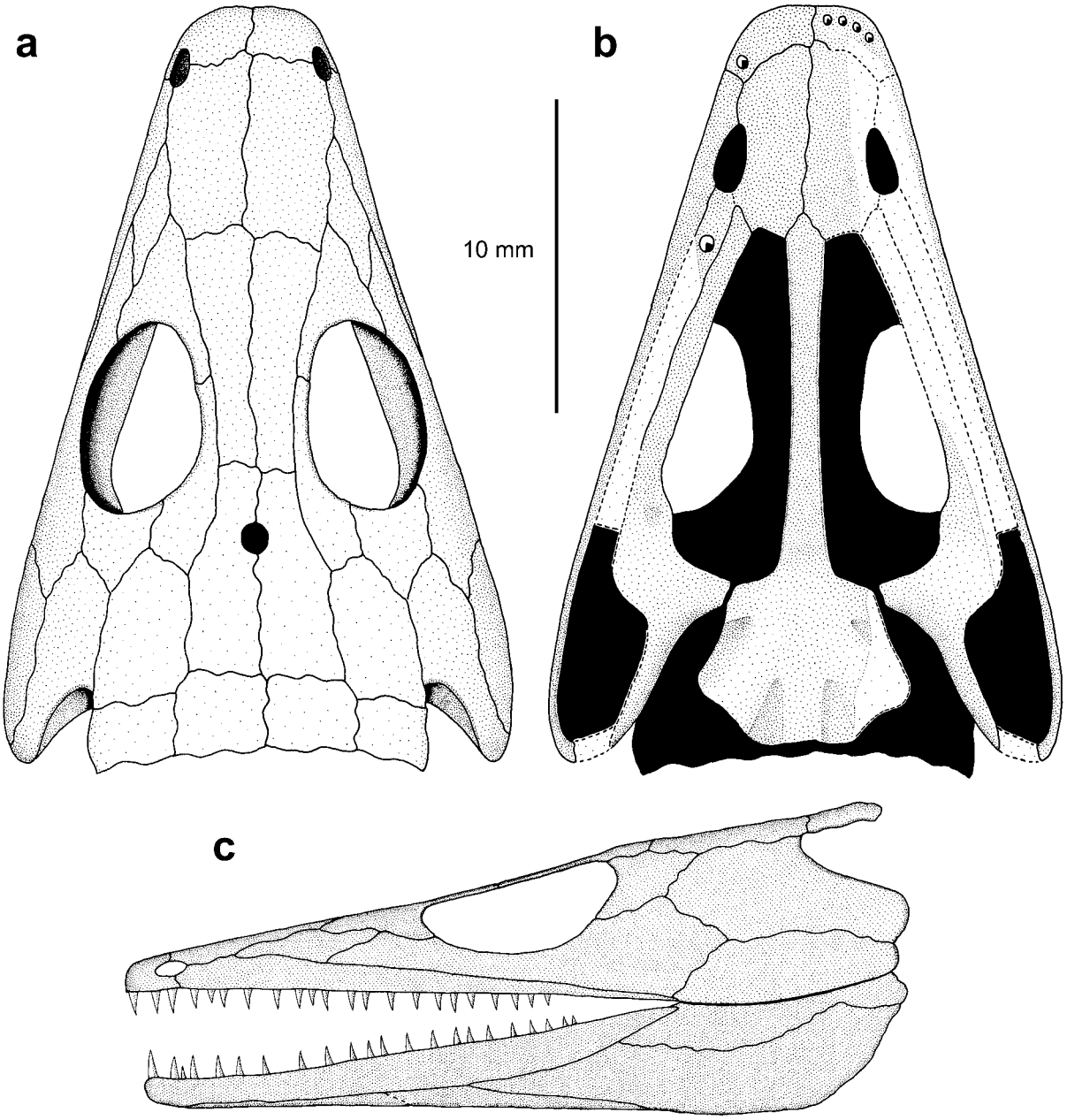

Figure 2 *Archegosaurus decheni*. Reconstruction of a small larval skull (sl circa 25 mm) based on a wax model, mainly after SMF A 71 and GMBS P/497: (a) dermal skull roof in dorsal view; (b) palate, the parasphenoid is supplemented after MB.Am.222; (c) lateral view of the skull, mandible reconstructed after MB.Am.134.

4.2. The bones of the dermal skull roof

Figures 6–14 show different skulls of *A. decheni*. The dermal skull roof (except for the septomaxilla, see below) is already well ossified in the smallest known individual with a skull length of 18 mm. As in osteolepiform fishes (Cote *et al.* 2002) and most temnospondyls (Boy & Sues 2000), the neurocranium starts to ossify distinctly later than the dermal skull bones (see section 8).

The premaxillae are paired massive bones which form the anteriormost part of the snout. Their median suture accounts for approximately 10–15% of preorbital length in the smallest specimens, whereas it increases to more than 20% in the largest skulls. The ossification centre is slightly elevated, forming the eminentia praemaxillaris (Fig. 14b). A premaxillary foramen (foramen praemaxillare) as reported by Gubin (1997) cannot be found in the investigated specimens. An alary process (Fig. 13) is present medial to the external naris in some specimens, whereas it is missing in others (polymorphism).

The maxilla is connected to the premaxilla lateral to the naris by a short suture. It attains its maximum depth at about the level of the anterior tip of the lacrimal. Its depth decreases constantly from this point posteriorly until it contacts the quadratojugal by a very narrow suture (Figs 2, 3c). During growth, the maxilla exhibits distinct positive allometry in length. In dorsal view, its lateral margin is straight in the smallest larvae. In further ontogeny, it becomes increasingly concave laterally.

The septomaxilla (Fig. 11) is a small, rounded triangular bone which is found in skulls beyond 50 mm length (e.g., MB.Am.193, MB.Am.227, MB.Am.138, MB.Am.117). In most specimens it is poorly preserved or is absent. The septomaxilla borders the external naris posteriorly and possesses a concave anterior margin. It sutures with the nasal and maxillary bones. The exposed part of the septomaxilla exhibits dermal sculpture like the adjacent bones of the dermal skull roof. It reaches further posteriorly on the ventral side of the

https://doi.org/10.1017/S0263593300001279 Published online by Cambridge University Press

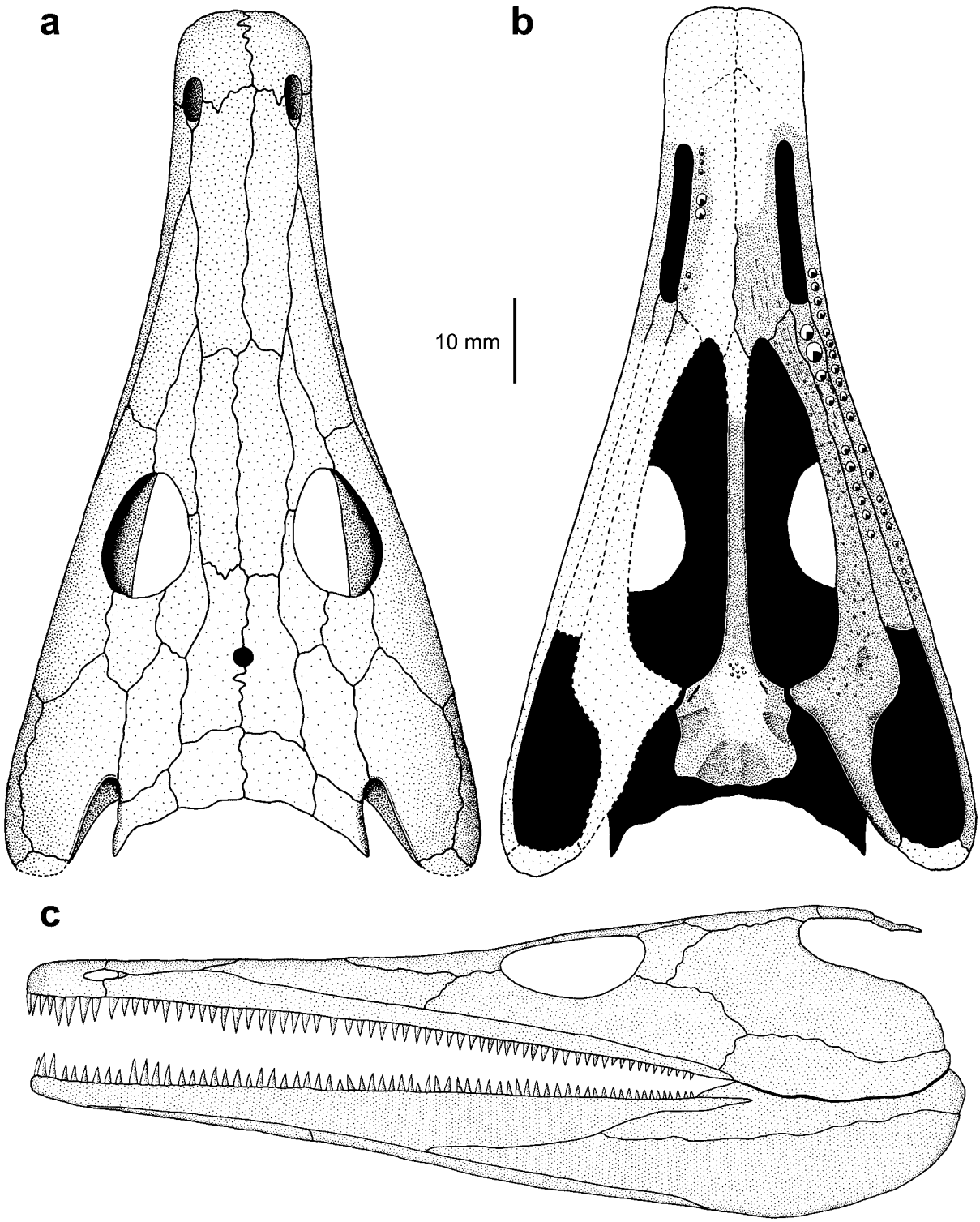

Figure 3 *Archegosaurus decheni*. Reconstruction of a larval skull (sl circa 90 mm): (a) dermal skull roof in dorsal view, based mainly on MB.Am.317 and 121; (b) palate, based on MB.Am.121, 236, 194, and 317; (c) lateral view of the skull, based on IGS U II 1/2.

dermal skull roof than on the dorsal side, as is indicated in MB.Am.193. This morphology is also known in *Eryops* (Panchen 1967). The septomaxilla is broken off the dermal skull roof in MB.Am.227 and is somewhat displaced in MB.Am.117. This is also the case in several other temnospondyls (Schoch 2001) and may indicate a weak connection to the adjacent bones. A small portion of roughened bone is visible ventral to the posterior margin of the naris in MB.Am.138. This structure represents a ventral process of the septomaxilla.

The lacrimal possesses a rhomboidal shape in small larvae. It exhibits distinct proportional elongation and narrowing during size increase of the skull. It constitutes almost 60% of the preorbital length in the largest skulls. The lacrimal is excluded from the orbital margin by a prefrontal–jugal contact, and there is no contact between lacrimal and naris or septomaxilla because of a broad suture between the nasal and the maxilla. As also remarked by Boy & Sues (2000), no nasolacrimal duct (ductus nasolacrimalis) can be determined in any size stage. A lacrimal of comparable proportional length in

https://doi.org/10.1017/S0263593300001279 Published online by Cambridge University Press

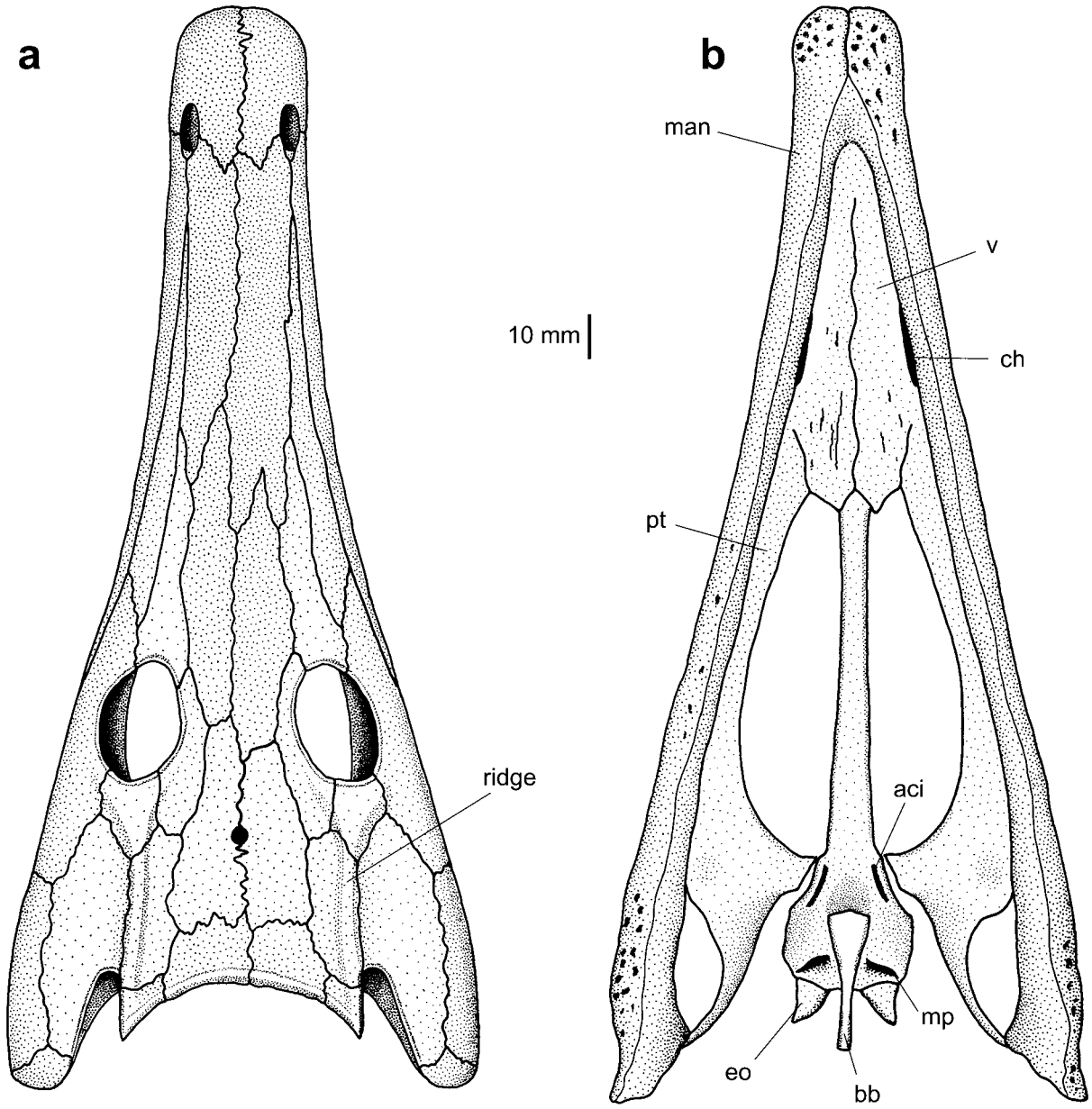

Figure 4 *Archegosaurus decheni*. Reconstruction of an early adult skull (sl circa 220 mm): (a) dermal skull roof in dorsal view, outline of skull reconstructed after MB.Am.953, the cranial sutures are based on MB.Am.117; (b) palate with mandible, basibranchial, and exoccipital, based on MB.Am.953.

adult skulls is only present in the archegosaurid *Collidosuchus* (Gubin 1986).

The nasal is an elongated rectangular bone that occupies most of the snout area. It elongates proportionally with increasing skull length. The ratio of length to width of single nasal bones is approximately 2:1 in small individuals, and 7:1 in the largest ones. The nasal reaches its maximum width anterior to the tip of the lacrimal. As in most other rostrum-bearing stereospondylomorphs, the nasal contributes greatly to preorbital length. Exceptions are *Collidosuchus*, in which it is distinctly shorter than the frontal (Gubin 1986), and many lonchorhynchine trematosaurs in which the premaxillae are the most elongate bones (Schoch & Milner 2000).

The frontal is an elongate rectangular bone whose length increases only slightly during growth relative to its width. It reaches its maximum width in its centre, anterior to the orbits. The maximum width of the frontals is slightly narrower than that of the nasals in most skulls. In small individuals, the frontal is longer than the nasal. These two bones have approximately the same length in skulls beyond 80 mm in length, and the nasal is longer than the frontal in most of the largest skulls.

The prefrontal is a narrow triangular bone that undergoes considerable proportional elongation during size increase of the skull. It tapers anteriorly to terminate near the anterior border of the frontals. The postfrontal forms the main part of the median border of the orbit. A narrow anterior process of this bone sutures with the prefrontal anteromedial to the orbit and excludes the frontal from the orbital margin. The postorbital has a rhombic shape and is proportionally short as compared to plesiomorphic stereospondylomorphs such as *Capetus* (Sequeira & Milner 1993) and *Sclerocephalus* (Boy 1988).

A characteristic element in the skull roof of *A. decheni* is the jugal. The part lateral to the orbit is distinctly narrower than in plesiomorphic stereospondylomorphs like *Sclerocephalus* and *Cheliderpeton* (Boy 1993b). The jugal width lateral to the middle of the orbit is smaller than half the orbital width in all size stages of *A. decheni*; in the smallest known skulls it is

https://doi.org/10.1017/S0263593300001279 Published online by Cambridge University Press

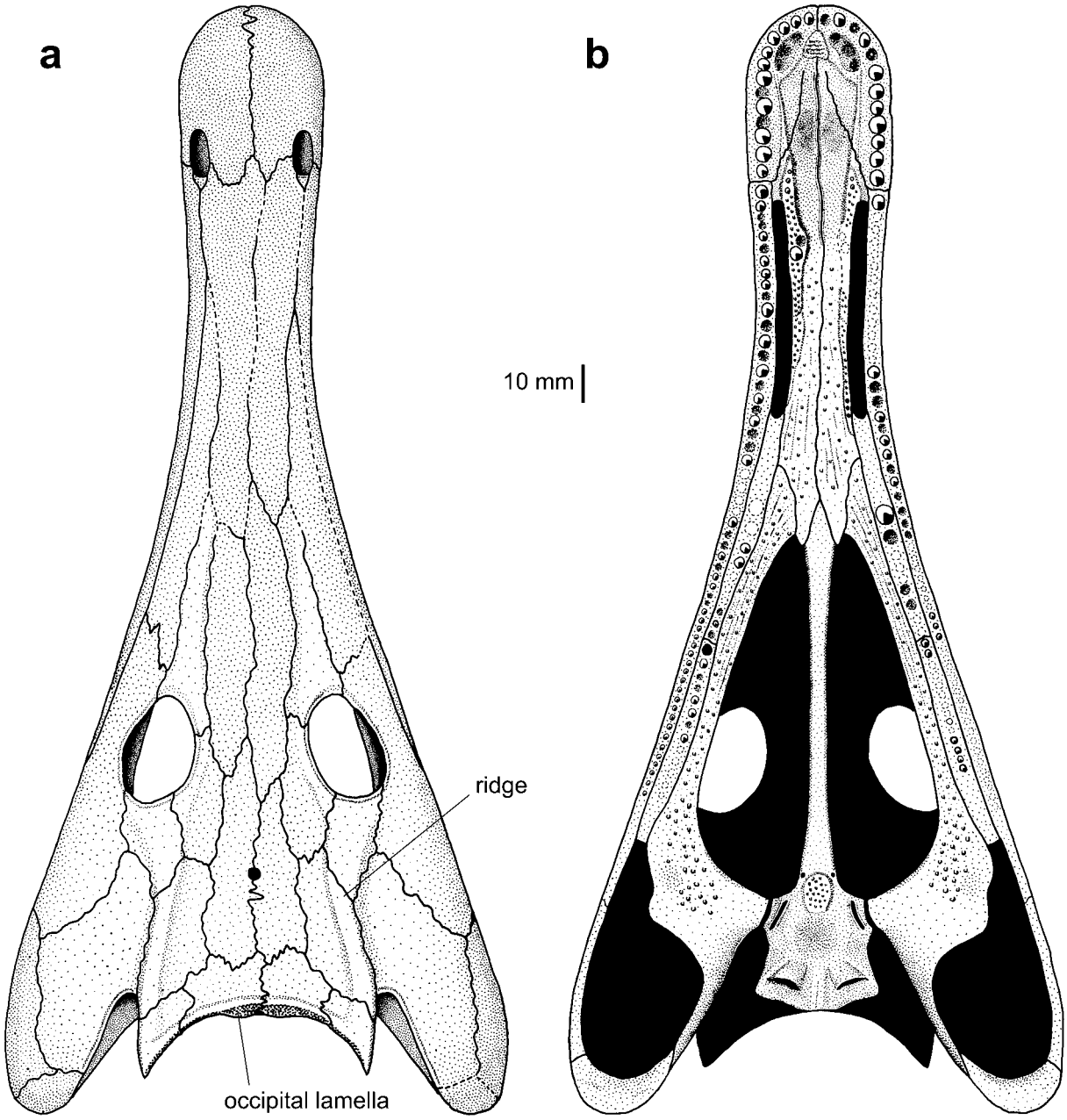

Figure 5 *Archegosaurus decheni*. Reconstruction of an adult skull (sl circa 280 mm): (a) dermal skull roof in dorsal view, based on MB.Am.116; (b) palate, based on MB.Am.116.

smaller than one third the orbital width. The jugal reaches its maximum depth in its postorbital part, in which it forms the anterior portion of the cheek region. According to Gubin (1997), the jugal sends out a ventral alary process on the palate posterior to the ectopterygoid. No specimen of the investigated size series shows this structure. Only the palate of MB.Am.121 might exhibit an insula jugalis. However, this cannot be determined with certainty because preservation in this part is poor.

The slender, rectangular supratemporal forms a small portion of the dorsomedial border of the squamosal embayment. It establishes a long suture with the squamosal. The parietal is of elongated rectangular shape. It narrows anteriorly nearby the pineal opening and forms a concave anterolateral border with the postfrontal. It is shorter than the frontal in all known size stages. In smaller specimens, it is distinctly broader than the frontal. It becomes proportionally narrower in larger skulls so that it attains approximately the same width as the frontal.

Postparietal and tabular bones possess a concave posterior margin, except in the smaller specimens (Fig. 2). During increase of skull length, the concavity is strengthened. A distinct occipital lamella (Fig. 5) is present on the posterior margin of the skull table for insertion of the epaxial musculature. The tabular forms a 'horn' that grows posteriorly with positive allometry. The lateral margin of the tabular is slightly convex. A tapering, narrow tabular extension is present which is directed posteroventrally (see section 4.6.3, Fig. 16).

The squamosal is of rhombic shape and forms the anterior and lateral margin of the squamosal embayment. The quadratojugal is a stout bone which narrows anteriorly and forms a very short suture with the posterior end of the maxilla. A paraquadrate opening (foramen paraquadratum) cannot be determined in the investigated skulls.

4.3. Sutures of the dermal skull roof

As in many temnospondyls, the sutures between the dermal skull roofing bones are more strongly interdigitated in large specimens than in small ones. In the smallest known specimens of *A. decheni*, the sutures are relatively straight. The interdigitation of longitudinal as well as of transverse sutures

https://doi.org/10.1017/S0263593300001279 Published online by Cambridge University Press

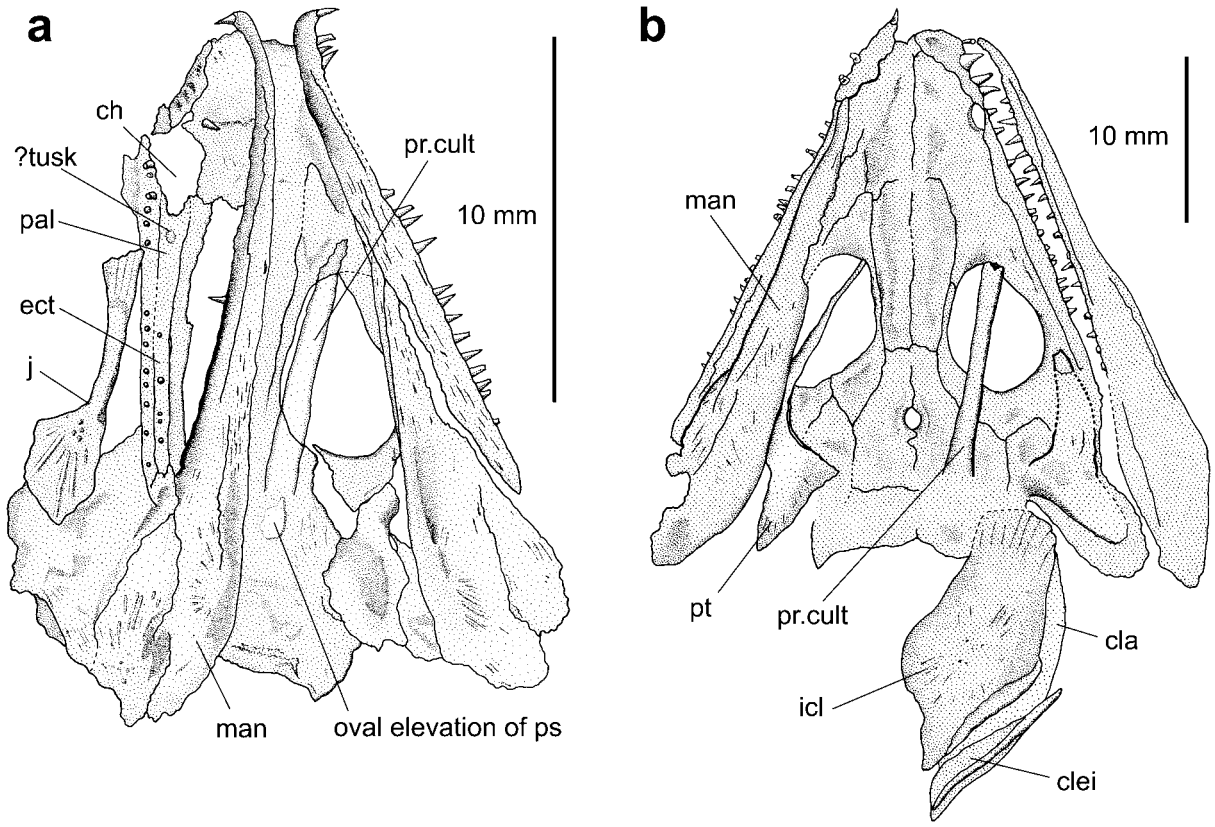

Figure 6 Larval skulls of *Archegosaurus decheni*: (a) MB.Am.134 (sl=18 mm); (b) BMNH-42755 (plaster cast, sl=31 mm).

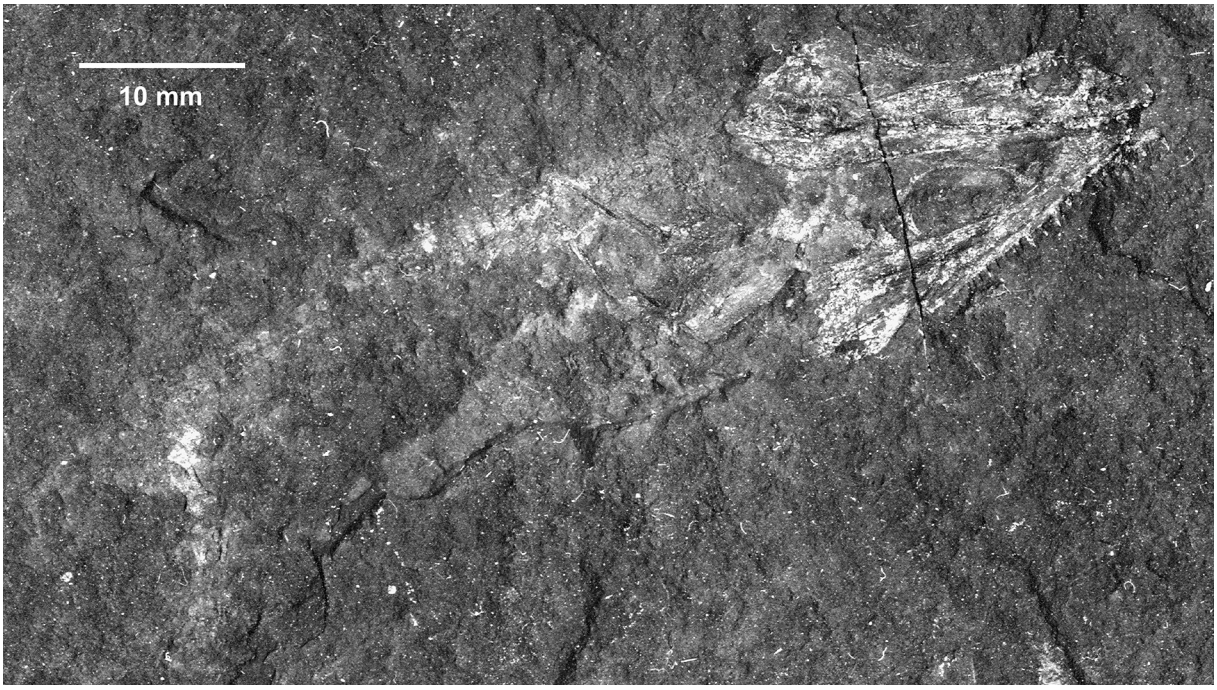

Figure 7 *Archegosaurus decheni*. MB.Am.134 (sl=18 mm), this complete skeleton is the smallest known specimen.

increases quickly during increase of skull length, especially in the postorbital skull region. The interparietal suture is strongly interdigitated with a distinct zigzag-suture immediately posterior to the pineal opening. This can be recognised especially in large skulls but is foreshadowed in the smaller ones. Frontals, nasals, and premaxillae show interdigitating median sutures, with the median suture between the premaxillae forming a distinct zigzag. In contrast, the maxillary–jugal, maxillary–lacrimal and lacrimal–prefrontal sutures are almost straight, even in the largest skulls. The transverse sutures of the bones of the median series (premaxilla, nasal, frontal, parietal, postparietal) may show individual variation. An example is MB.Am.117 (sl=207 mm), in which the suture between frontal and nasal is extremely interdigitated.

https://doi.org/10.1017/S0263593300001279 Published online by Cambridge University Press

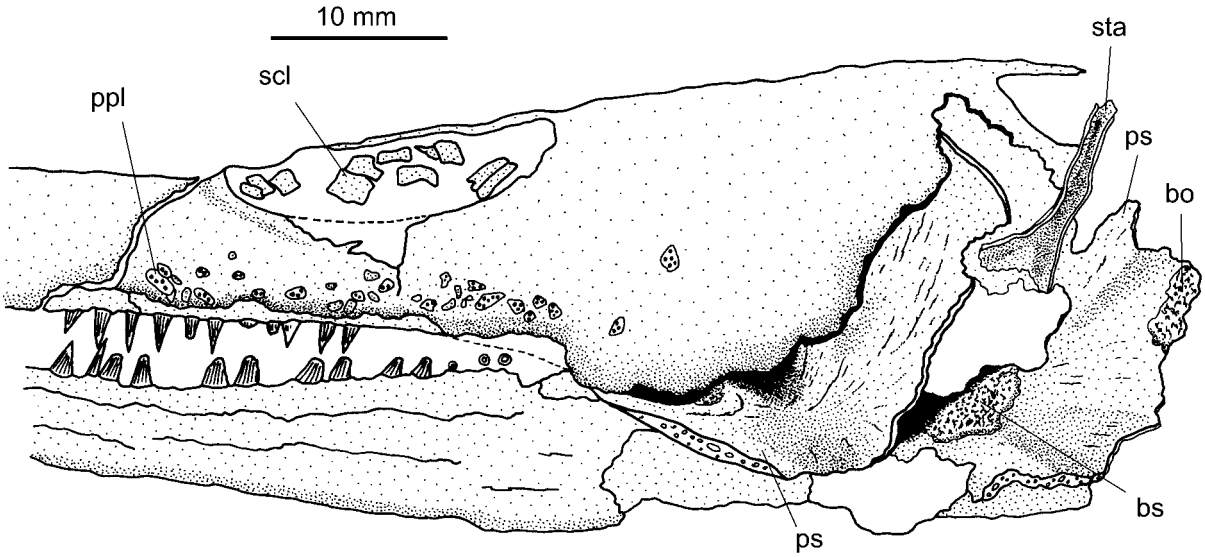

Figure 8 *Archegosaurus decheni*. Posterior region of skull in lateral view (sl circa 115 mm), showing details of palate, neurocranium, and stapes.

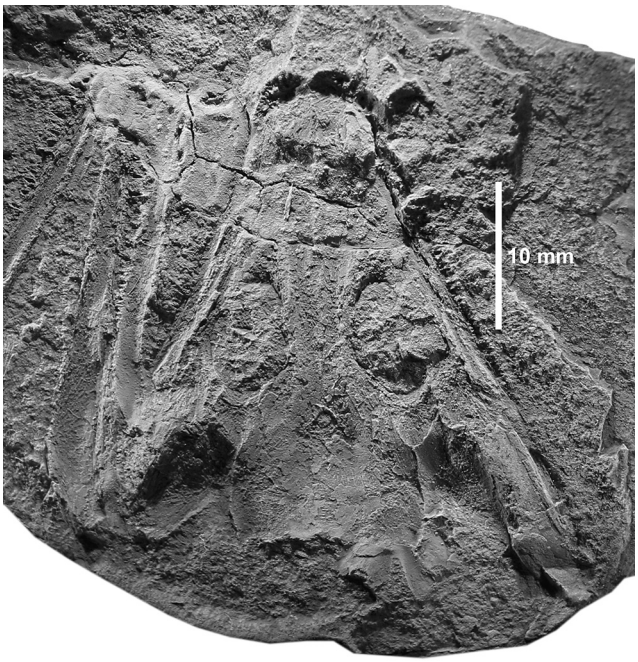

Figure 9 *Archegosaurus decheni*. MB.Am.220a (sl=32 mm), larval skull in ventral view.

4.4. Ontogenetic changes in dermal sculpture

In the smallest specimens, pits are located in the ossification centres of the dorsal sides of the dermal skull roofing bones. Fine grooves radiate from the centres through the otherwise smooth bone surface (e.g., MB.Am.134, sl=18 mm, Fig. 6a; MB.Am.222b, sl=30 mm, Fig. 12a). This type of sculpture is considered a larval characteristic in *Sclerocephalus haeuseri* (Boy 1988) and several other temnospondyls (Boy & Sues 2000).

At a skull length of around 50 mm, the radial grooves have become slightly deeper and broader, and the pits in the ossification centres have become larger on the preorbital skull. The sculpture, however, is still weak and mostly radially oriented. On the postorbital skull table, the sculpture is advanced compared to the preorbital part. Ridges form a polygonal sculpture on the entire tabular, on the postparietal at least in its centre (incomplete preservation), in the centre and posterior part of the supratemporal, and to a lesser degree in the centres of squamosal, postorbital, quadratojugal, and jugal bones. The largest parts of these bones, surrounding their centres, consist of radial furrows which are slightly deeper and broader than in smaller skulls (e.g., MB.Am.221b, sl=51 mm, Fig. 12b; MB.Am.179, sl=53 mm). This pattern of sculpture has been characterised as early metamorphic in many temnospondyls (Boy & Sues 2000).

In skulls of approximately 80 mm length, the sculpture is clearly more expressed (visible in MB.Am.227b, sl circa 84 mm, Fig. 13a). The ridges are proportionally stronger than in smaller skulls and form broader, deeper and more regular polygons and furrows. The centres of the bones consisting of polygonal sculpture are enlarged. On the nasal, the polygonal sculpture is still restricted to a small area in its centre. Boy & Sues (2000) described this stage of sculpture in temnospondyls as late metamorphic. In skulls beyond 100 mm in length, the regions with polygonal sculpture are expanded and the polygons are formed more regularly (e.g., MB.Am.235, sl circa 125 mm, Fig. 13b), a pattern which was characterised as adult in temnospondyls (Boy & Sues 2000).

During further growth, polygonal sculpture develops slowly on the bones of the preorbital skull roof. For example, only a small area of polygonal sculpture is present on the nasal in MB.Am.138 (sl=144 mm). Regions of elongated furrows and ridges are present anterior and posterior to this area. Such ridges and furrows can also be seen on the anterior part of the prefrontal and the anterior and posterior region of the lacrimal.

In skulls beyond 200 mm length (e.g., MB.Am.117, sl=207 mm, Fig. 14a; MB.Am.116, sl=279 mm, Fig. 14b), the regions of polygonal sculpture are greatly expanded even on the preorbital skull roof bones. Elongated furrows and ridges are restricted to small areas, being most conspicuous on the anterior part of the quadratojugal, the posterior part of the jugal, and the posterolateral part of the squamosal. In the slightly depressed region anteromedial to the orbits, the sculpture is less intensive.

4.5. Lateral line sulci of the dermal skull roof

The lateral line system in *A. decheni* does not consist of continuous furrows, but of single oval or long-oval depressions on the dorsal side of the dermal skull roof and the labial side of the mandible. The course of the lateral line system of the skull roof is shown in Figures 12–15.

https://doi.org/10.1017/S0263593300001279 Published online by Cambridge University Press

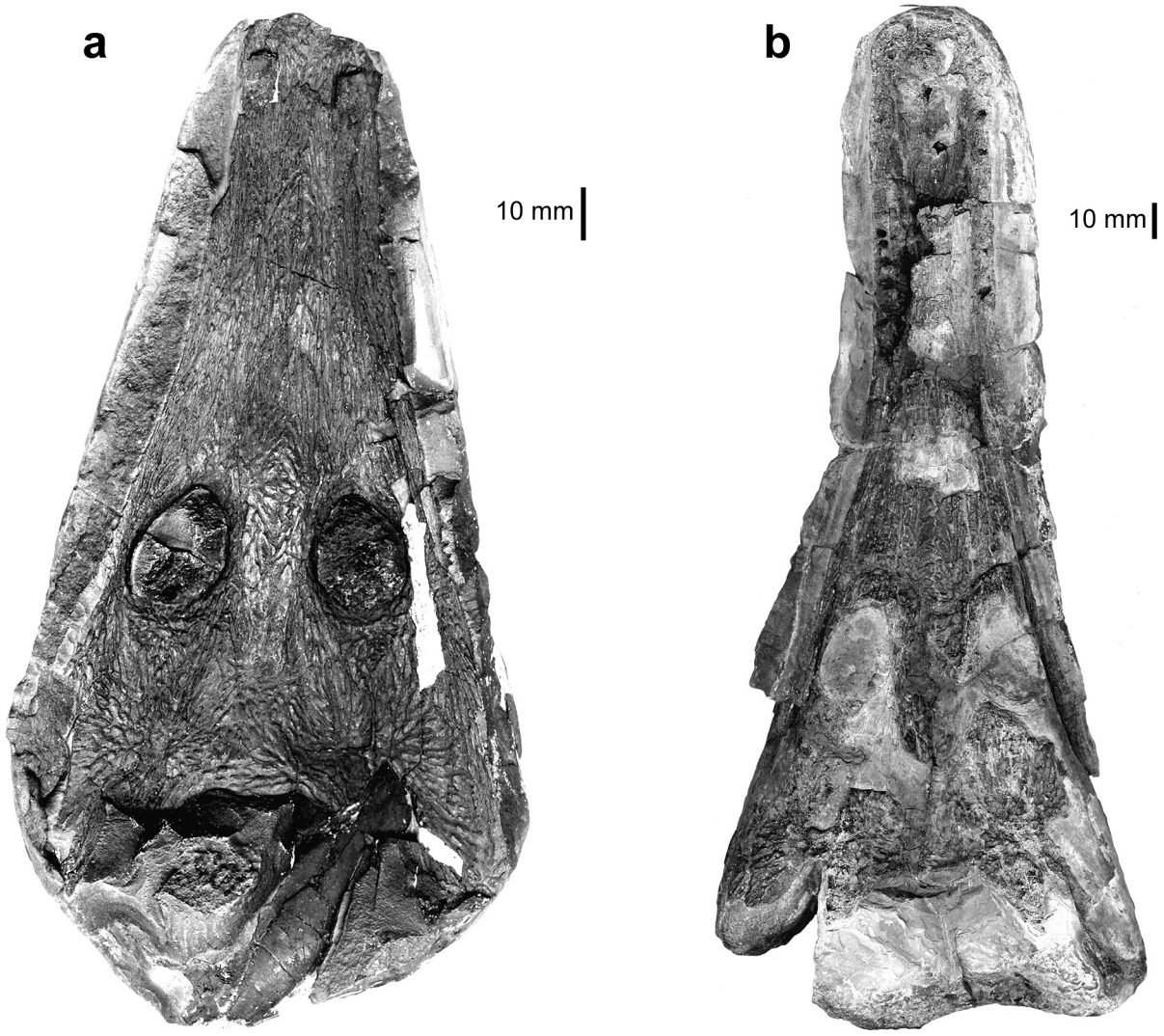

Figure 10 Skulls of *Archegosaurus decheni*: (a) MB.Am.138b (sl=144 mm), late larval skull, natural mould of the dermal skull roof; (b) MB.Am.139a (sl=242 mm), adult skull in dorsal view.

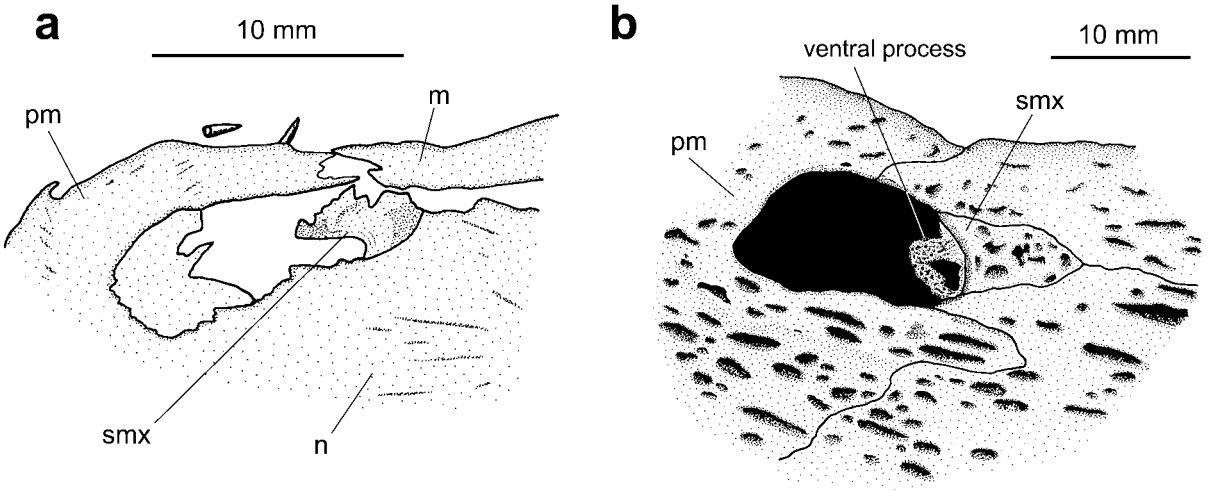

Figure 11 *Archegosaurus decheni*. Septomaxilla, anterior is left: (a) MB.Am.193 (sl=54 mm), in ventral view; (b) MB.Am.138 (sl=144 mm), latex cast in dorsal view, the ventral process of the septomaxilla is visible in the narial opening.

4.5.1. Development. MB.Am.222b (sl=30 mm, Fig. 12a) is the smallest specimen in which lateral line sulci are visible, with a weak furrow detectable on the postorbital. In general, the sulci become deeper and broader in larger skulls. They consist of narrower but longer grooves in smaller individuals as compared to large skulls. The most distinct sulci are located in the ossification centre of the frontal, on the postfrontal (supraorbital sulcus), and the postorbital and the posterior jugal (infraorbital sulcus), in medium-sized and large skulls.

https://doi.org/10.1017/S0263593300001279 Published online by Cambridge University Press

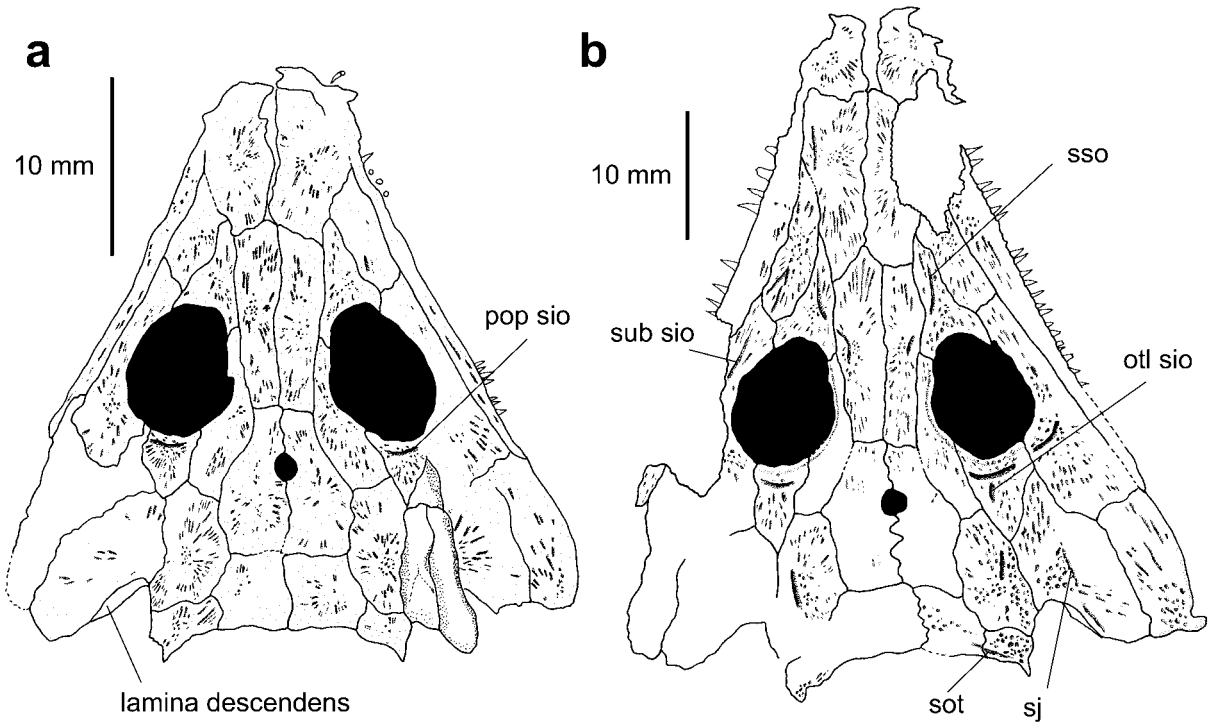

Figure 12 *Archegosaurus decheni*. Development of dermal sculpture. Skulls in dorsal view: (a) MB.Am.222 (sl = 30 mm); (b) MB.Am.221 (sl = 51 mm).

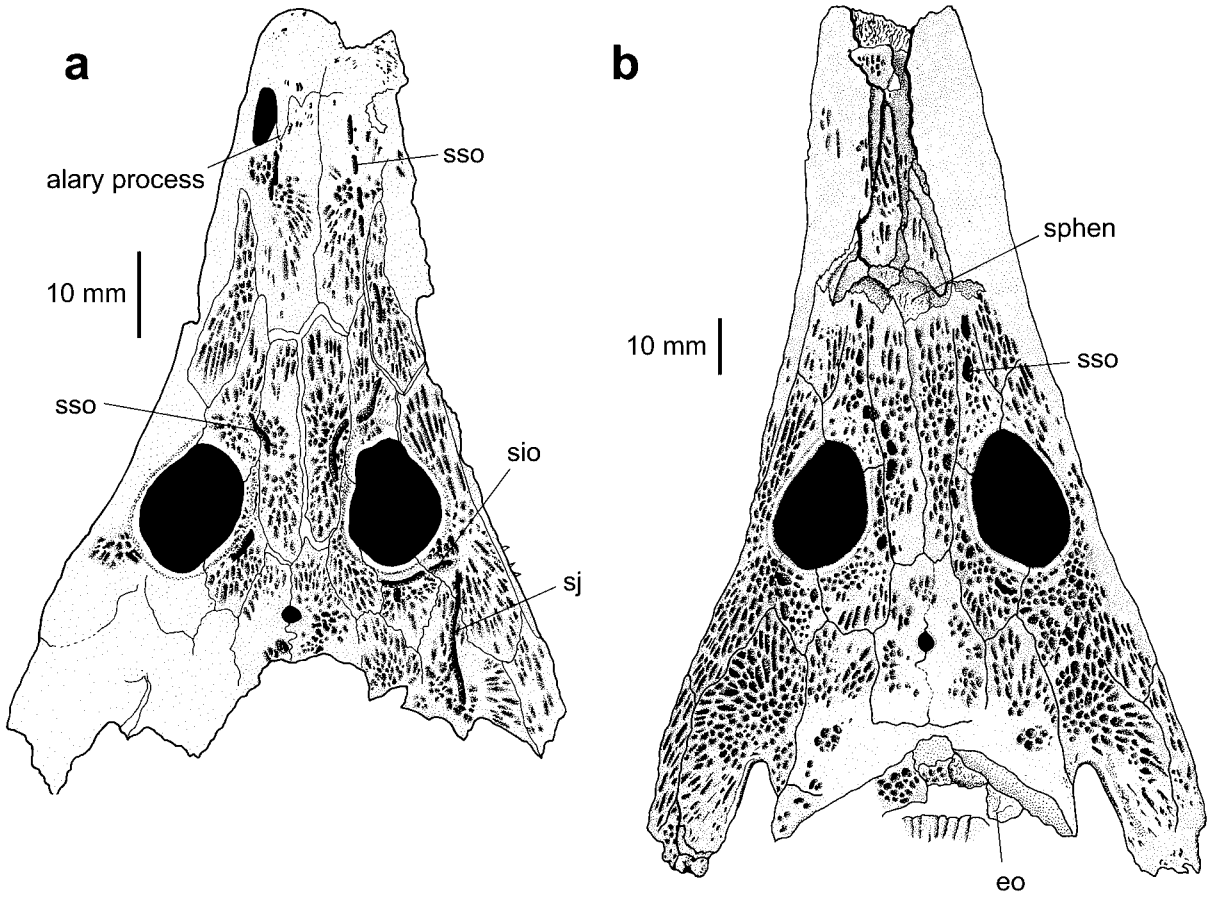

Figure 13 *Archegosaurus decheni*. Development of dermal sculpture. Skulls in dorsal view: (a) MB.Am.227 (sl circa 84 mm); (b) MB.Am.235 (sl circa 125 mm).

4.5.2. Variation. The course of the lateral line sulci exhibits individual variation in *A. decheni*. The supraorbital sulcus runs on the median part of the lacrimal instead of the anterior part of the prefrontal on the right side of MB.Am.227

https://doi.org/10.1017/S0263593300001279 Published online by Cambridge University Press

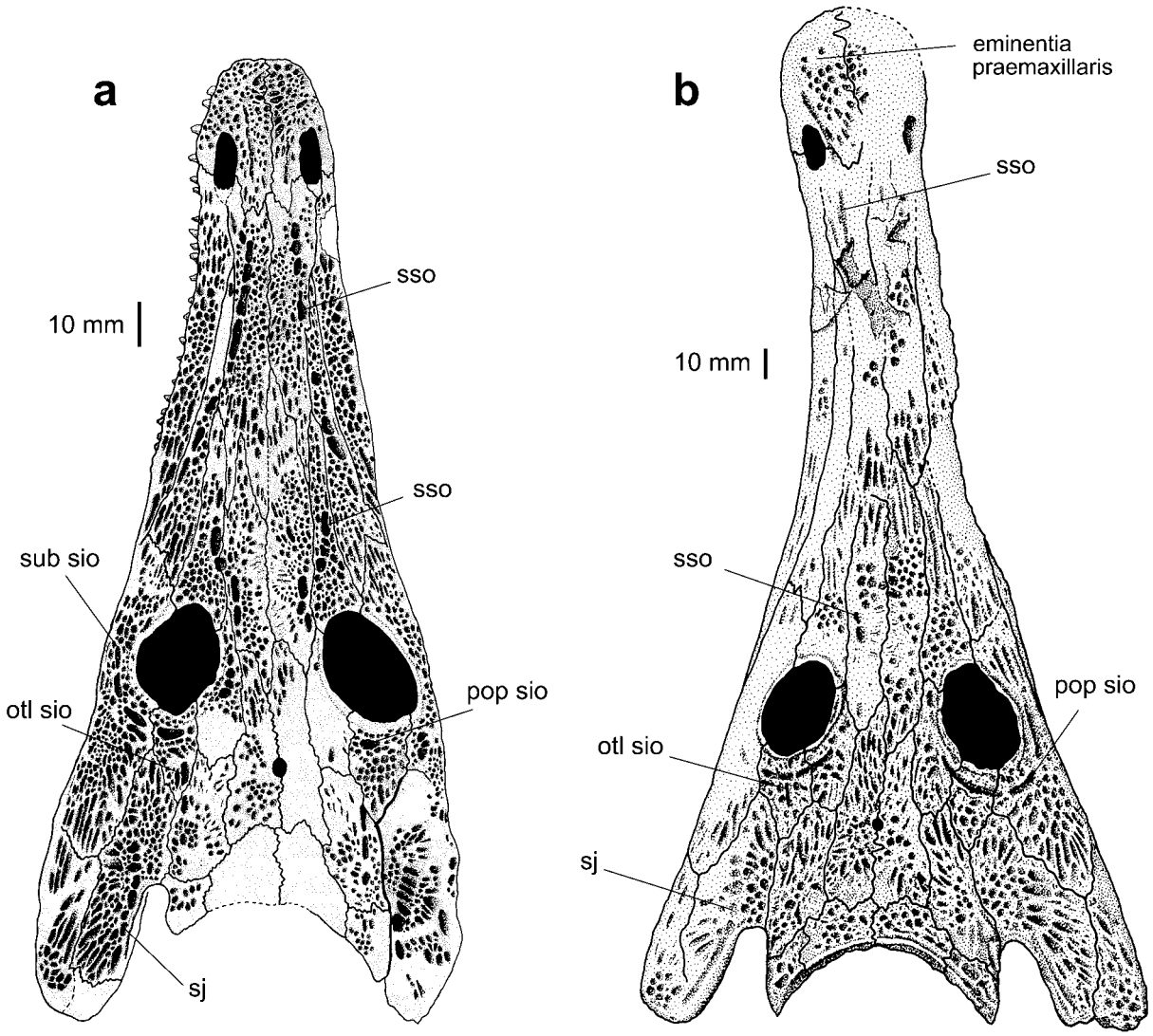

Figure 14 *Archegosaurus decheni*. Development of dermal sculpture. Skulls in dorsal view: (a) MB.Am.117 (sl=207 mm); (b) MB.Am.116 (sl=279 mm, neotype).

(sl circa 84 mm, Fig. 13a). This resembles the situation in many stereospondyls, in which the supraorbital sulcus also transverses a part of the lacrimal, e.g. *Rhinesuchus* (Watson 1962), *Benthosuchus*, *Metoposaurus*, *Cyclotosaurus*, *Trematosaurus* (Bystrow 1935), and *Mastodonsaurus* (Schoch 1999).

MB.Am.221 (sl=51 mm, Fig. 12b) exhibits a peculiar structure on the left lacrimal. Posterior to its ossification centre, the sulcus branches off in two parts. It is implausible that this structure represents the nasolacrimal duct because its posterior ends are not directed towards the orbit, but distinctly lateral to it. It represents the anterior part of the infraorbital sulcus that shows an aberrant branching. Similar individual branching of lateral lines is also known in trematosaurids (R. R. Schoch, pers. comm. 2002).

In MB.Am.117, a second depression is visible on the squamosal lateral to the anterior part of the jugal sulcus. It is less deep but broader than the regular lateral lines and is crossed by radial ridges and grooves of the dermal sculpture. It is not clear if this structure represents a part of the lateral line system.

4.6. The ventral side of the dermal skull roof

4.6.1. Orbitotemporal crest and capsular crest. The orbital crest (crista orbitotemporalis) and the capsular crest (crista capsularis) are well developed in all skulls independent of their size (Fig. 16). Pfannenstiel (1932) was the first to mention the orbitotemporal crest (*Parietalleiste*, Taenia marginalis) in *A. decheni* and illustrated the part on the ventral side of the parietal, while Gubin (1997) described the course of the orbitotemporal and capsular crest. In contrast to Gubin's description, the orbitotemporal crest starts anteriorly on the posterior part of the lacrimal and continues on the prefrontal in the investigated specimens (MB.Am.180, MB.Am.171, MB.Am.986, GMBS P/828). As described by Gubin, it subsequently runs on the postfrontal and curves medially on the parietal towards the pineal opening, which it encircles. In this region, the crest is most pronounced. It courses towards the postparietal posterior to the pineal opening, bends sharply in an anterolateral direction and merges with the capsular crest. In contrast to Gubin's description, this curvature is actually located not anterior, but posterior to the suture between parietal and postparietal (MB.Am.233, MB.Am.117a, MB.Am.156, MB.Am.986, GMBS P/494a). Then the capsular crest runs via the supratemporal to the fossa paroccipitalis of the tabular (see section 4.6.3). Posterior to the pineal opening, the crest becomes flatter and broader.

As interpreted by Wilson (1941) for the stereospondyl *Buettneria*, the described crests reflect the outline of the braincase. The orbitotemporal crest probably served for attachment of the dorsolateral parts of the sphenethmoid and the sella turcica region. This is indicated by a fragment of the posterior part of the sphenethmoid bone that is attached to the medial margin of this crest in GMBS P/494a. However, the

https://doi.org/10.1017/S0263593300001279 Published online by Cambridge University Press

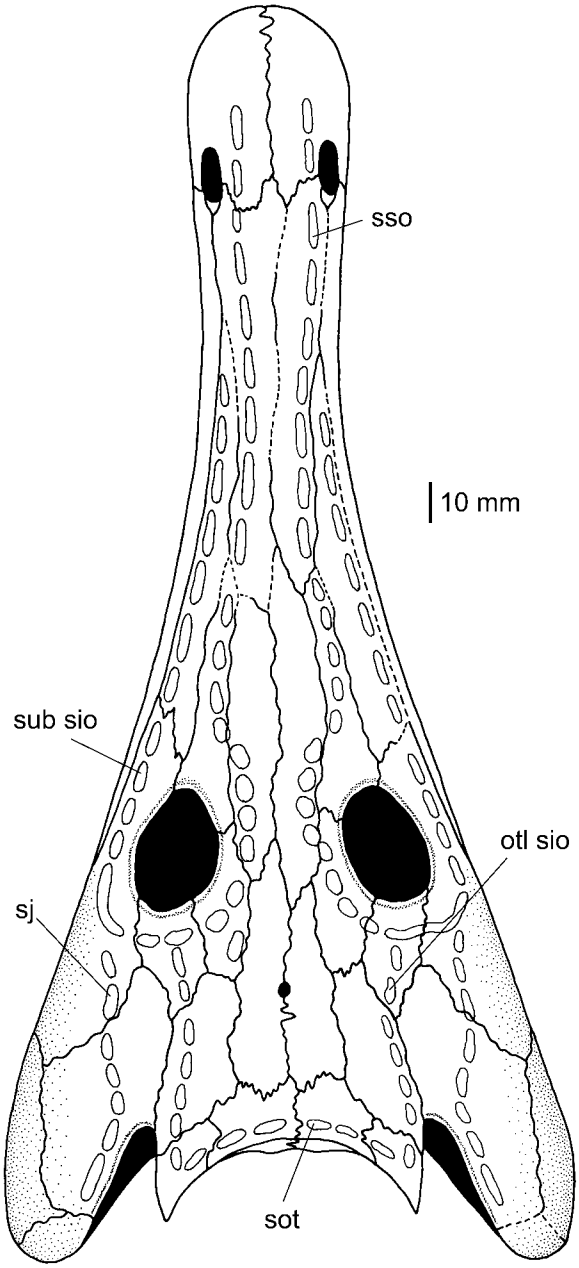

Figure 15 *Archegosaurus decheni*. Reconstruction of the lateral line sulci of the dermal skull roof. Based on several specimens.

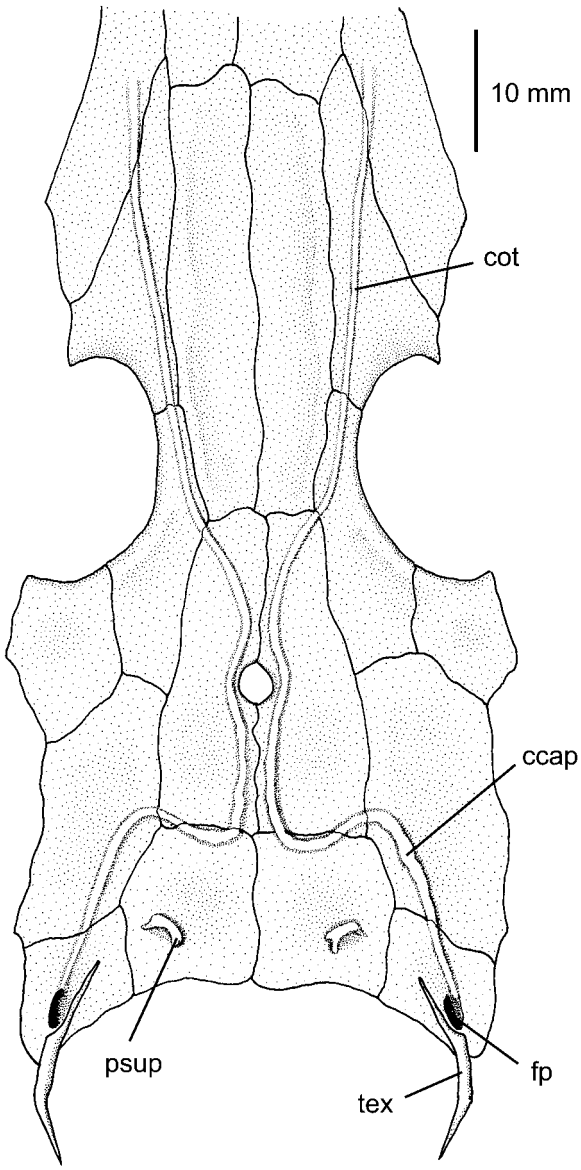

Figure 16 *Archegosaurus decheni*. Reconstruction of the ventral side of the dermal skull roof of a juvenile specimen showing the orbitotempral and paroccipital crests, the tabular extension, the supraoccipital process, and the paroccipital fossae. The paroccipital process of the tabular is ossified only in adult specimens. Based on several specimens.

distance between the left and right crest in the region between and anterior to the orbits is larger than the width of the sphenethmoid bone as indicated in MB.Am.116. This suggests a lateral continuation of the sphenethmoid in cartilage. Judging by the outline of the capsular crest, it probably served for attachment of the otic ossification and its cartilaginous extension.

4.6.2. Narial region. A broad and shallow depression medial and posterior to the narial opening extends parallel to the longitudinal axis of the skull (MB.Am.150, MB.Am.174, GPIT/Am/20). It begins shortly anterior to the narial opening and extends medially, so that the median half of the naris lies in this depression. The depression continues posterior to the narial opening in the region of the nasal-maxillary boundary and the anterior tip of the lacrimal; then it narrows, flattens and finally disappears. Depressions are also visible on the ventral surface of the skull roof in *Tersomius* posteromedial to the naris on the nasal, lacrimal and prefrontal (Carroll 1964); in *Eryops* posterior to the naris on the nasal, lacrimal and maxilla (Sawin 1941); as well as in *Buettneria perfecta* posterior to the naris on the nasals (Wilson 1941). These round depressions are interpreted as locations of the cartilaginous nasal capsule. According to its shape in *A. decheni*, the capsule was rather small and proportionally elongate and narrow.

4.6.3. Squamosal, postparietal, and tabular. In small skulls, the descending lamina (lamina descendens) of the squamosal is visible along the lateral margin of the squamosal embayment (Fig. 12). This lamina is more conspicuous in larger skulls. It was connected with the ascending lamina (lamina ascendens) of the pterygoid in the living animal.

The ventrally directed supraoccipital process of the postparietal is visible for the first time in a specimen of 67 mm skull length (MB.Am.204). In larger specimens (MB.Am.228; MB.Am.233; MB.Am.138a; MB.Am.117), it is more conspicuous and resembles the Greek letter π (Fig. 16). It sutured with the vertical column of the exoccipital (Fig. 28).

No ossified paroccipital process is present on the ventral side of the tabular in small and middle-sized skulls. Instead, there is a quite distinct depression (fossa paroccipitalis, Fig. 16), which extends almost parallel to the lateral margin of the tabular (MB.Am.204, sl=67 mm; MB.Am.233, sl=

https://doi.org/10.1017/S0263593300001279 Published online by Cambridge University Press

127 mm), comparable to the morphology in *Dvinosaurus* (Shishkin 1973, p. 34, fig. 6). The paroccipital process of the exoccipital was housed in this fossa. The capsular crest runs lateral to the fossa paroccipitalis. An ossified paroccipital process formed by the tabular is present in skulls beyond about 200 mm length (Fig. 28).

The tabular extension is visible in MB.Am.138a (sl=145 mm). It starts on the ventral side of the tabular horn as a flattened crest that courses medial to the fossa paroccipitalis to the tip of the tabular horn (Fig. 16). Thereby the depth of the crest increases rapidly. It has reached its maximum depth and width below the tip of the tabular horn. It continues posterior to the tabular horn in a posteroventral direction. Finally, it becomes narrower again and bends sharply in a posteromedial direction. GMBS P/403 (sl=41 mm) is the smallest specimen in which a tabular extension is visible.

5. The palate

The following description of the palate is mostly based on large specimens because they show the most details. It is supplemented by the description of middle-sized and small specimens to document ontogenetic alteration.

5.1. Palatal openings

The length of the interpterygoid vacuities measures slightly more than one third of the skull length in the largest skulls, approximately 40% in medium-sized, and almost half the skull length in small specimens. These differences result from the proportional elongation of the snout during size increase of the skull. The interpterygoid vacuities are framed laterally and posterolaterally by the pterygoids, anteriorly by the vomers and posteriorly and medially by the parasphenoid.

The choanae are extremely elongated and account for more than 20% of the skull length in adults (Fig. 5b). Their lateral margin is concave, corresponding to the margin of the snout. They are more than 4 times longer than the external nares and lie behind the posterior narial margins. The choanae are framed anteriorly and medially by the vomer, posteriorly by the palatine and laterally by the maxilla. In medium-sized specimens (skull lengths 80–150 mm), the choana is already elongated, though it is proportionally shorter than in large skulls (Fig. 18b). In GMBS P/497 (sl=24 mm; Fig. 20b), the choanal margin is poorly preserved; nevertheless, its length can be estimated as approximately 10% of the skull length.

The subtemporal fenestrae are bordered medially by the pterygoid, posteriorly by the quadrate and laterally by the quadratojugal. There is no unambiguous evidence of an insula jugalis sensu Gubin (1997) that excludes the ectopterygoid from the subtemporal fenestra.

5.2. The bones of the palate

5.2.1. Premaxilla. A shelf of the premaxilla (lamina palatina) forms the anterior part of the palate (Fig. 17). A reniform to oval depression, the anterior palatal fossa, is situated anterolaterally on each premaxilla. Its longitudinal axis is directed anteromedially. The fossa itself possesses three roundish depressions; a larger one is situated between two smaller ones in MB.Am.116. Probably they admitted the teeth of the symphysis of the lower jaw when the mouth was closed. A nearly triangular elevation situated medial to the fossae has a roughened surface with transverse striae. This structure, situated on the shelf of the premaxilla, is the 'tuberculum subrostrale medium' (Gubin 1986) or 'premaxillary tubercle' (Holmes 2000). Gubin (1986, p. 73), who described a very similar structure in the archegosaurid *Collidosuchus*, presumed that it 'served as a shock absorber in closing of the mouth'. The premaxilla sutures posteriorly with the maxilla and vomer. The vomers extend far anterior between the premaxillae. The premaxilla is excluded from the choanal margin by maxillary-vomer contact anterior to the choana.

5.2.2. Vomer. The vomers grow with distinct positive allometry. In adults, they are distinctly elongate and narrow, measuring almost half the length of the skull. In medium-sized skulls (80–150 mm skull length), the length of the vomers accounts for less than 40% of the skull length, corresponding to the lesser elongation of the snout. They measure only 25% of the skull length in the smallest known larvae. An elevated strip of bone bearing teeth and denticles begins anteromedial to the choana and extends posteriorly parallel to the medial choanal margin at least in large and medium-sized skulls (Fig. 17, 18b). On its widest part, the elevation bears a large tusk with appropriate, anteromedially located replacement pit. Apart from these teeth, the elevation is covered densely by denticles.

The vomers are bordered anterolaterally by the premaxilla and have a short posterolateral contact with the maxilla. They form the anterior and medial border of the choana. The vomer borders the palatine posterior to the choana and forms a posterolateral connection with the pterygoid. Each vomer forms a posteriorly directed, short, pointed process (parasphenoidal process) on its posterior margin. The anterior part of the cultriform process extends between these processes. Posterior to the vomerine tusks, the surface of the vomer is covered by scattered denticles.

The dorsal surface of the vomer (Fig. 18a) is smooth, and the torus parachoanalis is well developed. This torus is a dorsal bulge that borders the choana medially and probably strengthens the region of the vomerine tusks. The parasphenoidal sulcus is located in the dorsal midline of the vomers and receives the anterior portion of the cultriform process (Fig. 18a).

5.2.3. Maxilla. The maxilla contacts the premaxilla a short distance anterior to the choana. Its maximum width is lateral to the posterior part of the choana in large skulls. It narrows posteriorly before it borders with the quadratojugal by a posteromedially directed suture. The maxilla forms the lateral border of the choana. Posterior to the choana, it borders medially with palatine and ectopterygoid.

5.2.4. Palatine. The palatine is slender and forms the posterior choanal margin. In large skulls, its anterior part is toothless, the anteriormost tooth being a tusk with adjacent tooth pit. It is the largest tooth in the skull. In contrast, the large palatine tusk is situated proportionally much closer to the posterior margin of the choana in small and medium-sized skulls (Fig. 18b). The palatine is broadened in the region of tusk and pit. In rare cases, two tusks can be present simultaneously on the palatine. There is space for 6–8 teeth posterior to the tusks. These teeth are slightly larger than the adjacent maxillary teeth in MB.Am.116. The exact number of palatine teeth in other specimens cannot be determined because of poor preservation. Apart from a questionable pit for the large palatine tusk in the anterior part, no teeth are preserved on the palatine in the smallest specimen (MB.Am.134, sl=18 mm, Fig. 6a). However, the tooth row on the ectopterygoid (see below) indicates that there was probably also a tooth row present on the palatine. The palatine borders the vomer medially for a short distance but is mostly bordered by the pterygoid (GMBS P/426, MB.Am.116). It sutures posteriorly with the ectopterygoid and laterally with the maxilla (Fig. 17a).

5.2.5. Ectopterygoid. The ectopterygoid is also a slender element and slightly shorter than the palatine. The anterior

https://doi.org/10.1017/S0263593300001279 Published online by Cambridge University Press

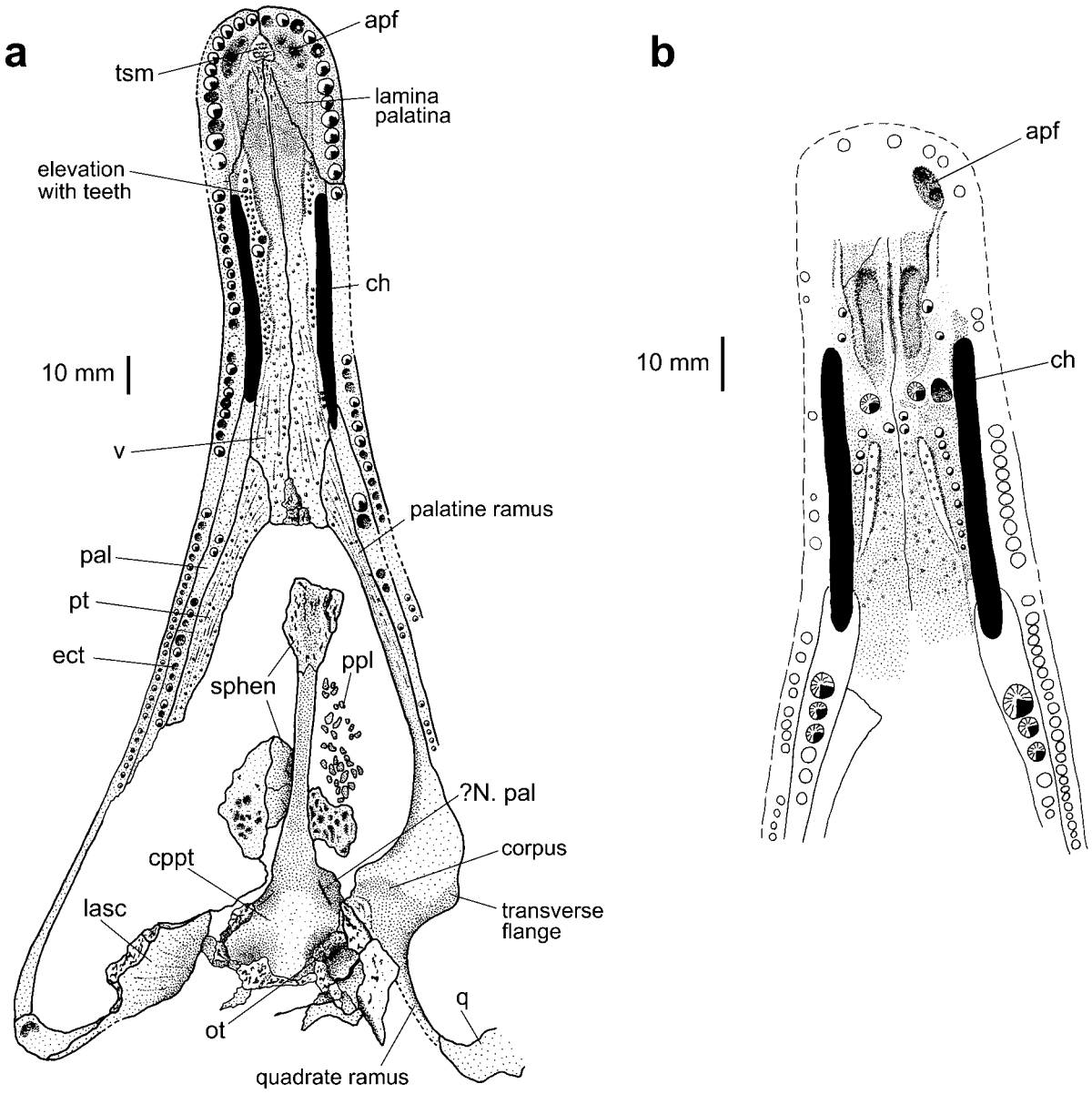

Figure 17 *Archegosaurus decheni*. Palates of large specimens: (a) Type A palate: MB.Am.116 (sl=279 mm, neotype), ventral surface of premaxilla, vomer, and palatine are preserved as negative impression, parasphenoid and pterygoid are preserved in dorsal view; (b) Type B palate: MB.Am.117 (sl=207 mm) in ventral view.

teeth of the ectopterygoid are slightly larger than the posterior ones on the palatine and the adjacent ones on the maxilla (Fig. 17a). The number of teeth cannot be unambiguously determined, but there is space for at least 14 in MB.Am.116. No tusks are present on the ectopterygoid. It sutures medially with the pterygoid and laterally with the maxilla. The ectopterygoid possesses a continuous row of teeth also in the smallest available specimen (MB.Am.134, sl=18 mm, Fig. 6a), although the number of teeth cannot be determined.

5.2.6. Pterygoid. The pterygoid can be divided into three discrete parts, the palatine ramus, the corpus, and the quadrate ramus (Fig. 17a). The palatine ramus is elongated and narrow compared to many other temnospondyls. At its anterior end, it broadens distinctly and is connected with the vomer. It is separated from the cultriform process by the parasphenoidal process of the vomer (see section 5.2.2). The palatine ramus is laterally connected with the palatine and ectopterygoid. A furrow for the anterior, unossified portion of the palatoquadrate is present near the medial margin on the dorsal side of the palatine ramus. The corpus of the pterygoid has a basicranial ramus that is shorter and sturdier than in *Sclerocephalus haeuseri* (Boy 1988). In its proportions, it resembles that of late juvenile *Chelideperton latirostre* (Boy 1993b). A cavity in the basicranial ramus can neither be excluded nor identified because of poor preservation. On the dorsal side, the corpus of the pterygoid and the posterior part of the palatine ramus is strengthened by the torus marginalis on the margin of the interpterygoid vacuity. The conical recess, that holds the basipterygoid process of the basisphenoid, is clearly visible in a large skull (SMF A35b) at the base of the ascending lamina of the pterygoid (Fig. 26b). A transverse flange (Fig. 17a) of the pterygoid is developed in large and middle-sized specimens, whereas it is only slightly developed in skulls smaller than about 70 mm in length. The posterolaterally directed quadrate ramus is distinctly smaller than the palatine ramus and overlaps the median part of the quadrate. The quadrate ramus forms an elevated ascending lamina (Fig. 17a).

The pterygoid, with the exception of the quadrate ramus, is covered by denticles with posteriorly curved tips. On the corpus of the pterygoid, the denticles are distinctly larger than in the other regions of the pterygoid.

https://doi.org/10.1017/S0263593300001279 Published online by Cambridge University Press

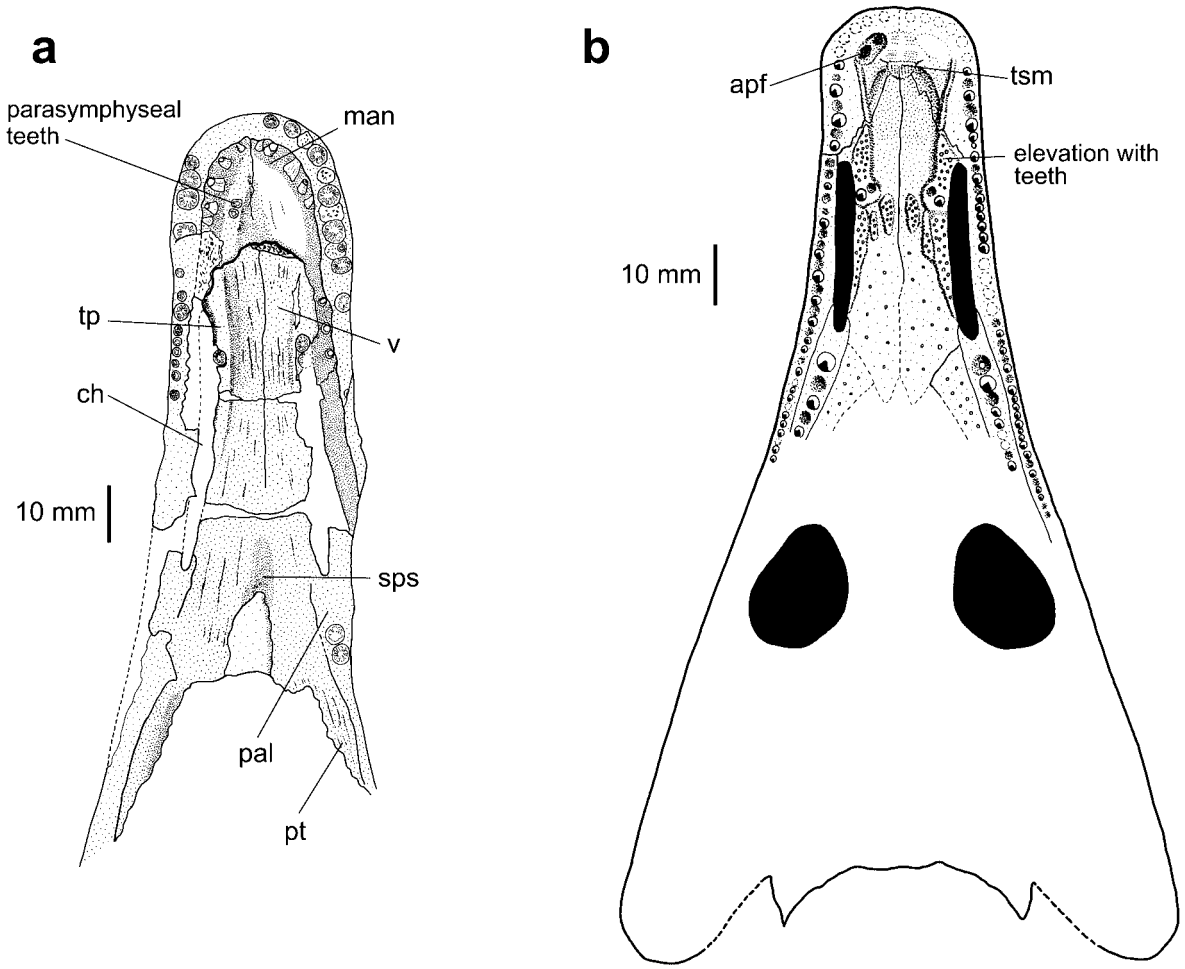

Figure 18 *Archegosaurus decheni*. Palates: (a) GPIT/Am/20 (sl=181 mm) in dorsal view, two parasymphyseal teeth are preserved on the left mandibular ramus; (b) MB.Am.155 (sl=134 mm, plaster cast) in ventral view.

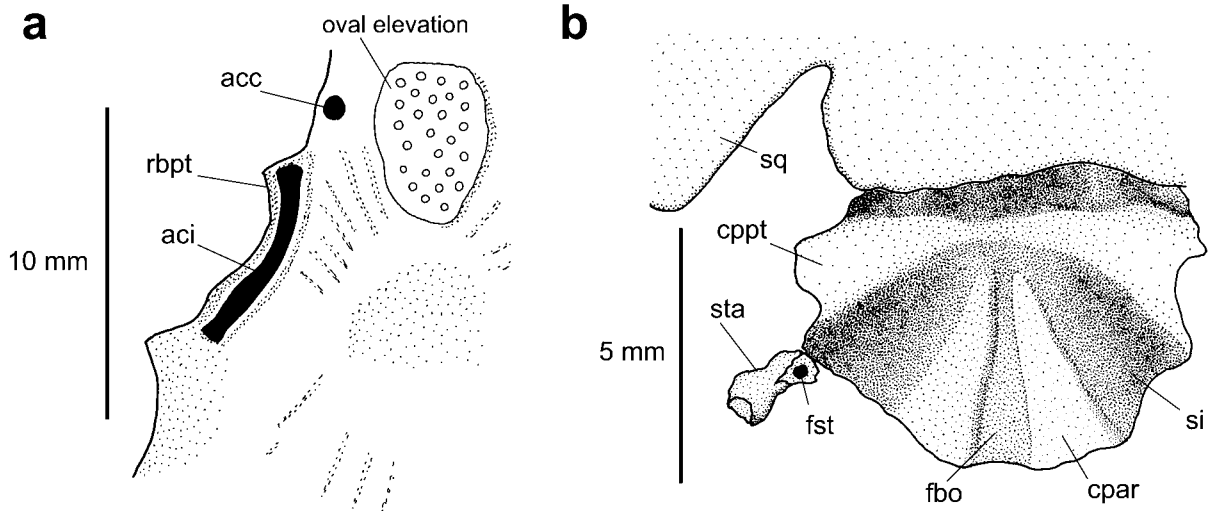

Figure 19 *Archegosaurus decheni*. Basal plate of parasphenoid: (a) MB.Am.253 (sl circa 160 mm) in ventral view, showing the furrow for the internal carotid artery and the entrance foramen for the intracranial branch of this artery; (b) MB.Am.140 (sl=28 mm) in dorsal view with stapes.

5.2.7. Parasphenoid. The basal plate of the parasphenoid is about as long as wide in large specimens (Fig. 5b). In its overall shape, it broadens posteriorly. It is proportionally broader in small specimens than in larger ones (e.g., MB.Am.140, sl=27·8 mm).

Anteriorly, the basal plate possesses an oval, slightly elevated area covered with denticles, which is best visible in middle-sized and large skulls (Fig. 19a). This oval elevation is also visible in the smallest specimen (MB.Am.134, sl=18 mm, Fig. 6a), although no denticles are preserved. In one specimen (MB.Am.155a, sl=134 mm), the denticles extend over the whole ventral surface of the cultriform process. In the region of the basicranial articulation, a distinct furrow for the internal carotid artery (Gubin 1997) runs in anteromedial direction posterolateral to the dentigerous area (Fig. 19a). In specimen MB.Am.253b, a foramen is visible anterior to the furrow at the

https://doi.org/10.1017/S0263593300001279 Published online by Cambridge University Press

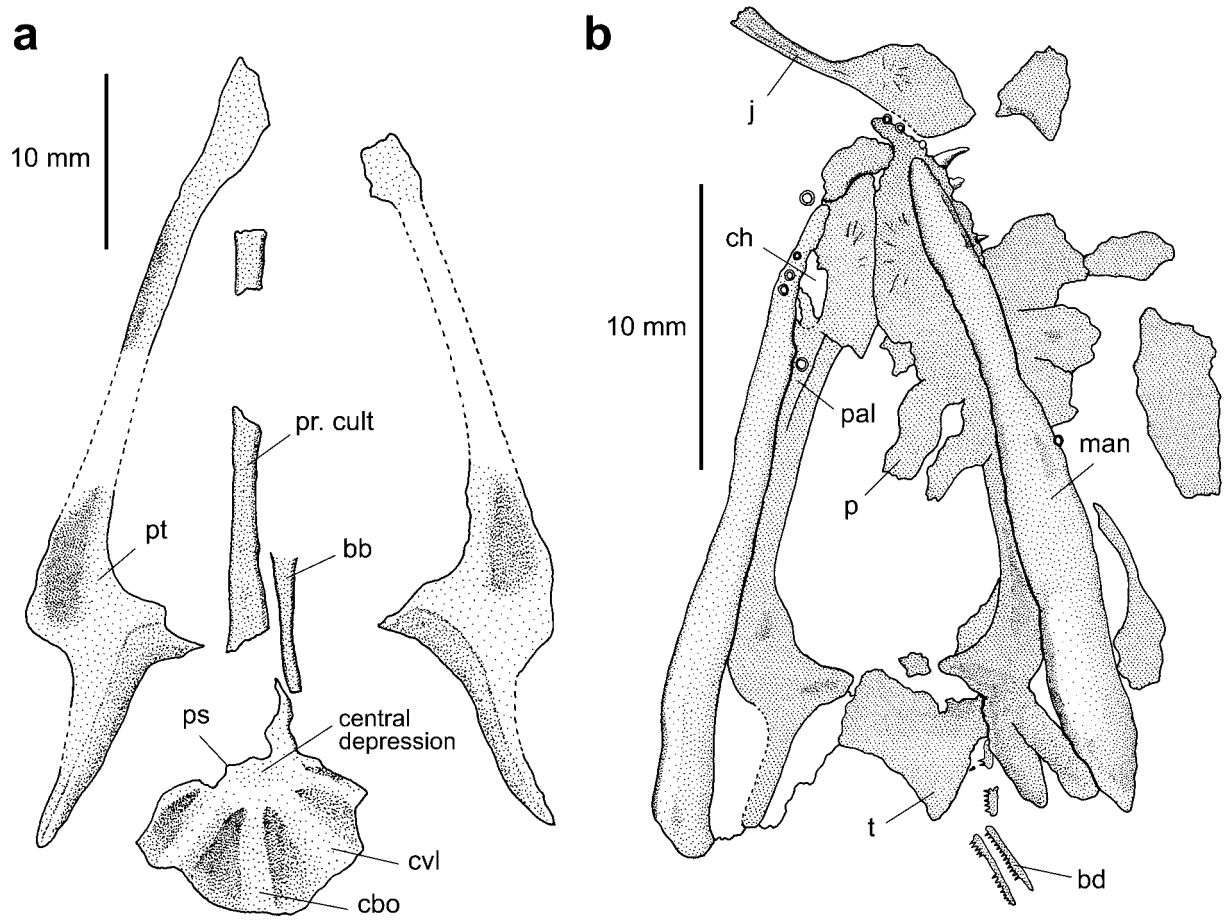

Figure 20 *Archegosaurus decheni*. Palates of small specimens: (a) SMNS 81994 (sl circa 65 mm) in ventral view with basibranchial; (b) GMBS P/497 (sl circa 24 mm) in ventral view, this is the smallest known articulated palate in *A. decheni*.

base of the cultriform process (Fig. 19a), representing the entrance for the intracranial branch of the internal carotid, comparable to the situation in the intasuchid *Intasuchus silvicola* (Shishkin 1968) and the archegosaurid *Platyoposaurus* (Gubin 1991). A round, shallow depression is situated in the centre of the ventral surface of the basal plate (Figs 19a, 20a). Shallow furrows and ridges radiate from this depression, resembling the sculpture of the dermal skull roof (Fig. 19a). Distinct paired muscular pockets for the insertion of the hypaxial musculature are situated posterolateral to the central depression (Fig. 4b). The ventrolateral crest runs anterolateral to these pockets from the margin of the central depression in posterolateral direction (Fig. 20a). The low and broad basioccipital crest extends between the muscular pockets from the posterior margin of the basal plate to the central depression (Figs 20a, 24a).

The transversely orientated parapterygoid crest (Figs 17a, 19b, 25b, 26, 27) is present on the anterior part of the dorsal side of the basal plate of the parasphenoid (terminology after Bystrow & Efremov 1940; synonym: crista parafenestralis, Säve-Söderbergh 1936; Shishkin 1973). This crest broadens laterally. The paroccipital crest runs posterolaterally on each side, separated from the parapterygoid crest by the sulcus intercristatus (Figs 19b, 26a). The fossa basioccipitalis is situated between the left and right of the paroccipital crest (Fig. 19b). On the dorsal side of the basal plate, a somewhat narrower furrow is visible in about the same position as the ventral furrow of the internal carotid artery on the ventral side (Fig. 17a). It possibly carried the palatine nerve, comparable to the situation in *Benthosuchus sushkini* (Shishkin 1968). A foramen is visible in MB.Am.227 anterolateral to the ossified socket of the basisphenoid (Fig. 26a). It possibly represents the outlet foramen of the internal carotid artery.

The cultriform process is dorsally concave. It is only slightly convex or even planar on the ventral side. The cultriform process gets proportionally more slender during size increase of the skull.

5.2.8 Palatal plates. In skulls beyond 50 mm length, ossified plates of irregular shape and size (Figs 8, 17) are frequently found in the region of the interpterygoid vacuities. As observed by Meyer (1858), they possess denticles on one side. They are slightly curved posteriorly like the denticles on the vomer, pterygoid and parasphenoid. Judging from their position, they must have covered a canvas of skin that was present in the interpterygoid vacuities. The denticles are of different size. The largest are found in the region behind the orbits, i.e., in the posterior part of the interpterygoid vacuities, such that an area with larger denticles was present in the posterolateral part of the palate together with the denticles of the corpus of the pterygoid. Among archegosaurids, denticle-bearing palatal plates have been reported also in *Prionosuchus* (Cox & Hutchinson 1991).

5.3. Palatal dimorphism

Two different patterns of palatal dentition can be distinguished, here called type A and type B. Type A, represented by specimens MB.Am.116 (Fig. 17a), MB.Am.138 (Fig. 18b) and the vomer illustrated by Gubin (1997, p. 105, fig. 1b), possesses the pattern that is described in section 5.2.2: no continuous tooth row medial to the choana, but a tusk with an anteromedially located tooth pit. Type B, represented by MB.Am.117 (Fig. 17b), MB.Am.155, MB.Am.136, as well as by a specimen

https://doi.org/10.1017/S0263593300001279 Published online by Cambridge University Press

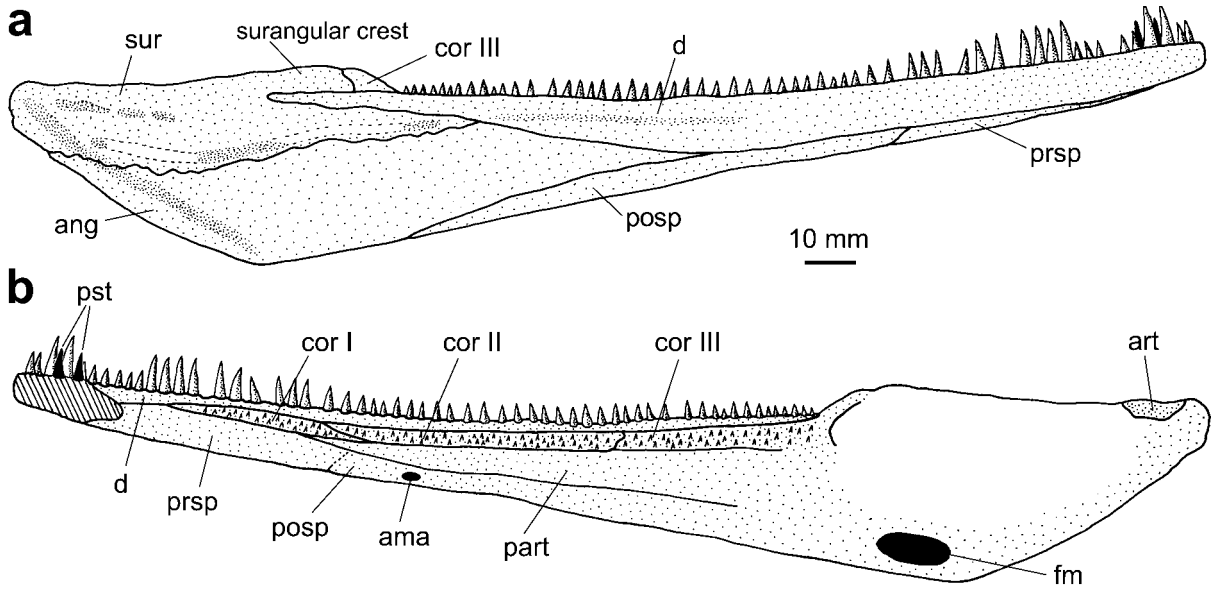

Figure 21 *Archegosaurus decheni*. Reconstruction of the mandible of a large individual: (a) labial view; (b) lingual view. Based on MB.Am.117 and MB.Am.258, supplemented after MB.Am.953. Two of the four parasymphyseal teeth are shown in black.

illustrated by Hofker (1926, p. 115, figs 6, 7), possesses a continuous row of middle-sized teeth medial to the choana. This row may run either directly parallel to the choana, or in anteromedial direction at an acute angle to the choanal margin. Additional one or two middle-sized teeth are present close to the intervomerine suture posteromedial to the vomerine tusk. It is possible that the two different patterns of vomerine dentition in *A. decheni* can be attributed to sexual dimorphism. Unfortunately, a sufficient number of adequately preserved specimens is not available to confirm this assumption.

6. The lower jaw (mandible)

6.1. The mandible of adult specimens

The mandible of adult specimens will be described first (Figs 21, 22). Its shape is elongated and low. The depth of the symphysis is approximately one fifth of the maximum depth of the mandible. In labial view the surangular crest is low (Fig. 21a), and the retroarticular process formed by the surangular is short. The angle of the jaw is approximately 135°.

6.1.1. Labial side. The dentary extends from the symphysis approximately 4/5 of the mandible length. It sutures ventrally with the pre- and postsplenial and reaches its maximum depth at mid length. The dentary ascends from this point at an angle of circa 15°, suturing posteroventrally with the angular and surangular. The dentary occupies the main part of the anterior half of the labial side of the mandible.

The pre- and postsplenials are poorly preserved in most cases, and the suture between is mostly not detectable. They are elongated, narrow bones and form the ventral edge of the anterior two thirds of the mandible. The presplenial participates with the dentary in the formation of the symphysis (see section 6.1.3). The postsplenial is more than 1·5 times the length of the presplenial.

The angular forms the posteroventral part of the lower jaw. Dorsally, it sutures with the surangular, and sends out an anterior process between the dentary and postsplenial. It forms the ventral edge of the mandible at its deepest part.

The surangular forms the main part of the low surangular crest, which is formed anteriorly by a small portion of coronoid III. Laterally, the surangular is overlapped by a narrow posterior process of the dentary. The surangular of the largest specimens is proportionally deeper in its posterior part than in *Sclerocephalus* and *Cheliderpeton* (Boy 1988, 1993b). It cannot be determined in the present material to which extent the surangular participates in the jaw articulation.

The course of the lateral line sulci of the mandible is shown in Figure 22. It corresponds with the situation seen in most early tetrapods and temnospondyls.

6.1.2. Lingual side. The dentary forms the dorsal edge of the lingual side and is shallow. Anteriorly, it becomes deeper in the region of the symphysis (see section 6.1.3). It does not participate posteriorly in the margin of the adductor fossa. Medially, it sutures with the coronoids. Three narrow, long coronoids are present. Coronoid I does not participate in the formation of the symphysis. Coronoid III forms the anterior and anterolateral margin of the adductor fossa. Denticles present on all three coronoids can also be observed in early tetrapods such as *Acanthostega* (Ahlberg & Clack 1998). This is also the case in the basal temnospondyl *Balanerpeton* (Milner & Sequeira 1994), and, among stereospondylomorphs, in *Sclerocephalus* (Schoch 2003), the archegosaurid *Platyoposaurus* (Gubin 1991), and in many stereospondyls (Schoch & Milner 2000). The stereospondylomorph *Cheliderpeton* (Boy 1993b) exhibits denticles only in the posterior region of the coronoid row, probably on coronoid III.

The splenials form the ventromedial margin of the anterior lingual ramus of the mandible. The postsplenial is penetrated by a comparatively large foramen in its anterior part, that is also present in *Eryops* (Sawin 1941), *Dvinosaurus* (Shishkin 1973), *Sclerocephalus*, *Onchiodon*, and (smaller) in *Cheliderpeton* (Boy 1988, 1990, 1993b). According to Shishkin (1973), it serves for the passage of the anterior mylohyoid artery. The presplenial participates in formation of the symphysis (see section 6.1.3.).

Similar to *Cheliderpeton* (Boy 1993b), the prearticular is distinctly elongate and tapers in a narrow anterior process that terminates between coronoid I and the presplenial. The lingual wall of the adductor fossa is crushed in the investigated specimens. An oval Meckelian fenestra can be determined in the ventral part of this region (MB.Am.953).

https://doi.org/10.1017/S0263593300001279 Published online by Cambridge University Press

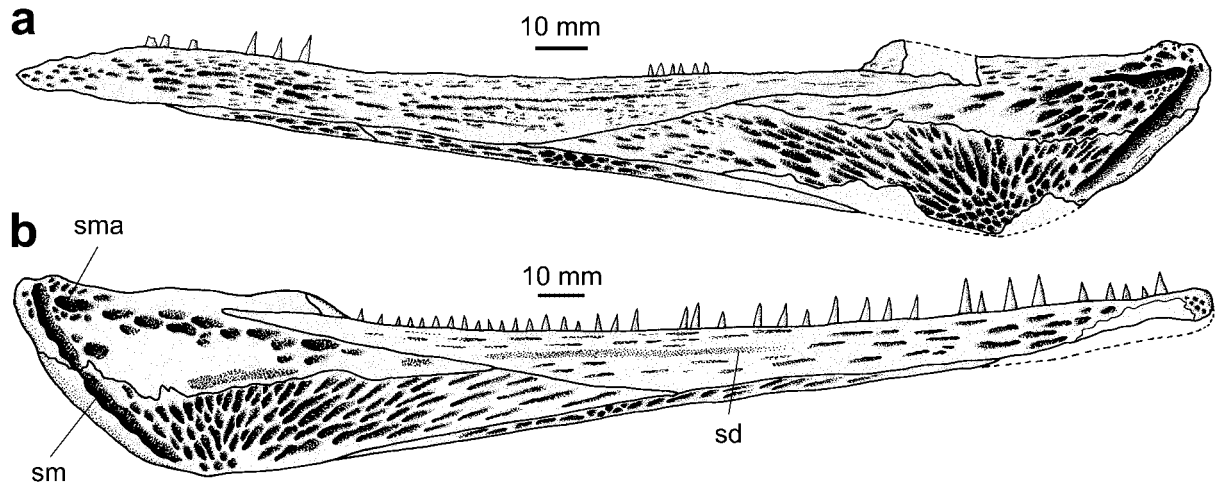

Figure 22 *Archegosaurus decheni*. Sculpture of mandible in labial view: (a) MB.Am.117b (sl=207 mm); (b) MB.Am.258b (sl circa 250 mm).

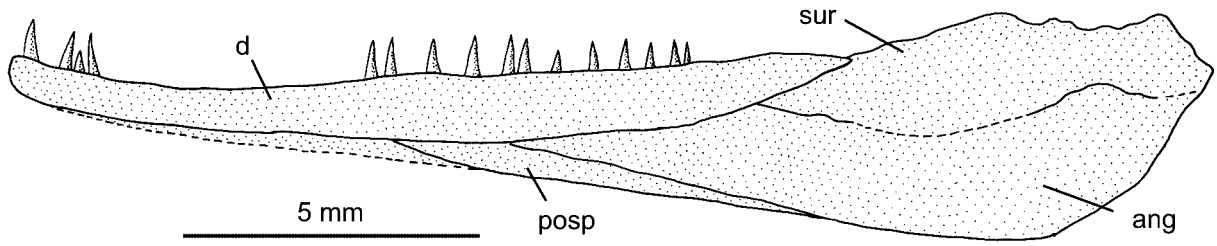

Figure 23 *Archegosaurus decheni*. Reconstruction of the mandible of the smallest specimen in labial view (MB.Am.134, sl=18 mm).

6.1.3. Symphysis. The symphysis is rarely preserved in *A. decheni*. As Whittard (1928) recognised, it is formed by dentary and presplenial (Fig. 21b). In the region of the symphysis, the anterior part of the mandibular ramus broadens medially and forms the symphyseal lamina. In contrast to the description of Whittard, the dentary forms the dorsal part of the lamina. A low crest that bears the symphyseal fangs is located on the lamina medial to the marginal tooth row. Two bases of dentary symphyseal fangs are visible in MB.Am.258, and two fangs alternating with two tooth pits are present on each ramus in GMBS P/635. Also two dentary symphyseal fangs are visible in the posterior part of the symphyseal lamina of the left ramus in GPIT/Am/20; there have probably been additional teeth in the anterior part which is not adequately preserved (Fig. 18a). The diameter of the bases of the dentary symphyseal fangs is smaller than that of the adjacent marginal teeth. One symphyseal fang plus replacement pit on the dentary medial to the marginal tooth row seems to be the plesiomorphic condition in tetrapods (see Ahlberg & Clack 1998). Also among plesiomorphic stereospondylomorphs, two parasymphyseal tooth loci are present in *Cheliderpeton* (Boy 1993b) and *Melosaurus* (Golubev 1995). There are no more than two parasymphyseal fangs in stereospondyls, although an additional arcade of small teeth has been reported medial to the marginal teeth in metoposaurids and *Parotosuchus* (Jupp & Warren 1986; Warren & Davey 1992; Schoch & Milner 2000). The higher number of parasymphyseal fang loci can be regarded as autapomorphy of *A. decheni*.

6.1.4. Articular and retroarticular process. The articular is preserved as a roughened bone anterior to the retroarticular process in MB.Am.258a and MB.Am.117. MB.Am.258a (ml=280 mm) is an internal cast of the posterior part of the lower jaw; the articular is visible as a hollow with remnants of bone. It is wedge-shaped in lateral view, with the tip directed ventrally. Its dorsal surface (articulation surface) is not preserved. The retroarticular process is very short and formed by the surangular alone.

6.2. Ontogeny of the mandible

The mandible is preserved in labial view in the smallest known specimen with a skull length of 18 mm (MB.Am.134, Fig. 23). It is somewhat sturdier and proportionally less elongated than in large specimens. The surangular crest is proportionally lower and only slightly elevated above the dentary. Coronoid III may not participate in the surangular process; this can be proven only in specimens beyond 50 mm skull length. The posterior process of the dentary is shorter and blunter than in larger specimens. Only the posterior part of the postsplenial can be identified; further anterior, no sutures can be traced.

During further ontogeny, the postsplenial becomes longer with respect to the presplenial, but the retroarticular process barely increases proportionally in length. At a skull length of 206 mm, the articular is ossified, but it probably ossified much earlier in ontogeny.

7. Marginal dentition

7.1. Teeth of the upper jaw

The tooth-bearing bones of the upper jaw are the premaxilla and maxilla. The dentition in the largest specimens will be described first. Morphology of single teeth in *A. decheni* has been described by Goldfuss (1847) and Meyer (1858). In general, marginal teeth are pointed conical, round in cross-section at their bases, and slightly curved lingually. The dentine is infolded. The upper jaw provides space for approximately 70 teeth (Fig. 5). The premaxilla bears 12–13 teeth. Premaxillary teeth increase in size from rostral to abrostral, so that the largest marginal teeth of the upper jaw are situated

https://doi.org/10.1017/S0263593300001279 Published online by Cambridge University Press

anterior to the suture between premaxilla and maxilla, where the premaxilla is broadened. The maxilla bears approximately 55 teeth. Maxillary teeth No. 2–10 are distinctly smaller than the large premaxillary teeth and the first maxillary tooth in MB.Am.116. The following six maxillary teeth are again larger, and the tooth-bearing part of the bone is broader. The large tusk of the vomer is situated nearby the 'gap' that is formed by the smaller teeth on the anterior part of the maxilla. The subsequent teeth decrease constantly in size. Overall, the teeth of premaxilla and maxilla exhibit a size differentiation with two zones of smaller teeth (Fig. 3c).

7.2. Teeth of the lower jaw

Tooth-bearing elements are the dentary and coronoids I–III. Four large tooth loci are present posterior to the marginal teeth in the symphyseal region. The dentary has space for approximately 65–70 marginal teeth (Fig. 21). Beginning anteriorly, there are 2–3 smaller (or medium-sized) teeth, followed abrostrally by 2–3 very large teeth. Abrostrally, 6–7 quite small teeth are situated, followed posteriorly by 6–7 larger teeth. The subsequent teeth decrease constantly in size. Thus, quite small teeth are located on the dentary, opposed to the large premaxillary teeth, and large dentary teeth are opposed to smaller anterior maxillary teeth.

Whittard (1928) illustrated two symphyseal teeth on the presplenial. These teeth have to be assigned to the symphyseal lamina of the dentary according to the specimens investigated here (see section 6.1.3). The coronoids I-III bear no larger teeth, but many small denticles.

7.3. Ontogeny of dentition

7.3.1. Differentiation of size. The marginal teeth are not as differentiated in small larvae (Fig. 2). From rostral to abrostral, the size of the teeth decreases more or less constantly. Slight differentiation is first seen in a specimen of 38 mm skull length (MB.Am.218). Here the anterior maxillary teeth are smaller as compared to the premaxillary teeth and also as compared to the posterior ones. The opposing dentary teeth are larger than the maxillary teeth. The differentiation is distinct in skulls beyond 60 mm in length.

7.3.2. Infolding of dentine. All marginal teeth possess a smooth surface in the smallest larvae, no infolding is visible in cross-sections, and the pulp cavity is proportionally large. These features are typical of the teeth of small temnospondyl larvae (Bystrow 1938; Boy & Sues 2000). A first infolding of dentine, suggested by slight longitudinal striae in *A. decheni*, appears in the basal region of the large premaxillary teeth with a diameter of approximately 0·2 mm in MB.Am.140 (sl=28 mm). The other teeth retain their smooth surface. The striae are still poorly developed at a skull length of about 40 mm, but they are visible on the remaining teeth. A tooth in cross-section was described and illustrated by Goldfuss (1847), Burmeister (1850), and Meyer (1858). The infolding remains simple even in adults. The largest specimen of *A. decheni* in which tooth bases are well visible in cross section has a skull length of more than 210 mm (MB.Am.136). The base of the largest tooth measures more than 5 mm in diameter. Its pulp cavity is comparatively large, the primary folds are not folded secondarily, and there are no secondary cavities. Teeth of juvenile *Benthosuchus* (diameter slightly less than 4 mm; Bystrow & Efremov 1940) and *Metoposaurus* (diameter of about 5 mm; Warren & Davey 1992), for instance, exhibit a proportionally very constricted pulp cavity and the infolding of dentine is complex. This shows that the degree of infolding is not always a degree of the tooth size, as already pointed out by Warren & Davey (1992).

7.3.3. Number of teeth. The number of teeth in the upper as well as in the lower jaw increases with the proportional elongation of the snout during growth. It is, however, particularly difficult to determine the number of teeth in the smallest specimens. The dentary of the smallest larva has an estimated space for approximately 45–50 teeth. In MB.Am.220 (sl=32 mm), the complete upper jaw has space for approximately 60–65 teeth, whereas MB.Am.236 (sl=82 mm) has approximately 70 teeth in the upper jaw.

8. Ontogeny of endocranial ossifications (neurocranium and palatoquadratum)

8.1. The exoccipital

Both exoccipitals are visible from their ventral side posterior to the basal plate of the parasphenoid in a specimen of 53 mm skull length (BSM 1869 III 6, Fig. 24a). In MB.Am.225 (sl=70 mm, Fig. 24b) and NNM 39072 (sl=96 mm), the exoccipitals are medially constricted with a flattened, vertically oriented process. This process may represent the processus lamellosus *sensu* Bystrow & Efremov (1940). In IGS U II 1/2 (sl>90 mm), the exoccipital possesses the constricted shape described above, but the flattened process is not visible (Fig. 31b). The paroccipital process of the exoccipital is first visible in a skull of 181 mm length (GPIT/Am/20).

The exoccipital is better ossified in specimens with a skull length beyond 200 mm. The following description is based on MB.Am.237b (sl=220 mm, Fig. 25), NNM39040 (sl=195 mm), SMF A 35b (sl circa 200 mm, Fig. 26b), MB.Am.953 (sl=226 mm), and PIMUZ A/II 0061 (sl=236 mm). The vertical column of the exoccipital sends out a slender dorsal process which sutures with the supraoccipital process of the postparietal (Fig. 28). The paroccipital process extends in a dorsolateral direction towards the tabular. It sutures with the corresponding paroccipital process of the tabular (this process is visible in skulls beyond 200 mm length, see section 4.6.3) and forms the ventral, slightly concave border of the posttemporal fenestra (Fig. 28). A deepening on the posterolateral side of the left vertical column indicates the vagus foramen (for the nerves IX – XI, Fig. 25a). Medial to the vertical column, the anteromedially directed, ventrally situated submedullar process is visible and has an almost horizontal dorsal surface. The occipital condyle is posterior to the ventral half of the vertical column. The whole occipital condyles are paired, and the basioccipital participates only to minor degree. The surface of the occipital condyle is roughened, indicating a coverage of cartilage in life.

8.2. The basioccipital

A trace of the basioccipital is first visible in a specimen of approximately 84 mm skull length (MB.Am.227, Fig. 26a). It is a wedge-shaped, roughened area on the posteromedial, dorsal surface of the basal plate of the parasphenoid.

Again, the basioccipital is best visible in skulls beyond 200 mm in length (MB.Am.237, Fig. 25; SMF A35b, Fig. 26b). This wedge-shaped bone extends between the exoccipitals and otic ossifications and reaches anterior almost to the region of the basicranial articulation. An antero-posteriorly directed strip with a distinctly roughened surface is visible in the median part of the otherwise smooth and flat basioccipital in SMF A35b (Fig. 26b). The basioccipital is overlapped in its posterolateral part by the submedullar process of the exoccipital (Fig. 25), as in the archegosaurid *Platyoposaurus* (Efremov 1933). The basioccipital becomes slightly narrower dorsally (Fig. 28). The dorsal surface is concave in this part, probably

https://doi.org/10.1017/S0263593300001279 Published online by Cambridge University Press

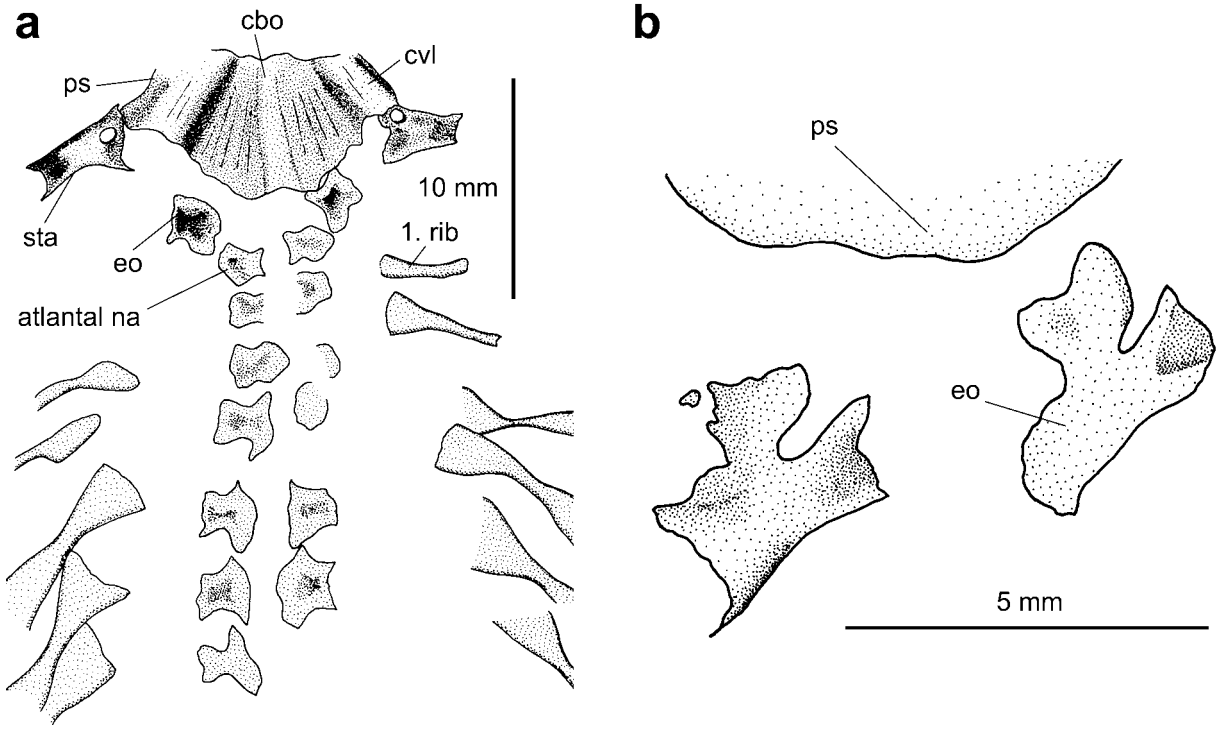

Figure 24 *Archegosaurus decheni*. Exoccipitals: (a) BSM 1869 III 6 (sl=53 mm), parasphenoid, exoccipital, stapes, and anterior trunk region in ventral view; (b) MB.Am.225 (sl=70 mm), parasphenoid with exoccipitals preserved posteriorly.

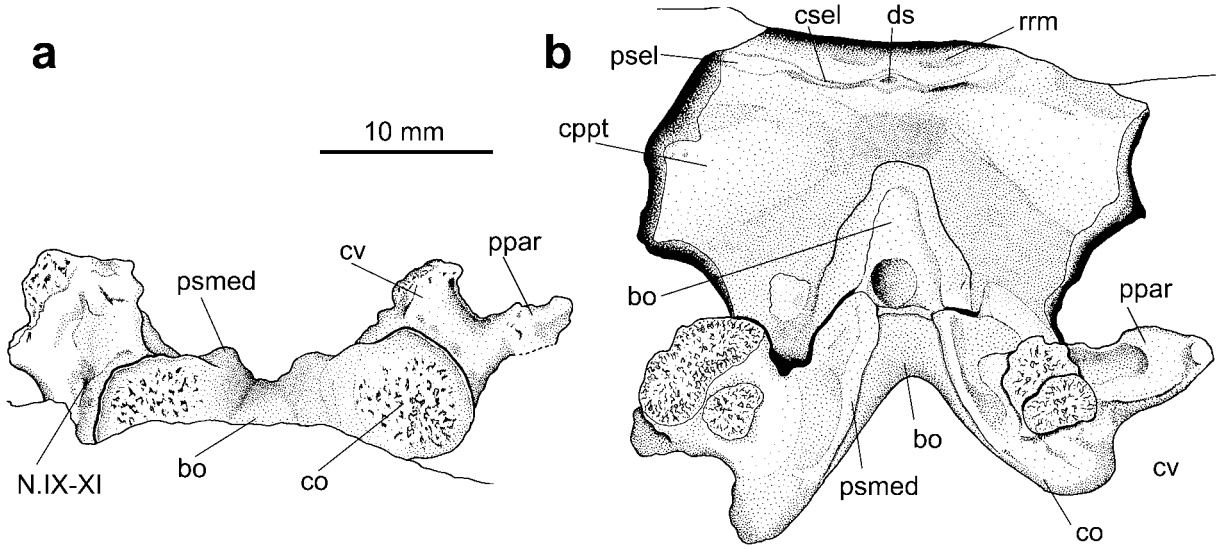

Figure 25 *Archegosaurus decheni*. Neurocranial elements in MB.Am.237b (sl circa 220 mm, silicone cast): (a) posterior view; (b) dorsal view.

for accommodation of the notochord; this dorsal depression extends anteriorly to the region of the anterior margin of the submedullar processes.

8.3. The otic region

The dorsal surface of the basal plate of the parasphenoid is distinctly roughened and slightly elevated in the posterolateral part of the paroccipital crest in SMF A3 (sl=144 mm), as ossification of the otic region has just started in skulls of this size. The otics, however, are rarely visible, and they are poorly preserved or absent in the large specimens as well. A partially preserved bone is present in the otic region in MB.Am.116 (sl=279 mm, Fig. 17a) on the lateral part of the dorsal side of the basal plate, posterior to the parapterygoid crest. It is posteriorly connected with the exoccipital and medially connected with the basioccipital. It represents the ventral and lateral part of the opisthotic. Anteriorly, the bone continues as a narrow process that extends over the parapterygoid crest in direction to the basipterygoid process. This part can be interpreted as the prootic. The material is too poorly preserved to ascertain if a suture is present between the opisthotic and the possible prootic.

The dorsal side of the opisthotic is irregular and roughened in MB.Am.237a (sl=220 mm; Fig. 27b), SMF A35b (sl circa 200 mm; Fig. 26b), and MB.Am.136a (sl=211 mm; Fig. 27a). An ascending process of the otic as in *Eryops* (Sawin 1941) is not preserved in these skulls. The oval fenestra is not detectable, and the prootic is not preserved. In MB.Am.953 (sl=226 mm), the opisthotic is a deep element that possesses an ascending process which probably reached the dermal skull

https://doi.org/10.1017/S0263593300001279 Published online by Cambridge University Press

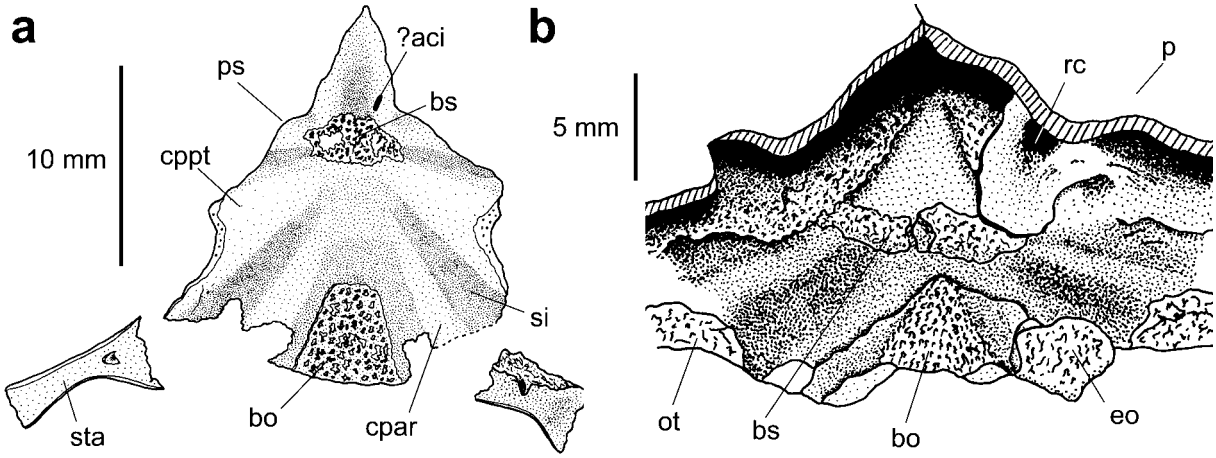

Figure 26 *Archegosaurus decheni*. Neurocranial elements: (a) MB.Am.227 (sl circa 84 mm), basal plate of parasphenoid in dorsal view with traces of basisphenoid and basioccipital; (b) SMF A35b (sl circa 200 mm) in posterodorsal view, the dermal skull roof is removed. The conical recess of the right pterygoid is visible.

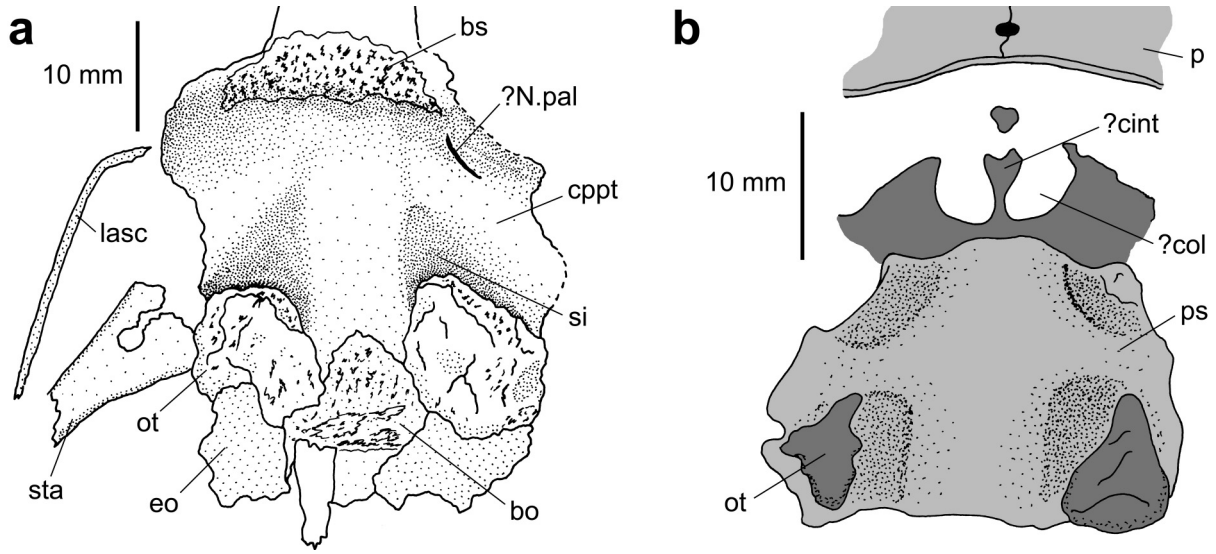

Figure 27 *Archegosaurus decheni*. Neurocranial elements: (a) MB.Am.136a (sl=211 mm) in dorsal view with stapes and ascending lamina of pterygoid; (b) MB.Am.237b (sl circa 220 mm), basal plate of parasphenoid in posterodorsal view, with remnants of the opisthotics and parts of the ?sphenethmoid in cross-section.

roof. The prootic portion is obscured by bones of the dermal skull roof.

8.4. The basisphenoid

A porous elevation of bone is present on the dorsal side of the basal plate of the parasphenoid in MB.Am.227a (sl circa 84 mm) at the base of the cultriform process (Fig. 26a). This structure represents the initial ossification of the basisphenoid. The porous bone at this location is more elevated in MB.Am.123 (sl=93 mm) and GMBS P/426 (sl circa 115 mm, Fig. 8). In skulls beyond 200 mm length (MB.Am.237b, 136a, SMF A 35b), the basisphenoid consists of a transversely orientated strip of bone that is located anterior to the parapterygoid crest (Figs 25b, 26b, 27a). It diminishes in depth towards its centre and forms a thin crest (*crista sellaris*) dorsally. In its lowest point, the crest is somewhat broadened and possesses a small and shallow deepening, which may represent the dorsum sellae. Laterally, the depth of the basisphenoid increases and the crest becomes broader, forming the lateral sellar processes. Anteriorly, the basisphenoid slopes abruptly to the floor formed by the parasphenoid. In dorsal view, the crista sellaris is concave anteriorly. Its broadened part in the middle forms a small anterior process that gives the crest the shape of a low, anteriorly opened 'w'. Paired shallow depressions are present on the anterior surface of the basisphenoid, anterolateral to the small deepening in the middle. They probably represent the recesses for the origin of the rectus eye muscles. The basipterygoid process of the basisphenoid remains cartilaginous.

8.5. The basipterygoid region

The basipterygoid region of *A. decheni* is insufficiently preserved in most specimens. An articulated parasphenoid and pterygoid are present in the largest specimen (MB.Am.116, Fig. 17a), but the nature of the articulation cannot be determined. The basipterygoid ramus of the parasphenoid is short (Fig. 19a). Its articulation facet is anteromedially aligned and laterally concave. Although the parasphenoid has formed a slightly overlapping suture with the basicranial ramus of the pterygoid, at least in medium-sized skulls (MB.Am.253, sl=circa 160 mm), a degree of mobility cannot be ruled out because the articulation is not tightly indented. This is similar to the situation in the archegosaurids *Platyoposaurus* (Efremov 1933) and *Bashkirosaurus* (Gubin 1981). A distinct recessus conoideus is preserved on the dorsal side of the pterygoid in SMF A35b (Fig. 26b). This structure articulates with the

https://doi.org/10.1017/S0263593300001279 Published online by Cambridge University Press

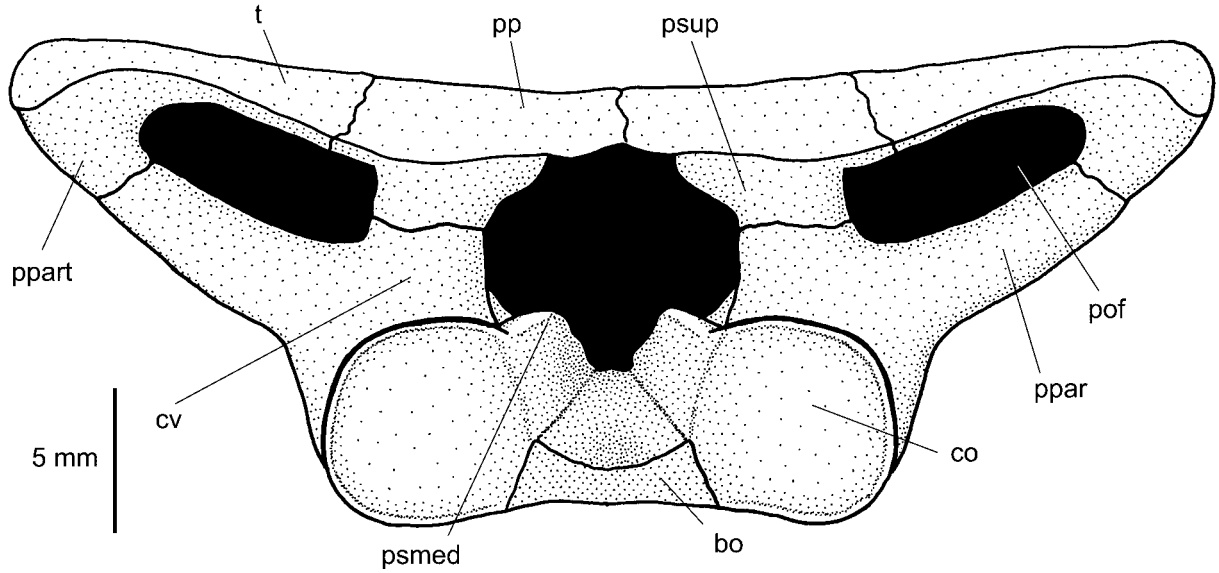

Figure 28 *Archegosaurus decheni*. Reconstruction of the occiput of an adult specimen in posterior view.

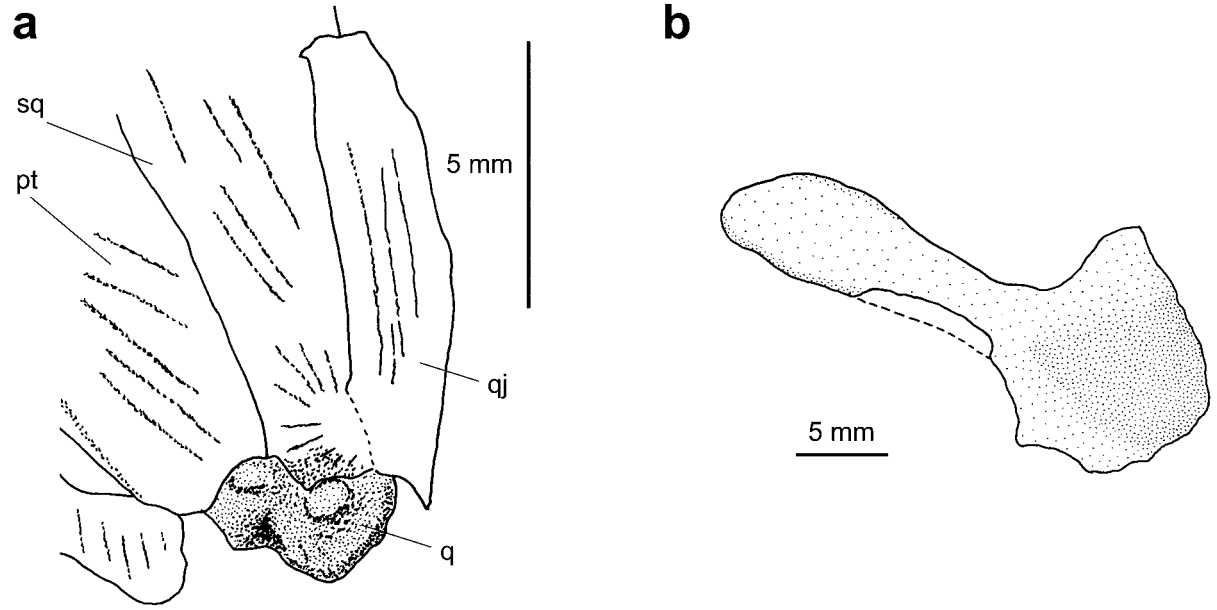

Figure 29 *Archegosaurus decheni*. Palatoquadrate ossifications: (a) BSM 1869III6 (sl = 53 mm), quadrate in ventral view; (b) MB.Am.237b (sl circa 220 mm), epipterygoid in posterior view.

basipterygoid process of the basisphenoid that remained cartilaginous, even in adult specimens (section 8.3).

8.6. The sphenethmoid and sella turcica region

The sphenethmoid is ossified in a skull of approximately 125 mm in length (MB.Am.235, IGS U III 4/5, Fig. 13b), but most of it is obscured by dermal bones. MB.Am.235 and IGS U III 4/5 are plaster casts of an original skull which is unfortunately lost. The sphenethmoid is preserved fragmentarily in MB.Am.116 (sl = 279 mm, Fig. 17a). The preserved part is 80 mm long; its posterior end is situated on the cultriform process anterior to the basal plate.

In MB.Am.237 (sl = 220 mm, Fig. 27b), the neurocranium is preserved in cross-section 9 mm posterior to the pineal opening, at the anterior end of the basal plate of the parasphenoid. A median crest rises and broadens dorsally from an ossified base that is situated on the basal plate. The crest divides a cavity that is framed laterally by concave walls which are curved medially in their dorsal part. It cannot be determined whether the lateral walls contact the dermal skull roof. Possibly this structure represents the cross-section of the posterior portion of the sphenethmoid. The median crest may represent the interolfactorial crest, that divides the olfactorial canal of the sphenethmoid.

8.7. Palatoquadrate ossifications

Epipterygoid and quadrate form the ossified parts of the palatoquadrate in *A. decheni*. Both elements are poorly preserved.

An ossified quadrate is preserved for the first time in BSM 1869 III 6 (sl = 53 mm, Fig. 29a). It is a short, stout bone that establishes a squamate suture with the ascending lamina of the pterygoid by overlapping it internally (Fig. 17a). It is connected anterolaterally with the quadratojugal and dorsally with the descending lamina of the squamosal.

https://doi.org/10.1017/S0263593300001279 Published online by Cambridge University Press

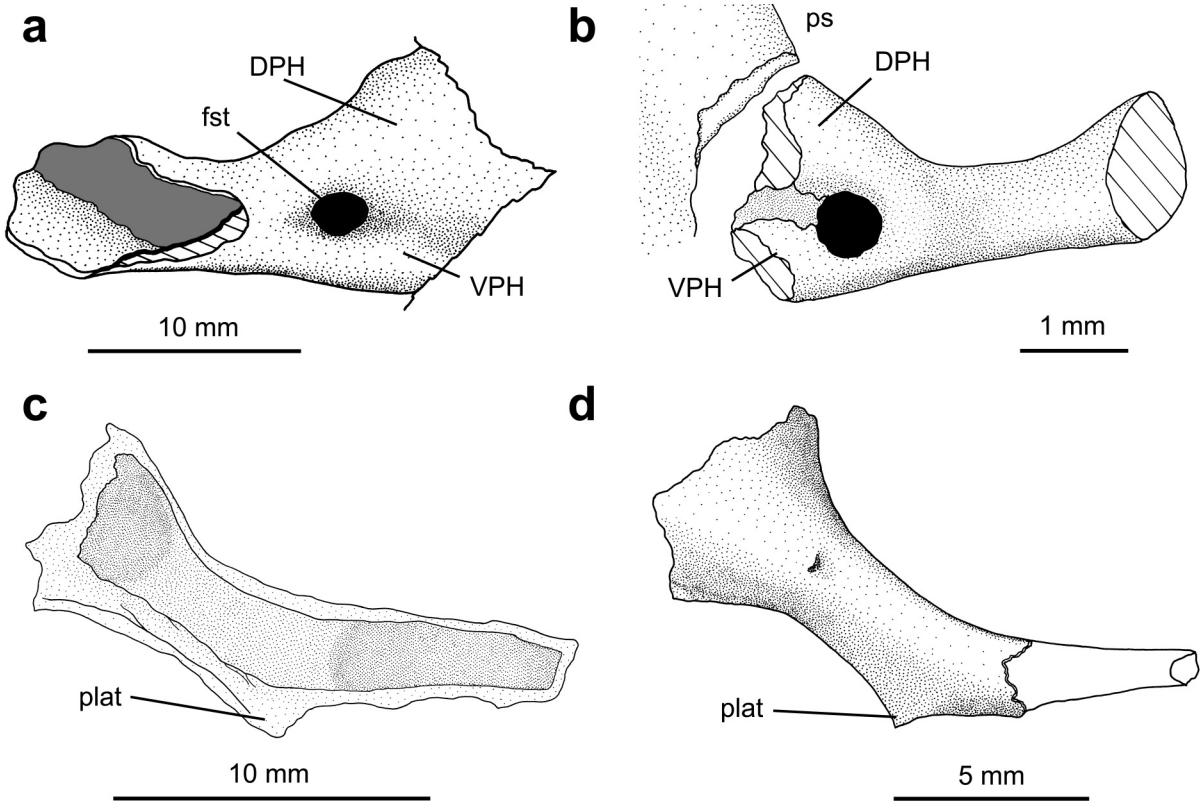

Figure 30 *Archegosaurus decheni*. Stapes: (a) GPIT/Am/20 (sl=181 mm), proximal part in dorsal view; (b) GMBS P/403 (sl=41 mm), in posteroventral view; (c) SMNS 81850 (sl=150 mm), the stapes is broken so that its inner surface is visible; (d) GMBS P/503 (sl circa 115 mm).

The epipterygoid appears to ossify late in ontogeny. An ossified element is present anterolateral to the basal plate of the parasphenoid in SMF A 3 (sl=144 mm). This bone has a broadened base from which a column-like process ascends, and may represent the epipterygoid in which the base with the ascending process is already ossified. An ascending bone is present on the right basicranial ramus of the pterygoid in MB.Am.237a (sl=220 mm, Fig. 29b). It possesses a broadened base and a slender shaft that is directed dorsomedially and contacts the dermal skull roof.

9. Visceral skeleton

9.1. The stapes (columella)

The stapes is broken in part and counterpart in most specimens, so that its shape and inner structure is frequently visible, but rarely its outer surface. It is preserved in different sized skulls.

9.1.1. Morphology. The following description is based mainly on GPIT/Am/20 and MB.Am.275b. The stapedial foramen is located in the proximal part of the stapes (Fig. 30a, b). It is embedded in a longitudinal depression which diminishes in proximal and in distal direction; it becomes deeper again towards the incisura of the proximal stapedial head. The incisura divides the proximal end of the stapes into a narrower head ('processus basalis' after Bystrow & Efremov 1940; 'ventral proximal head', VPH, after Lombard & Bolt 1988), and a broader head, the footplate ('dorsal proximal head', DPH). The stapes is widest and deepest in its proximal part and is nearly oval in cross-section. It is compressed anteroposteriorly and bends in dorsodistal direction at an angle of 150 – 160°, then it broadens anteroposteriorly again. It ends abruptly in its distal part (dorsodistal process). A crest is present on the posteroventral side of the proximal portion of the stapes. Laterally, it forms a distinct lateral process, which was probably continued with cartilage in the living animal (Fig. 30c, d). In anterior and posterior view, respectively, the stapes becomes more slender a short distance distal to the stapedial foramen; it broadens again in the region of the lateral process.

9.1.2. Comparison. Bolt & Lombard (1985) argued that the temnospondyl stapes, except for that of *Dvinosaurus*, is very similar to the anuran stapes and lacks any distal processes. In contrast, Boy (1988) and Schoch (2002) showed that the stapes of *Sclerocephalus haeuseri* also has a distinct lateral process similar to *Dvinosaurus*. Previously, Efremov (1933) had pointed out that the stapes of the archegosaurid *Platyoposaurus* bears a small, thin process that is directed to the ascending lamina of the pterygoid (Efremov 1933, p. 128, fig. 8). The stapes of *Archegosaurus decheni* is similar to that of *Sclerocephalus* and *Platyoposaurus* in possessing a comparable lateral process.

9.1.3. Position and orientation of the stapes. The broad DPH articulates with the ossified opisthotic in MB.Am.136a, which is connected with the basal plate of the parasphenoid in the sulcus intercristatus (Fig. 27a). The exact nature of the articulation of the VPH with the basal plate cannot be determined because of incomplete preservation in this region. In GPIT/Am/20 (sl=181 mm), the stapes is preserved *in situ* (Fig. 30a). The DPH is situated posterodorsally to the VPH. The stapedial artery runs in anterodorsal to posteroventral direction in *A. decheni*.

Bolt & Lombard (1985) reported that the distal end of the stapes is directed into the squamosal embayment in all adequately preserved temnospondyls they had investigated. This was corroborated by new findings in almost undistorted skulls of *Mastodonsaurus* (Schoch 1999). It is obvious that the distal portion of the stapes projects into the squamosal embayment in some three-dimensionally preserved skulls of *A. decheni*, too (e.g., MB.Am.257, SMF A 35).

https://doi.org/10.1017/S0263593300001279 Published online by Cambridge University Press

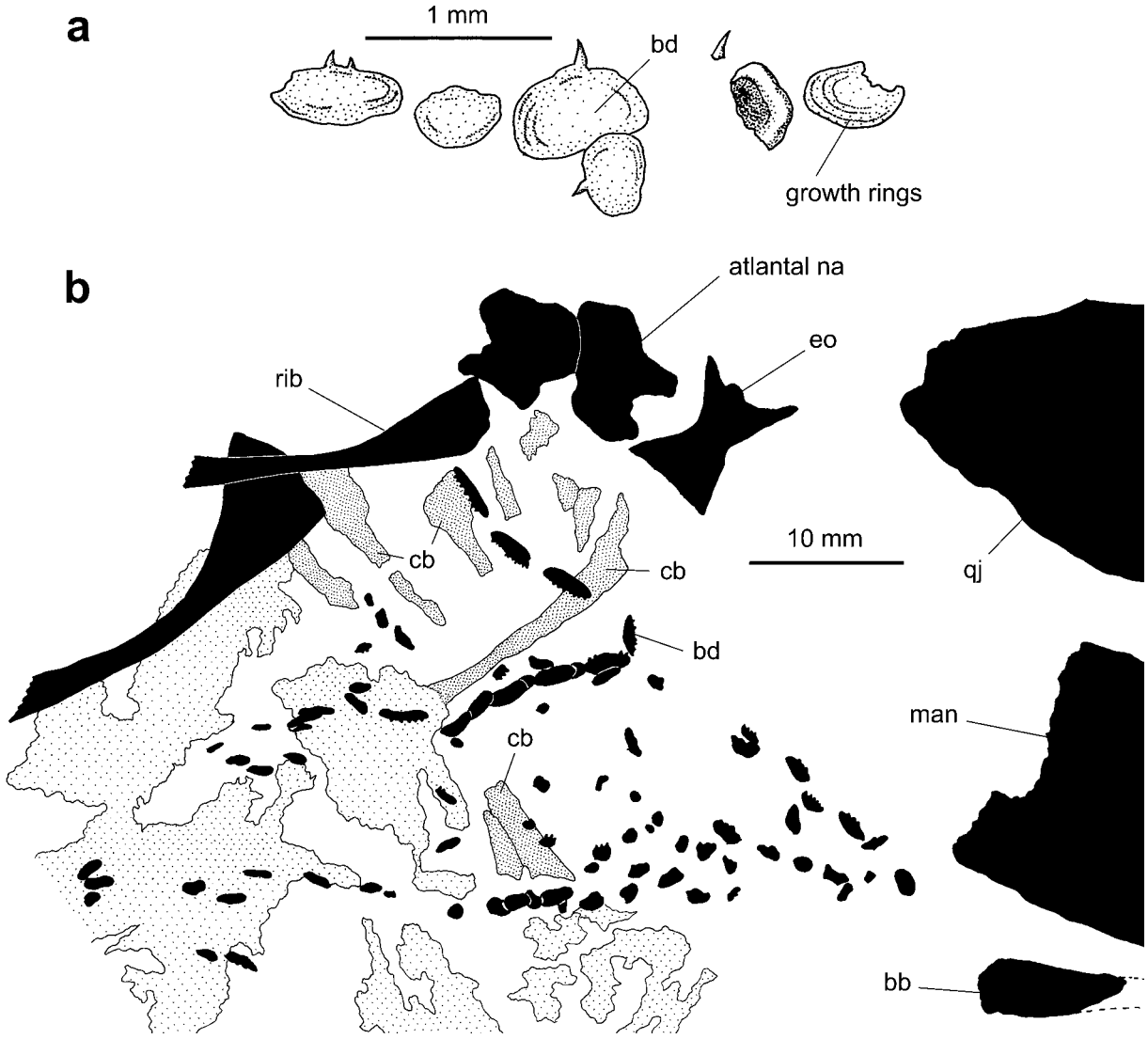

Figure 31 *Archegosaurus decheni*. Hyobranchium of IGS U II 1/2 (sl circa 90 mm): (a) the denticle-bearing branchial platelets exhibit concentric rings that can be interpreted as growth rings; (b) buccopharyngeal region: the posterior part of the basibranchial, branchial denticles, and carbonised remains of the cartilaginous ceratobranchials (densely stippled) are present. Carbonised remains of skin or gills are widely stippled.

9.1.4. Ontogeny. No stapes is preserved in the smallest specimens (18–25 mm skull length). The stapes is visible for the first time in an individual of 28 mm skull length (MB.Am.140, Fig. 19b). The ossified portion of the stapedial shaft grows with positive allometry in length during ontogeny, so that the stapes becomes proportionally longer and more slender in larger skulls. The portion of the stapes proximal to the stapedial foramen ossifies increasingly during ontogeny.

9.2. Branchial denticles

Four rows of denticle-bearing branchial platelets on both sides posterior to the skull indicate the presence of four pairs of cartilaginous ceratobranchials in the living animal. The platelets have been described by Witzmann (2004), and only additional information is given here. Concentric rings are visible on the branchial platelets in IGS U II 1/2 (sl circa 90 mm) that obviously represent growth rings (Fig. 31a). At least four rings are recognisable. Growth rings have not been reported in branchial platelets of temnospondyls. Branchial platelets can be demonstrated in specimens up to 150 mm skull length.

9.3. The basibranchial

A basibranchial (or copula) ventral to the parasphenoid was identified by Meyer (1858) as a median element of the hyobranchial apparatus. This bone is visible in GPIT/Am/233 (sl=46 mm) and PIMUZ A/II 0019 (sl=50 mm) lateral to the cultriform process. It is slightly broadened both in its anterior and posterior part. As shown by Hofker (1926), the basibranchial broadens distinctly in its anterior part during increasing skull length. Such a development is also visible in *Sclerocephalus* (Boy 1974, 1988) and *Onchiodon* (Boy 1990), and apparently represents a plesiomorphic pattern in temnospondyls.

The adult morphology of the basibranchial is visible in MB.Am.953 (sl=226 mm, Fig. 4b), and measures 35 mm. It broadens in its anterior third which is six times the width of the shaft.

9.4. Further remains of the hyobranchial skeleton and external gills

In IGS U II 1/2 (sl circa 90 mm), carbonised remains visible posterior to the basibranchial, between the branchial platelets (Fig. 31b), may be the remnants of skin or of the gills itself. At least four rod-like imprints are visible that are aligned anteroventrally, parallel to rows of branchial platelets. A further rod-like structure is aligned anterodorsally. Parallel and slightly ventral to this rod, a row of branchial platelets is visible. These carbonised structures can

https://doi.org/10.1017/S0263593300001279 Published online by Cambridge University Press

be interpreted as remains of cartilaginous branchial arches, probably the ceratobranchials. No unambiguous remains of further hyobranchial elements can be demonstrated in *A. decheni*. Three pairs of external gills like those in salamander larvae have been demonstrated in *A. decheni* (Witzmann 2004); their branches are preserved as thin carbonised layers. They can be recognised up to a skull length of 80 mm (TM 1169).

10. Discussion

10.1. Recognition of growth series

The series of 181 skulls investigated here satisfies the criteria listed by Schultze (1984) to identify a fossil growth series. First, all specimens were collected in the same locality, in the region of Lebach between Rümmelbach and Gresaubach in the Saarland, SW Germany. Secondly, they derive from the same horizon, the lower part of the 'Toneisensteinlager' of the Humberg Black Shale. Thirdly, skulls of every size can be distinguished by similar morphology as follows. The skull is distinctly more slender than that of any other temnospondyl in the Saar–Nahe Basin. Its lacrimal is excluded from the naris (or septomaxilla) by a broad maxillary-nasal contact. In contrast, the lacrimal contacts the naris and septomaxilla in larvae of *Sclerocephalus* and *Cheliderpeton* (Boy 1988, 1993b). In addition, the jugal is distinctly narrower in all size stages of *A. decheni* as compared to *Sclerocephalus* and *Cheliderpeton* of comparable size. Finally, the prefrontal of *A. decheni* tapers distinctly at its anterior end. In contrast, the prefrontal is always proportionally shorter and broader in *Sclerocephalus* and *Cheliderpeton* of equal skull length.

10.2. Capture of prey

10.2.1. Small larvae. According to Deban & Wake (2000), all extant urodele larvae and most water-dwelling adults capture prey items by using suction-feeding. The hyobranchial apparatus moves ventrally and posteriorly and depresses the floor of the mouth. The resulting expansion of the buccal cavity is further supported by lateral movements of the cheek, enabled by a joint between the jaw suspensorium and skull table (Schoch & Carroll 2003). This produces negative pressure in the buccal cavity, and water including prey items flows rapidly into the mouth. The floor of the mouth rises again during mouth closure, and water is expelled posterolaterally through the opened gill clefts. These clefts permit unidirectional flow of water through the buccal cavity, resulting in more effective suction feeding (Lauder & Shaffer 1986). Additionally, flaps of skin, the 'labial lobes', restrict the gape to the anterior part of the mouth (Erdman & Cundall 1984), leading to a higher velocity of the inflowing water and to control of its direction. Skulls with a short snout, blunt shape, and restricted gape are most adapted to suction feeding (Taylor 1987).

The smallest larvae of *A. decheni* have proportionally short snouts in relation to larger individuals. However, their skulls are slender, the gape is proportionally large, and the skull roof is akinetic. Marginal teeth that extend far posterior both on maxilla and dentary indicate that 'labial lobes' similar to aquatic urodeles were absent (Fig. 2c). Thus the inflow of water during mouth opening was undirected and not restricted to the anterior part of the mouth. Probably *A. decheni* relied on this uncontrolled suction effect when capturing small prey items (e.g., the syncarid crustacean *Uronectes*, preserved as remains in some specimens). The gill clefts permitted an unidirectional flow of water through the mouth cavity, and the branchial dentition prevented the prey from escaping through the gill clefts, analogous to the gill rakers of extant salamander larvae (Deban & Wake 2000). The large gape, as well as the robust conical teeth, indicate that small individuals also fed on large prey. Remains of prey found in small individuals of *A. decheni* (e.g., MB.Am.220, sl = 32 mm) consist of comparatively large specimens of the acanthodian *Acanthodes* sp., which are too large to be ingested solely by suction feeding. It is probable that *A. decheni* performed a forward strike towards the prey with jaw prehension. In conclusion, it can be assumed that suction feeding was not elaborate as in urodeles and thus not crucial in prey capture in small *A. decheni*. This hypothesis is supported by the fact that the hyobranchial apparatus was cartilaginous in small larvae, not ossifying until approximately 45 mm skull length. In contrast, extant suction feeding urodeles possess a well-ossified hyobranchial apparatus, whereas it is for the most part cartilaginous in non-suction feeding forms (Deban & Wake 2000). The suction-feeding dissorophoids *Apateon* and *Micromelerpeton* exhibit ossified ceratohyals and hypobranchials (Boy 2003). The marginal teeth of small larvae do not show the size differentiation that is present in larger specimens. Small individuals of *A. decheni* were obviously euryphagous.

10.2.2. Larger larvae and postlarval specimens. The marginal dentition differentiates in size with the proportional elongation and narrowing of the snout, similar to *Sclerocephalus* and *Cheliderpeton* (Boy 1988, 1993a, b). In skulls beyond 60 mm length, distinct size differentiation of the marginal teeth is present (Fig. 3c). The snout of middle-sized and large *A. decheni* is too slender and the gape too large to generate a strong suction effect. According to Taylor (1987), a lateral strike is the most effective mode of capturing prey for predators with long and narrow snouts. In contrast, moving forward on the prey with opened jaws constitutes greater resistance in water and affords precise approach to the prey (Taylor 1987). Thus the long, flat snout of *A. decheni* can be regarded as an adaptation to a lateral strike. This mode of feeding can be observed in extant long-snouted crocodiles and gharials (Cleuren & De Vree 2000), in the long-snouted actinopterygian *Lepisosteus* (Lauder & Norton 1980), as well as in marine mammals such as the platanistid river dolphins (Werth 2000). Most probably, *A. decheni* grabbed prey items with the anterolateral region of the snout, in which dentition shows the opposite size distribution in the upper and lower jaw as well as the largest marginal teeth. This adjustment of teeth allows better holding and killing of slippery and moveable prey. The large palatine and vomerine tusks, the comparatively long row of medium-sized teeth on palatine and ectopterygoid, and the symphyseal teeth of the dentary helped to fix and kill the prey.

After the prey was killed, it had to be repositioned before swallowing, analogous to extant crocodiles (Cleuren & De Vree 2000) and *Lepisosteus* (Lauder & Norton 1980). The large interpterygoid vacuities in *A. decheni* indicate that the eyeballs, together with the dentigerous palatal plates, assisted in the intrabuccal transport and swallowing by retraction into the mouth cavity, as seen in extant anurans and urodeles.

With the proportional elongation and narrowing of the snout during ontogeny, *A. decheni* increasingly preyed on fish, mostly *Acanthodes* sp. and occasionally on *Paramblypterus* sp., as nutrition remains indicate (see also Boy 1993a). It is important to emphasise that the ontogenetic change in *A. decheni* from small, euryphagous larvae to large, mainly ichthyophagous predators did not happen in a sudden kind of metamorphosis, but through a gradual process.

10.3. Ontogeny and function of the hyobranchial apparatus

In order to discuss the possible metamorphosis of the hyobranchium in *A. decheni*, it is necessary to consider functional aspects in feeding and breathing.

10.3.1. Basibranchial. The ossification of the basibranchial has been regarded as an indicator of the metamorphic phase in different temnospondyls (Boy & Sues 2000). However, in *A. decheni* the ossification of the basibranchial is no indicator of metamorphosis because it ossified at a skull length of approximately 45 mm, whereas the larval branchial platelets are present up to a skull length of 150 mm. Apart from the branchial platelets, the basibranchial is the only part of the hyobranchium that ossified in *A. decheni*. This is probably correlated with its role as the point of attachment for the hyobranchial musculature that rotated the hyobranchial apparatus to generate negative pressure in the buccal cavity during suction feeding, as well as to press air into the lungs for aerial respiration. Additionally, rotation of the hyobranchial apparatus obviously functioned to depress the mandible, because the retroarticular process is very poorly developed in *A. decheni* (Fig. 21). Mandibular depression by the hyobranchial apparatus might have been common in stem-stereospondyls, because the retroarticular process is absent or very small, and thus a strong depressor musculature was not able to insert on the lower jaw (Schoch & Milner 2000). Furthermore, the basibranchial probably also supported a developing, but simple, tongue pad and its musculature (see section 10.3.2). Mandibular depression by hyobranchial musculature is probably a plesiomorphic feature of gnathostomes because this muscle is also responsible for mouth opening in actinopterygians and dipnoans in addition to the m. epaxialis and m. levator operculi (Lauder & Reilly 1994).

10.3.2. Ceratobranchials. The presence of branchial denticles shows that *A. decheni* did not transform its hyobranchial apparatus at least until 150 mm skull length, i.e., four pairs of cartilaginous ceratobranchials were present until this size. The branchial denticles demonstrate that the gill clefts were still open. At a skull length of 150 mm, *A. decheni* has a distinctly elongated and slender snout. Therefore it must have performed the same mechanisms of prey capture as the adult specimens. Thus there is no reason to assume that the ceratobranchials underwent morphological changes during further growth, though the branchial platelets were resorbed and the gill clefts closed. If this interpretation is correct, *A. decheni* retained the pattern of four pairs of ceratobranchials as an adult, comparable in this respect to many larval or neotenic urodeles and to a certain degree to extant larval and metamorphosed gymnophionans (Stadtmüller 1936). As inferred from the size of the branchial platelets, the four cartilaginous ceratobranchials in *A. decheni* were slender elements.

The resorption of branchial denticles in middle-sized specimens is not correlated with a change in the mode of feeding, but it suggests the degeneration of external gills. As described in section 10.2.1, open gill clefts improve suction feeding effectivity. However, branchial denticles are still present in specimens whose snouts are too long and slender to feed by suction. Thus one can assume that the gill clefts served solely for gill breathing in larger larvae and indicate the presence of external gills until a skull length of around 150 mm.

Unfortunately, the morphology of the ceratobranchials after resorption of branchial platelets is not known in temnospondyls because they remained cartilaginous. Exceptions are a few forms, such as *Dvinosaurus* (Sushkin 1936) and *Gerrothorax* (Hellrung 2003), that are interpreted as perennibranchiate neotenes. It is possible that adult non-perennibranchiate temnospondyls still possessed three or four pairs of ceratobranchials in contrast to metamorphosed urodeles. This would be the plesiomorphic situation as compared to urodeles, whose remodelling of the hyobranchium would then be apomorphic (Stadtmüller 1936; Boy 1974). This hypothesis is supported by the fact that the most plesiomorphic metamorphosing urodele taxon, the hynobiids, have two pairs of ceratobranchials after metamorphosis, whereas all other taxa have only one pair after metamorphosis (Deban & Wake 2000). Boy (1985) also suspected that the hyobranchial apparatus of adult temnospondyls might have been quite similar to that of their larvae. He was lead to this consideration by his finding of ossified hypohyals and hypobranchials besides the 'adult' (i.e., anteriorly distinctly widened) basibranchial in the terrestrial dissorophoid *Micropholis*. However, it is also possible that early terrestrial temnospondyls such as *Dendrerpeton* or *Balanerpeton* evolved a remodelling of a larval into an adult hyobranchial apparatus that supported a moveable tongue, analogous to metamorphosed urodeles. If the later temnospondyls evolved from such terrestrial forms which remodelled the hyobranchium during ontogeny, then the retention of four pairs of ceratobranchials in *A. decheni* would be a paedomorphic trait.

10.4. Ontogeny of lateral line sulci

Small individuals of *A. decheni* exhibit almost no traces of lateral line sulci on the dermal skull bones, whereas they become more distinct during further growth. Boy (1988) reported a similar development in *Sclerocephalus*. Here the lateral line sulci are deeper in metamorphic and juvenile specimens than in larval ones. The only difference to *A. decheni* is their disappearance in the adult stage because of a change to a semi-terrestrial mode of life. The small dissorophoid *Micromelerpeton credneri* has lateral line sulci only on nasals in small specimens; the other parts of the lateral line sulci are visible much later in ontogeny, and the jugal sulcus is only traceable in some of the largest individuals (Boy 1972).

This development in *A. decheni* and other temnospondyls could be dependent on the thickness of the dermal skull roofing bones and the overlying skin, respectively. The skin may have been proportionally thicker relative to bone thickness in early growth stages, so that the lateral lines did not contact the surface of the bones. It is feasible that in further ontogeny the skin in *A. decheni* and other temnospondyls became proportionally thinner to the degree the bone sculpture was intensified, and thus the lateral lines came to lie on the bone surface. An extant analogue might be some hylid anurans, in which the lower layers of the dermis are increasingly replaced by hyperossifying bone during ontogeny (Trueb 1973).

10.5. Life history of *Archegosaurus decheni*

Can we draw conclusions from skull morphology as to whether *A. decheni* changed its habitat after resorption of the external gills, or whether it underwent a kind of metamorphosis? Most significant in this respect is the retention of lateral line sulci on the dermal skull roof and mandible of the largest specimens. They are a strong indicator of a primarily aquatic mode of life (Schoch 2001). A further indicator might be the morphology of the septomaxilla. This bone serves as origin for the constrictor and dilatator muscles that open and close the naris in urodeles (Lapage 1928; Panchen 1967). Narial muscles guarantee a tight closure of the external nares in the terrestrial plethodontids. These urodeles feed exclusively on land and their buccal cavity has to be kept free from water (Panchen 1967). As Panchen supposed, the septomaxilla served as origin of comparable

https://doi.org/10.1017/S0263593300001279 Published online by Cambridge University Press

muscles also in early tetrapods and temnospondyls. In terrestrial temnospondyls such as *Edops* and *Eryops*, the septomaxilla is a quite large and elaborate bone that bears a long internal process. In contrast, it is less developed in supposed aquatic forms (Sawin 1941; Panchen 1967; Schoch 2001). However, as Schoch (2001) pointed out, the functional differences between the two types of septomaxillary bones are not apparent. The small septomaxilla of *A. decheni* has a poorly developed internal process and represents the 'aquatic type'. This might indicate that narial muscles were less developed in *A. decheni*, possibly because it performed aquatic feeding and the buccal cavity was mostly filled with water. This corresponds with the absence of a nasolacrimal duct in all growth stages of *A. decheni*. The nasolacrimal duct can be regarded as a terrestrial adaptation in tetrapods (Janvier 1996) because it discharges surplus tear fluids from the eye to the nasal capsule to moisten the nasal epithelium. In extant neotenic, water-dwelling urodeles such as *Amphiuma* and *Siren*, no nasolacrimal duct is developed (Duellman & Trueb 1986). Its absence in *A. decheni* suggests that mainly water flowed through the narial passage, and the olfactory epithelium functioned in water rather than in air. Further evidence for this hypothesis may be derived from the shape and position of the choana. As Schoch (2001) recognised, terrestrial temnospondyls such as eryopids and zatrachydids exhibit a modification of the choanae to large and rounded openings which are expanded medially. Extant terrestrial urodeles and anurans have a voluminous narial passage, and this is also the case in adult *Eryops* (Schoch 2001). In contrast, the slit-like and laterally aligned choanae of *A. decheni* are characteristic of aquatic temnospondyls (Schoch 2001). The narrow choanae and the small size of the nasal capsule (judging from the impression on the ventral side of the dermal skull roof, see section 4.6.2) might indicate that the narial passage was restricted as compared to terrestrial temnospondyls.

The resorption of external gills in *A. decheni* does not necessarily imply a transition to a terrestrial mode of life. As Schmalhausen (1968) emphasised, external gills in large animals are disadvantageous because they are vulnerable to predators or may easily be damaged. Lungs, which are a plesiomorphic character of the Osteichthyes (bony fishes plus tetrapods, Janvier 1996), were the main respiratory organ after resorption of gills. Juvenile and adult *A. decheni* probably swam to the water surface to gulp air, as do extant lungfishes and many aquatic urodeles. Possibly the skin served as accessory respiration organ. An extant example of a primarily aquatic amphibian that has resorbed its gills and closed the gill clefts is the large-growing urodele *Andrias* (Duellman & Trueb 1986).

It can be assumed that *A. decheni* possessed an impedance-matching ear because the stapes is a long and quite slender element that was directed into the squamosal embayment. However, it cannot be determined if the stapes had the function to transmit airborne vibrations (such as in the majority of extant anurans) or if it had an auditory function underwater. Instead of a tympanic membrane, the tympanic annulus bears a cartilaginous disc that serves as receiver of aquatic sound waves in pipid anurans (Wever 1985). Therefore the presence of an impedance-matching ear in *A. decheni* is no indicator of terrestriality.

Considering these data, it can be assumed that *A. decheni* was primarily water-dwelling, not only as a gill-breathing larva, but throughout its life history. Furthermore, the life history of *A. decheni* does not include a metamorphosis in the sense of Alberch (1989), who defined metamorphosis as a condensement and synchronisation of developmental events in a short period of time. In contrast, the ontogeny of *A. decheni* shows gradual morphological changes. Developmental events such as initial ossifications of different skeletal elements are dissociated over a long period of time, if we take skull length as a crude proxy of individual age. The only abrupt alteration is the resorption of branchial platelets in middle-sized individuals, probably correlated with closure of gill clefts and resorption of external gills. However, this is not synchronous with any other morphological change visible in the skeleton, and does not constitute a metamorphosis. Also, the formation of polygonal sculpture, regarded as an indicator of metamorphosis in different temnospondyls (Bystrow 1935; Boy & Sues 2000), is not a metamorphic character in *A. decheni*. According to the sculptural classification of Boy & Sues (2000), the metamorphic stage would start at a skull length of approximately 50 mm in *A. decheni*, and the adult (or postmetamorphic) stage at 120 mm. However, in this size stage, the larval branchial platelets are still present.

Development of *A. decheni* is decelerated in many regards as compared to other temnospondyls. This includes the late ossification of the basibranchial, the long retention of denticle-bearing branchial platelets and external gills, and the degree of dentine infolding of marginal teeth, which remains simple even in adult individuals. In spite of this, the elongation of the snout can be interpreted as a peramorphic trait, probably caused by acceleration of the growth rate. Its proportional length is exaggerated as compared to more plesiomorphic temnospondyls such as *Dendrerpeton* or *Sclerocephalus*.

In conclusion, the life history of *A. decheni* includes a larval phase but no metamorphosis, similar in this respect to extant lepidosirenid lungfishes (Rose & Reiss 1993). The larval phase ended with resorption of branchial denticles. The subsequent juvenile and adult phases can only be separated arbitrarily. Uncinate processes of the ribs start to develop at a skull length of around 200 mm (pers. obs.), and this developmental event might be defined here as the beginning of the adult phase. Compared with the life histories of other temnospondyls such as *Sclerocephalus* (Boy 1988; Schoch 2003), *Onchiodon* (Boy 1990), and *Cheliderpeton* (Boy 1993b), the larval phase was much extended in *A. decheni*. This long duration of larval development is probably correlated with the similar mode of life in larvae and adults. An extant example might be the giant salamander *Cryptobranchus*, whose larval phase lasts approximately five years, and which is aquatic throughout its life history (Duellman & Trueb 1986).

11. Acknowledgements

I am much indebted to Hans-Peter Schultze (Lawrence) and Rainer Schoch (Stuttgart) who provided support and encouragement as well as constructive critique. I also want to thank Jürgen Boy (Mainz) for discussion and for the loan of specimens. Kathrin Dietze (Berlin) helped me to prepare a three-dimensional wax-model of a larval skull. Annalisa Gottmann (Bonn) made the photographs of the type specimens of *A. decheni*. I also gratefully acknowledge Peter Bartsch, Thomas Gassner, René Grube, Oliver Hampe (Berlin), Hanna Hellrung (Stuttgart), Jozef Klembara (Bratislava), Dieter Korn (Berlin), Jürgen Kriwet, Oliver Rauhut (München), Alexander Schmidt (Jena), Rodrigo Soler-Gijon, Sven Weidemeyer (Berlin), and Ralf Werneburg (Schleusingen) for various helpful comments and discussions. I am also grateful to Andrew Milner and one anonymous reviewer who have helped to improve the article substantially.

I thank the following persons for access to their collections: Oliver Hampe and David Unwin (MB Berlin), Thomas Martin (FU Berlin), Martin Sander (IP Bonn), Gerhard Plodowski

and Jutta Oelkers-Schäfer (SM Frankfurt am Main), Jacob Leloux (TM Haarlem), Wolfgang Munk (SMN Karlsruhe), Jon de Vos (NNM Leiden), Jürgen Boy (PI Mainz), Helmut Mayr (BSM München), Rudolf Becker (GMB Saarbrücken), Jean-Claude Horrenberger and Jean-Claude Gall (IG Strasbourg), Rainer Schoch and Rupert Wild (SMN Stuttgart), Michael Maisch (GPI Tübingen), and Heinz Furrer (PIMU Zürich). Hans-Hartmut Krüger and Lutz Berner (Berlin) kindly prepared latex casts of various skulls of *Archegosaurus decheni*.

12. Abbreviations used in figures

acc—intracranial branch of arteria carotis interna
aci—arteria carotis interna
ama—arteria mylohyoideus anterior
ang—angular
apf—anterior palatal fossa
art—articular
bb—basibranchial
bd—branchial denticles
bo—basioccipital
bs—basisphenoid
cb—ceratobranchials
cbo—basioccipital crest
ccap—capsular crest
ch—choana
cint—crista interolfactoria
cla—clavicle
clei—cleithrum
co—occipital condyle
col—canalis olfactorius
cor—coronoid
cot—orbitotemporal crest
cpar—paroccipital crest
cppt—parapterygoid crest
csel—sellar crest
cv—vertical column
cvl—ventrolateral crest
d—dentary
DPH—dorsal proximal head
ds—dorsum sellae
ect—ectopterygoid
eo—exoccipital
fbo—basioccipital fossa
fm—Meckelian fenestra
fp—paroccipital fossa
fst—stapedial foramen
icl—interclavicle
j—jugal
lasc—ascendening lamina of pterygoid
m—maxilla
man—mandible
mp—muscular pockets
n—nasal
N.IX–XI—nerves IX–XI
N.pal—palatine nerve
na—neural arch
ot—opisthotic
otl sio—otic part of infraorbital sulcus
p—parietal
pal—palatine
part—prearticular
plat—lateral process
pm—premaxilla
pof—posttemporal fenestra
pop sio—postorbital part of infraorbital sulcus
posp—postsplenial
pp—Postparietal
ppar—paroccipital process of exoccipital
ppart—paroccipital process of tabular
ppl—palatal plates
pr.cult—cultriform process
prsp—presplenial
ps—basal plate of parasphenoid
psel—sellar process
psmed—submedullar process
pst—parasymphyseal teeth
psup—supraoccipital process
pt—pterygoid
q—quadrate
qj—quadratojugal
rbpt—basipterygoid ramus
rc—conical recess
rrm—recess for rectus eye muscle
scl—sclerotic plate
sd—dental sulcus
si—sulcus intercristatus
sio—infraorbital sulcus
sj—jugal sulcus
sm—mandibular sulcus
sma—accessory mandibular sulcus
smx—septomaxilla
sot—occipital commissure
sphen—sphenethmoid
sps—parasphenoidal sulcus
sq—squamosal
sso—supraorbital sulcus
sta—stapes
sub sio—suborbital part of infraorbital sulcus
sur—surangular
t—tabular
tex—tabular extension
tp—torus parachoanalis
tsm—premaxillary tubercle
v—vomer
VPH—ventral proximal head

13. References

Agassiz, L. 1833. *Recherches sur les Poissons fossiles*, Vol. 2, 1–336. Neuchâtel and Soleure: Petitpierre.

Ahlberg, P. E. & Clack, J. A. 1998. Lower jaws, lower tetrapods – a review based on the Devonian genus *Acanthostega*. *Transactions of the Royal Society of Edinburgh: Earth Sciences* **89**, 11–46.

Alberch, P. 1989. Development and the evolution of amphibian metamorphosis. *Fortschritte der Zoologie* **35**, 163–73.

Ammon, L. v. 1889. *Die permischen Amphibien der Rheinpfalz*. München: F. Straub.

Bolt, J. R. & Lombard, R. E. 1985. Evolution of the amphibian tympanic ear and the origin of frogs. *Biological Journal of the Linnean Society* **24**, 83–99.

Boy, J. A. 1972. Die Branchiosaurier (Amphibia) des saarpfälzischen Rotliegenden (Unter–Perm, SW-Deutschland). *Abhandlungen des Hessischen Landesamtes für Bodenforschung* **65**, 1–137.

Boy, J. A. 1974. Die Larven der rhachitomen Amphibien (Amphibia: Temnospondyli; Karbon – Trias). *Paläontologische Zeitschrift* **48**, 236–82.

Boy, J. A. 1976. Überblick über die Fauna des saarpfälzischen Rotliegenden (Unter–Perm). *Mainzer geowissenschaftliche Mitteilungen* **5**, 13–85.

Boy, J. A. 1977. Typen und Genese jungpaläozoischer Tetrapoden-Lagerstätten. *Palaeontographica* **A156**, 111–67.

Boy, J. A. 1985 Über *Micropholis*, den letzten Überlebenden der Dissorophoidea (Amphibia, Temnospondyli; Unter-Trias). *Neues Jahrbuch für Geologie und Paläontologie, Monatshefte* **1985**, 29–45.

Boy, J. A. 1987. Die Tetrapoden-Lokalitäten des saarpfälzischen Rotliegenden (?Ober-Karbon – Unter-Perm; SW-Deutschland) und die Biostratigraphie der Rotliegend-Tetrapoden. *Mainzer geowissenschaftliche Mitteilungen* **16**, 31–65.

Boy, J. A. 1988. Über einige Vertreter der Eryopoidea (Amphibia: Temnospondyli) aus dem europäischen Rotliegend (?höchstes Karbon – Perm). 1. *Sclerocephalus. Paläontologische Zeitschrift* **62**, 107–32.

Boy, J. A. 1990. Über einige Vertreter der Eryopoidea (Amphibia: Temnospondyli) aus dem europäischen Rotliegend (?höchstes Karbon – Perm). 3. *Onchiodon. Paläontologische Zeitschrift* **64**, 287–312.

Boy, J. A. 1993a. Synopsis of the tetrapods from the Rotliegend (Lower Permian) in the Saar–Nahe Basin (SW-Germany). *In* Heidtke, U. (ed.) *New Research on Permo-Carboniferous Faunas*. Pollichia-Buch **29**, 155–69.

Boy, J. A. 1993b. Über einige Vertreter der Eryopoidea (Amphibia: Temnospondyli) aus dem europäischen Rotliegend (?höchstes Karbon – Perm). 4. *Cheliderpeton latirostre. Paläontologische Zeitschrift* **67**, 123–43.

Boy, J. A. 2003. Paläoökologische Rekonstruktion von Wirbeltieren: Möglichkeiten und Grenzen. *Paläontologische Zeitschrift* **77**, 123—52.

Boy, J. A., Meckert, D. & Schindler, T. 1990. Probleme der lithostratigraphischen Gliederung im unteren Rotliegend des Saar–Nahe-Beckens (?Ober-Karbon – Unter-Perm; SW-Deutschland). *Mainzer geowissenschaftliche Mitteilungen* **19**, 99–118.

Boy, J. A. & Fichter, J. 1982. Zur Stratigraphie des Saarpfälzischen Rotliegenden (?Ober-Karbon–Unter-Perm); SW-Deutschland. *Zeitschrift der Deutschen Geologischen Gesellschaft* **133**, 607–42.

Boy, J. A. & Sues, H.-D. 2000. Branchiosaurs: Larvae, Metamorphosis and Heterochrony in Temnospondyls and Seymouriamorphs. *In* Heatwole, H. & Carroll, R. L. (eds) *Amphibian Biology 4: Palaeontology*, 1150–97. Chipping Norton: Surrey Beatty.

Burmeister, H. 1850. *Die Labyrinthodonten aus dem Saarbrücker Steinkohlengebirge*. Berlin: G. Reimer.

Bystrow, A. P. 1935. Morphologische Untersuchungen der Deckknochen des Schädels der Stegocephalen. 1. Mitteilung. Schädel der Stegocephalen. *Acta Zoologica* (*Stockholm*) **16**, 65–141.

Bystrow, A. P. 1938. Zahnstruktur der Labyrinthodonten. *Acta Zoologica* (*Stockholm*) **19**, 387–425.

Bystrow, A. P. & Efremov, I. A. 1940. *Benthosuchus sushkini* Efremov. A labyrinthodont from the Eotriassic of Sharzenga River. *Travaux de l'institut paléontologique académie de sciences de l'USSR* **10**, 1–152. [In Russian with English summary.]

Carroll, R. L. 1964. Early evolution of the dissorophid amphibians. *Bulletin of the Museum of Comparative Zoology, Harvard University* **131**, 161–250.

Cleuren, J. & de Vree, F. 2000. Feeding in Crocodylians. *In* Schwenk, K. (ed.) *Feeding*, 337–58. New York, Boston, and London: Academic Press.

Cote, S., R. L. Carroll, R. Cloutier, & Bar-Sagi, L. 2002. Vertebral development in the Devonian sarcopterygian fish *Eusthenopteron foordi* and the polarity of vertebral evolution in non-amniote tetrapods. *Journal of Vertebrate Paleontology* **22**, 487–502.

Cox, C. B. & Hutchinson, P. 1991. Fishes and amphibians from the Late Permian Pedra de Fogo Formation of Northern Brazil. *Palaeontology* **34**, 561–73.

Credner, H. 1882. Die Stegocephalen aus dem Rotliegenden des Plauen'schen Grundes bei Dresden. Dritter Theil. *Zeitschrift der Deutschen Geologischen Gesellschaft* **34**, 213–37.

Deban, S. M. & Wake, D. B. 2000. Aquatic feeding in salamanders. *In* Schwenk, K. (ed.) *Feeding*, 65–94. New York, Boston, and London: Academic Press.

Dechen, E. C. H. v. 1847. [Mittheilungen an Professor Bronn gerichtet]. *Neues Jahrbuch für Mineralogie, Geognosie, Geologie und Petrefakten-Kunde* **1847**, 319–23.

Duellman, W. & Trueb, L. 1986. *Amphibian Biology*. New York: McGraw-Hill.

Efremov, I. A. 1933. Neubeschreibung des Labyrinthodonten *Platyops stuckenbergi* aus den oberpermischen Ablagerungen des Flusses Kitjak, eines Nebenflusses der Wjatka. *Travaux de l'institut paléontologique académie de sciences de l'USSR* **2**, 117–64.

Erdman, S. & Cundall, D. 1984. The feeding apparatus of the salamander *Amphiuma tridactylum*: morphology and behavior. *Journal of Morphology* **181**, 175–204.

Goldfuss, G. A. 1847. *Beiträge zur vorweltlichen Fauna des Steinkohlengebirges*. Bonn: Naturhistorischer Verein für die preussischen Rheinlande.

Golubev, V. K. 1995. New species of *Melosaurus* (Amphibia. Labyrinthodontia) from the Kazanian of the Kama river drainage area. *Paleontological Journal* **29**, 107–19.

Goodrich, E. S. 1930. Studies on the structure and development of vertebrates. London: Macmillan & Co.

Gubin, Y. M. 1981. A new platyoposaurid from Bashkiria. *Paleontological Journal* **15**, 108–10.

Gubin, Y. M. 1986. New data on the archegosauroids of the East European Platform. *Paleontological Journal* **20**, 70–5.

Gubin, Y. M. 1991. [Permian archegosauroid amphibians of the USSR]. *Trudy Paleontologichesko Instituta Nauka SSSR* **249**, 1–138. [In Russian.]

Gubin, Y. M. 1997. Skull morphology of *Archegosaurus decheni* Goldfuss (Amphibia, Temnospondyli) from the Early Permian of Germany. *Alcheringa* **21**, 103–21.

Haubold, H. 1983. Die Lebewelt des Rotliegenden. Die Neue Brehm-Bücherei, Vol. **154**, 1–246. Wittenberg Lutherstadt: A. Ziemsen Verlag.

Hellrung, H. 2003. *Gerrothorax pustuloglomeratus*, ein Temnospondyle (Amphibia) mit knöcherner Branchialkammer aus dem Unteren Keuper von Kupferzell (Süddeutschland). *Stuttgarter Beiträge zur Naturkunde* **B330**, 1–130.

Hofker, J. 1926. *Archegosaurus Decheni* Goldfuss. Untersuchung des Schädelbaues. *Palaeontologia Hungarica* **2**, 109–30.

Holmes, R. R. 2000. Palaeozoic temnospondyls. *In* Heatwole, H. & Carroll, R. L. (eds) *Amphibian Biology 4: Palaeontology*, 1082–120. Chipping Norton: Surrey Beatty.

Jaekel, O. 1896. Die Organisation von *Archegosaurus. Zeitschrift der Deutschen Geologischen Gesellschaft* **3**, 505–21.

Jäger, G. 1850. Über die Übereinstimmung des *Pygopterus lucius* Agassiz mit dem *Archegosaurus Dechenii* Goldfuss. *Abhandlungen der mathematisch-physikalischen Klasse der Bayerischen Akademie der Wissenschaften* **5**, 879–86.

Janvier, P. 1996. *Early Vertebrates*. Reprint 2002. Oxford: Clarendon Press.

Jordan, H. 1849. Ergänzende Beobachtungen zu der Abhandlung von Goldfuss über die Gattung *Archegosaurus. Verhandlungen des naturhistorischen Vereins für Rheinlande und Westphalen* **6**, 76–81.

Jupp, R. & Warren, A. A. 1986. The mandibles of the Triassic temnospondyl amphibians. *Alcheringa* **10**, 99–124.

Königer, S., Lorenz, V., Stollhofen, H. & Armstrong, R. A. 2002. Origin, age and stratigraphic significance of distal fallout ash tuffs from the Carboniferous-Permian continental Saar–Nahe Basin (SW-Germany). *International Journal of Earth Sciences (Geologische Rundschau)* **91**, 341–56.

Konzhukova, E. D. 1956. [The Intan Lower Permian fauna of the northern Ural region]. *Trudy Paleontologichesko Instituta Nauka SSSR* **62**, 5–50. [In Russian.]

Kuhn, O. 1933. Labyrinthodontia. *In* Quenstedt, W. (ed.) *Fossilium Catalogus, I. Animalia*, **61**, 1–114.

Langenhan, A. 1909. *Fauna und Flora des Rotliegenden in der Umgebung von Friedrichroda*, Vol. 2. Friedrichroda: Selbstverlag.

Lapage, E. O. 1928. The septomaxillary. I. In the Amphibia Urodela. *Journal of Morphology* **45**, 441–71.

Lauder, G. V. & Norton, S. F. 1980. Asymmetric muscle activity during feeding in the gar, *Lepisosteus oculatus. Journal of Experimental Biology* **84**, 17–32.

Lauder, G. V. & Reilly, S. M. 1994. Amphibian feeding behavior: comparative biomechanics and evolution. *In* Bels, V. L., Chardon, M. & Vandewalle, P. (eds) *Biomechanics of feeding in vertebrates. Advances in comparative and environmental physiology* **18**, 163–95. Berlin: Springer Verlag.

Lauder, G. V. & Shaffer, H. B. 1986. Functional design of the feeding mechanism in lower vertebrates: unidirectional and bidirectional flow systems in the tiger salamander. *Zoological Journal of the Linnean Society* **88**, 277–90.

Lombard, R. E. & Bolt, J. R. 1988. Evolution of the stapes in Paleozoic tetrapods, conservative and radical hypotheses. *In* Fritzsch, B., Ryan, M. J., Wiczynski, W. & Walkoviak, W. (eds) *The evolution of the amphibian auditory system*, 37–67. New York: J. Wiley.

Lydekker, R. 1885. Indian Pre-Tertiary Vertebrata. The labyrinthodont from the Bijori group. Palaeontologia Indica **4** (1), 1–16.

Makowsky, A. 1876. Über einen neuen Labyrinthodonten '*Archegosaurus austriacus* nov. spec.' *Sitzungsberichte der Kaiserlichen Akademie der Wissenschaft* **73**, 155–66.

Meyer, H. v. 1858. Reptilien aus der Steinkohlenformation in Deutschland. *Palaeontographica* **6**, 59–219.

Milner, A. R. 1978. A reappraisal of the Early Permian amphibians *Memonomenos dyscriton* and *Cricotillus brachydens. Palaeontology* **21**, 667–86.

Milner, A. R. & Sequeira, S. E. K. 1994. The temnospondyl amphibians from the Viséan of East Kirkton, West Lothian, Scotland. *Transactions of the Royal Society of Edinburgh: Earth Sciences* **84** (for 1993), 331–61.

Panchen, A. L. 1967. The nostrils of choanate fishes and early tetrapods. *Biological reviews of the Cambridge Biological Society* **42**, 374–420.

Pfannenstiel, M. 1932. Gehirnkapsel und Gehirn fossiler Amphibien, eine biologisch-anatomische Studie. *Monographien zur Geologie und Paläontologie* **6**, 1–85.

Romer, A. S. 1939. Notes on branchiosaurs. *American Journal of Sciences* **237**, 748–61.

Romer, A. S. 1947. Review of the Labyrinthodontia. *Bulletin of the Museum of Comparative Zoology Harvard College* **99**, 1–368.

Rose, C. S. & Reiss, J. O. 1993. Metamorphosis and the vertebrate skull: ontogenetic patterns and Developmental Mechanisms. *In* Hanken, J. & Hall, B. K. (eds) *The Skull: Development*. Vol. 1, 289–346. Chicago and London: The University of Chicago Press.

Säve-Söderbergh, G. 1936. On the morphology of Triassic stegocephalians from Spitsbergen and the interpretation of the endocranium in the Labyrinthodontia. *Kunglinga Svenska Vetenskapsakademiens Handlingar* **16**, 1–181.

Sawin, H. J. 1941. The cranial anatomy of *Eryops megacephalus. Bulletin of the Museum of Comparative Zoology at Harvard College* **88**, 407–63.

Schmalhausen, I. I. 1968. *The Origin of Terrestrial Vertebrates*. New York and London: Academic Press.

Schoch, R. R. 1999. Comparative osteology of *Mastodonsaurus giganteus* (Jaeger 1828) from the Middle Triassic (Lettenkeuper: Longobardian) of Germany (Baden-Württemberg, Bayern, Thüringen). *Stuttgarter Beiträge zur Naturkunde Serie* **B278**: 1–175.

Schoch, R. R. 2001. Can metamorphosis be recognised in Palaeozoic amphibians? *Neues Jahrbuch für Geologie und Paläontologie, Abhandlungen* **230**, 335–67.

Schoch, R. R. 2002. The stapes and middle ear of the Permo-Carboniferous tetrapod *Sclerocephalus. Neues Jahrbuch für Geologie und Paläontologie, Monatshefte* **215**, 177–200.

Schoch, R. R. 2003. Early larval ontogeny of the Permo-Carboniferous temnospondyl *Sclerocephalus. Palaeontology* **46**, 1055–72.

Schoch, R. R. & Carroll, R. L. 2003. Ontogenetic evidence for the Paleozoic ancestry of salamanders. *Evolution and Development* **5**, 314–24.

Schoch, R. R. & Milner, A. R. 2000. *Teil 3 B, Stereospondyli. Handbuch der Paläoherpetologie*. München: Verlag Dr. Friedrich Pfeil.

Schultze, H.-P. 1975. Die Lungenfisch-Gattung *Conchopoma* (Pisces, Dipnoi). *Senckenbergiana lethaea* **56**, 191–231.

Schultze, H.-P. 1984. Juvenile specimens of *Eusthenopteron foordi* Whiteaves 1881 (osteolepiform rhipidistian, Pisces) from the Late Devonian of Miguasha, Quebec, Canada. *Journal of Vertebrate Paleontology* **4**, 1–16.

Sequeira, S. E. K. & Milner, A. R. 1993. The temnospondyl amphibian *Capetus* from the Upper Carboniferous of Nýřany, Czech Republic. *Palaeontology* **36**, 657–80.

Shishkin, M. A. 1968. On the cranial arterial system of the labyrinthodonts. *Acta Zoologica (Stockholm)* **49**, 1–22.

Shishkin, M. A. 1973. [The morphology of the early Amphibia and some problems of lower tetrapod evolution]. *Trudy Paleontologichesko Instituta Nauka SSSR* **137**, 1–257. [In Russian.]

Stadtmüller, F. 1936. Kranium und Visceralskelett der Stegocephalen und Amphibien. *In* Bolk, L., Göppert, E., Kallius, E. & Lubosch, W. (eds) *Handbuch der vergleichenden Anatomie der Wirbeltiere*, Vol. **4**. Berlin and Vienna: Urban & Schwarzenberg.

Steen, M. C. 1938. On the fossil amphibia from the gas coal of Nýřany and other deposits in Czechoslovakia. *Proceedings of the Zoological Society London* **B108**, 205–83.

Sushkin, P. 1936. Notes on the pre-Jurassic Tetrapoda from USSR. III. *Dvinosaurus amalitzky*, a perennibranchiate stegocephalian from the Upper Permian from North Dvina. *Trudy Paleontologichesko Instituta Nauka SSSR* **4**, 43–91.

Taylor, M. A. 1987. How tetrapods feed in water: a functional analysis by paradigm. *Zoological Journal of the Linnean Society* **91**, 171–95.

Tewari, A. P. 1960. Note on a new species of *Archegosaurus* from the Lower Gondwana of Risin Spur (Kashmir). *Current Science* **29**, 144–5.

Trueb, L. 1973. Bones, frogs, and evolution. *In* Vial, J. (ed.) *Evolutionary biology of the anurans*, 65–132. Columbia: University of Missouri Press.

Warren, A. A. & Davey, L. 1992. Folded teeth in temnospondyls – a preliminary study. *Alcheringa* **16**, 107–32.

Watson, D. M. S. 1919. The structure, evolution and origin of the Amphibia. The 'orders' Rhachitomi and Stereospondyli. *Philosophical Transactions of the Royal Society London* **B209**, 1–72.

Watson, D. M. S. 1962. The evolution of the labyrinthodonts. *Philosophical Transactions of the Royal Society London* **B245**: 219–65.

Werneburg, R. 1986. Erste Übersicht der permokarbonen Tetrapodenfauna des Thüringer Waldes. *Veröffentlichungen Naturhistorisches Museum Schleusingen* **1**, 41–6.

Werneburg, R. 1988. Die Amphibienfauna der Oberhöfer Schichten (Unterrotliegendes, Unterperm) des Thüringer Waldes. *Veröffentlichungen Naturhistorisches Museum Schleusingen* **3**, 2–27.

Werneburg, R. & Schneider, J. 1996. The Permian temnospondyl amphibians of India. *Special Papers in Palaeontology* **52**, 105–28.

Werth, A. 2000. Feeding in marine mammals. *In* Schwenk, K. (ed.) *Feeding*, 487–526. New York, Boston, and London: Academic Press.

Wever, E. G. 1985. *The amphibian ear*. Princeton, New Jersey: Princeton University Press.

Whittard, W. F. 1928. On the structure of the palate and mandible of *Archegosaurus decheni* Goldfuss. *Annals and magazine of Natural History* **10**, 255–64.

Wilson, J. A. 1941. An interpretation of the skull of *Buettneria*, with special reference to the cartilages and soft parts. *Contributions from the Museum of Paleontology, University of Michigan* **5**, 71–111.

Witzmann, F. 2004. The external gills of Palaeozoic amphibians. *Neues Jahrbuch für Geologie und Paläontologie, Abhandlungen* **232**, 375–401.

Woodward, A. S. 1905. Permo-Carboniferous plants and vertebrates from Kashmir. Vol. II. Fishes and labyrinthodonts. *Memoirs of the Geological Survey of India. Palaeontologia Indica. New Series* **2**, 10–13.

Yates, A. M. & Warren, A. A. 2000. The phylogeny of the 'higher' temnospondyls (Vertebrata: Choanata) and its implications for the monophyly and origins of the Stereospondyli. *Zoological Journal of the Linnean Society* **128**, 77–121.

Zittel, K. A. R. v. 1888. *Handbuch der Palaeontologie: I. Abtheilung. Palaeozoologie. Vol. III. Vertebrata (Pisces, Amphibia, Reptilia, Aves)*. Berlin: R. Oldenbourg.

FLORIAN WITZMANN Museum für Naturkunde, Institut für Paläontologie, Invalidenstraße 43, 10115 Berlin, Germany.

MS received 8 December 2004. Accepted for publication 28 June 2005.